Preprints.org

Review

B meson Decays in Confined Covariant Quark Model

Stanislav Dubnička , Anna Zuzana Dubničková , Mikhail Alekseevich Ivanov , Andrej Liptaj [*]

Article

B meson Decays in Confined Covariant Quark Model

Stanislav Dubnička [1],[‡] ⓘ, **Anna Z. Dubničková** [2],[‡] ⓘ, **Mikhail A. Ivanov** [3],[‡] ⓘ, **and Andrej Liptaj** [1],[‡],* ⓘ

1 Institute of Physics, Slovak Academy of Sciences, Bratislava, Slovakia
2 Faculty of Mathematics, Physics and Informatics, Comenius University, Bratislava, Slovakia
3 Bogoliubov Laboratory of Theoretical Physics, Joint Institute for Nuclear Research, Dubna, Russia
* Correspondence: Andrej.Liptaj@savba.sk
‡ These authors contributed equally to this work.

Abstract: The aim this text to present the confined covariant quark model (CCQM) and review its applications to the decays of B mesons. We do so in the context of existing experimental measurements and theoretical results of other authors, which we review also. The physics principles are in detail exposed for the CCQM, the other results (theoretical and experimental) are surveyed in an enumerative way with comments. We proceed by considering successively three categories of decay processes: leptonic, semileptonic and non-leptonic.

Keywords: quark model; symmetry; B meson decay

1. Introduction

The confinement property of quantum chromodynamics (QCD) implies it is not possible to study the strong force using the scattering of free quarks. The confinement itself being a manifestation of the strong force, one cannot but analyze more complex systems such as hadrons, i.e. bound states of quarks. All hadrons are colorless (white) objects, among them mesons consisting of two quarks only. Even though no stable mesons exist, the meson physics is often seen as the most simple testing ground of QCD.

Various measurement provided us so far with a large amount of experimental data (masses, decay rates) which challenges our ability to provide theoretical predictions. For the above-mentioned reasons, the perturbative calculations performed at partonic level need to be complemented by the so-called hadronic effects, which are non-perturbative in nature and originate in the long-range interaction between quarks and gluons. As of now, we do not have a well-established general method for a reliable computation of hadronic effects for arbitrary processes from first principles.

Our ability to describe mesons and other QCD states without model dependence is limited, yet improves in time. Light meson physics is often treated within the chiral perturbation theory (ChPT) based on an (approximate) flavor chiral symmetry of the QCD which is spontaneously broken. Assuming this symmetry together with constraints from the analyticity and unitarity, phenomenological Lagrangians were proposed in [1]. This allowed to reproduce the results from complicated methods of the current algebra. In [1] the Lagrangians have been given in the leading order only, the extension of this approach which included meson loops was formulated in two original papers [2,3]. Since, the ChPT proved to be a successful effective field theory approach with remarkable results [4,5], however the large masses of other quarks besides u, d and s exclude the heavy-quark physics from its applicability range.

A different approach is represented by non-perturbative methods, such as the Dyson-Schwinger equations. The latter were formulated decades ago [6–8] in terms of an infinite number of coupled differential equations imposed to the Green functions of the theory. With necessary simplifications results were derived first for abelian theories. Then the approach was extended also to the more complicated case of non-abelian theories [9], thus including QCD and hadronic physics. The application to heavy quarks was for the first time presented in [10].

A distinctive non-perturbative theoretical technique to investigate the strong interaction physics are the QCD sum rules [11,12]. The central object of interest are the correlation functions of interpolating quark currents treated using the operator product expansion (OPE) and expressed in term of a perturbative continuum contribution and a low energy parameterization. These are then matched assuming the quark-hadron duality. The results are derived in form of sum rules, the uncertainties have to take into account various necessary approximations. Among others, the results for leptonic decay constants and hadron transition form factors have been derived [13,14].

In the domain of heavy meson physics (which we are interested in) a specific tool is available: the approximate realization of the heavy quark symmetry gives rise to the heavy quark effective theory (HQET) [15–17]. The symmetry appears when the mass of the heavy quark goes to infinity and is the combination of a heavy quark flavor symmetry and the independence of hadronic properties on the heavy quark spin state. It allows for important simplifications and leads to results expanded in the inverse of the heavy quark mass.

An important model-independent approach with possibly very broad applicability is represented by numerical QCD calculations on the lattice. Here an important progress was made over last decades [18], nowadays predictions of form factors in weak decays of heavy particles become available [19–22]. The potential of the method is immense, since, as is evident from [23], the bulk of the experimental data in high-energy physics is related to hadrons and explaining them at few percent level accuracy would be a triumph.

However we are not at this point now and the possibility for lattice calculations to become the mainstream of theoretical predictions will depend on the future developments. Thus, despite the important achievements of the lattice QCD, model dependent methods remain the most popular and versatile tools in making QCD predictions with hadronic effects included. This is mainly due to the fact that the lattice QCD remains limited to a narrow set of specific processes while the model framework can be usually easily adopted to various settings, making thus predictions more easy to produce. This is especially true with relation to the B factories, i.e. very high-luminosity accelerator facilities nowadays in operation where a large number of various heavy hadron decays is registered and measured. Many of these approaches can be described as "quark" models, since they describe the hadron by considering its valence quarks using some specific assumptions or ansätze (see e.g. [24,25]).

In weak decays the various quark models are usually combined with a perturbative computation at the quark level. Here, it is customary to use an effective four-fermion theory derived using the OPE and governed by the low-energy Hamiltonian

$$\mathcal{H}_{\text{eff.}}^{b \to q} = \frac{G_F}{\sqrt{2}} V_{tb} V_{tq}^* \sum_i C_i(\mu) Q_i(\mu) \tag{1}$$

here written for the $b \to q \in \{s, d\}$ transition. $Q_i(\mu)$ are local operators expressed in terms of quark fields, $C_i(\mu)$ are the Wilson coefficients which can be evaluated perturbatively, V_{ij} are Cabibbo - Kobayashi - Maskawa (CKM) matrix elements and μ is the QCD renomalization scale. Its value is set to a typical momentum transfer which is for weak decays significantly smaller that the W mass. Thus W is effectively removed from (1), it enters in computations of $C_i(\mu)$. An excellent overview of weak decays is given in [26].

The heavy decay processes are of a special interest for the particle physics community for several reasons [27]. One of them is the determinations of the CKM matrix elements and the study of related questions such as the CP violation, unitarity triangle, baryogenesis and weak physics in general. Further, B factories are used to search for new exotic states including tetraquarks, pentaquarks, glueballs and so on. The collected data also allowed to study fragmentation processes, test the lepton universality, investigate possible lepton flavor violation and address the questions related to a new, beyond Standard Model (SM) physics [28,29].

Indeed, various new physics (NP) scenarios [30–36] predict deviations from the SM in B meson decay processes. Because of the very high luminosity the nowadays colliders have, there is a hope that even rare (small in number) deviations from the SM physics can be detected.

We use the confined covariant quark model (CCQM) [37] to investigate the b-physics processes. A dedicated effort was made in previous years and decades to cover most of the measured B meson data, and since they are large in number we believe it is appropriate to review them. We provide in this text the overview of the results from the perspective of the CCQM, but we also point to contributions and achievements from other approaches and authors. Up to some exceptions, the majority of our outcome was formulated in terms of the SM predictions which were compared to data. In this way possible tensions or deviations were identified or hypothesis about the nature of an exotic state were expressed. This then points to possible NP phenomena or better understanding of exotic particles, especially when there is an agreement with other theoretical works too.

The large quantity of various B-related results we published in the past does not allow us to review each decay in full details. We therefore define three categories and for each we present a demonstrative calculation with one or two example processes. The categories are leptonic, semileptonic and non-leptonic (radiative) decays.

The text is structured as follows: In Section 2 the general features of the CCQM are presented. The following three sections are dedicated to specific process categories, as mentioned above. Each has three subsections, one with a general overview, the second presenting in more details the computations for a chosen example process and the third where results obtained within the CCQM framework are summarized. The text ends with conclusion and outlook.

2. Confined covariant quark model

The key points for the model construction are

- Lorentz symmetry and invariant Lagrangian,
- compositeness and double counting,
- confinement of quarks,
- gauge symmetry and inclusion of electromagnetic (EM) fields,

which we address is this order. In an additional subsection we also briefly describe our computational techniques.

2.1. Lagrangian

To construct a theory with Lorentz symmetry one naturally recurs to a Lagrangian formulation. So is done for the CCQM which is an effective field approach where both, quark and hadronic fields occur. The quark-meson interaction term is written as

$$\mathcal{L}_{int} = g_M M(x) J_M(x) + \text{ H.c. }, \quad J_M(x) = \int dx_1 \int dx_2 F_M(x; x_1, x_2) \bar{q}_2(x_2) \Gamma_M q_1(x_1), \quad (2)$$

where M represents the mesonic field, q the quark one, g_M is their coupling and H.c. stands for the hermitian conjugate. The interpolating quark current J_M is non-local and the integral over the positions x_1, x_2 of constituent quarks is weighted by a vertex function F_M. The symbol Γ_M represents a combination of gamma matrices depending on the spin of M. For a scalar M one has $\Gamma_M = 1$, for pseudoscalar $\Gamma_M = \gamma^5$ and for a vector particle the expression is $\Gamma_M = \gamma^\mu$. In the latter case the mesonic field has a Lorentz index too (M_μ) and the indices are contracted.

The explicit form of F_M is driven by two requirements. First we constrain the positions of quarks so as to make the hadron be situated in their barycenter. For this a delta function is introduced where the weights in its argument depend on the constituent quark masses $w_i = m_i/(m_1 + m_2)$. Second, to

manifestly respect the Lorentz symmetry, the remaining dependence is written as a function of the spacetime interval

$$F_M (x; x_1, x_2) = \delta (x - w_1 x_1 - w_2 x_2) \, \Phi_M \left[(x_1 - x_2)^2 \right].$$ (3)

Further steps in the construction of F_M are done with respect to the computational convenience. Φ_M is assumed to have a Gaussian form in the momentum representation

$$\Phi_M \left[(x_1 - x_2)^2 \right] = \int \frac{d^4 k}{(2\pi)^4} e^{-ik(x_1 - x_2)} \widetilde{\Phi}_M \left(-k^2 \right), \quad \widetilde{\Phi}_M \left(-k^2 \right) = e^{k^2/\Lambda_M^2},$$ (4)

where Λ_M is a free parameter of the model related to the meson M. The square of the momentum in the argument of the exponential becomes negative in the Euclidean region $k^2 = -k_E^2$ which implies an appropriate fall-off behavior and removes ultraviolet divergences in Feynman diagrams. The question of other possible function forms of Φ_M was addressed in [38], where four different ansatzes were tested, each having a meaningful physical interpretation. The dependence of the results on the function form was found to be small.

Besides the hadron-related Λ_M, the CCQM comprises four "global" parameters: three constituent quark masses and one universal cutoff which plays a role in the quark confinement (as explained later). The values expressed in GeV are

$$m_q = m_{u,d} = 0.241, \quad m_s = 0.428, \quad m_c = 1.67, \quad m_b = 5.05, \quad \lambda = 0.181,$$ (5)

where we do not distinguish between the two light quarks and use the same mass for both. The values slightly changed in the past, they were few times [39,40] updated if significant new data become available. They were extracted by over-constrained global fits of the model on available experimental points.

The CCQM does not include gluons. The gluonic effects are effectively taken into account by the vertex function which is adjusted to describe data by tuning the free parameter it contains.

At last we have to mention that the CCQM is suitable for description of various multi-quark states including baryons [41,42] and tetraquarks [43]. In this text we focus on mesons, the approach is in other cases very similar: the interpolating quark current is constructed for a given number of quarks (more alternatives can be considered) and multiplied by the hadronic field to give the interaction Lagrangian.

2.2. Compositeness condition

The interaction of a meson is given by the Lagrangian (2): the meson fluctuates into its constituent quarks, these interact and afterwards combine back into a mesonic final state. Yet, (2) implies that both, quark and mesons, are elementary and this rises concerns about the double counting.

We address these questions by implementing the so-called compositeness condition [37,39,44] which originates in works [45–47] (see [48] for a review). The interaction of a meson through the creation of virtual quark states implies the mesonic field is dressed, i.e. its vertex and wave function need to be renormalized. This is reflected in the renormalization constant Z_M which can be interpreted as the overlap between the physical state and the corresponding bare state. By requiring $Z_M = 0$ we make this overlap vanish, i.e. the physical state does not contain bare state and can be regarded as a bound state. As a consequence the quarks exist only as virtual and quark degrees of freedom do not appear on the level of the physical state.

Z_M is expressed in terms of the derivative of the meson mass operator Π_M' (its scalar part for vector mesons)

$$Z_M = 1 - g_M^2 \Pi_M' \left(m_M^2 \right) = 0$$ (6)

and at one-loop level (Figure 1) is given by

$$\Pi'_{PS}(p^2) = \frac{-i}{2p^2} p^\alpha \frac{d}{dp^\alpha} \int d^4k\, \tilde{\Phi}^2_{PS}(-k^2) \text{tr}\left[\gamma^5 S_1(k+w_1 p)\gamma^5 S_2(k-w_2 p)\right], \tag{7}$$

$$\Pi'_V(p^2) = \frac{-i}{3}\left(g_{\mu\nu} - \frac{p_\mu p_\nu}{p^2}\right)\frac{1}{2p^2} p^\alpha \frac{d}{dp^\alpha} \int d^4k\, \tilde{\Phi}^2_V(-k^2)\text{tr}\left[\gamma^\mu S_1(k+w_1 p)\gamma^\nu S_2(k-w_2 p)\right], \tag{8}$$

for pseudoscalar and vector mesons respectively. The symbol S_i denotes the quark propagator $S_i = 1/(m_{q_i} - \gamma^\mu k_\mu)$ and the differentiation is done using the identity $d\Pi/dp^2 = (p^\mu\, d\Pi/dp^\mu)/(2p^2)$.
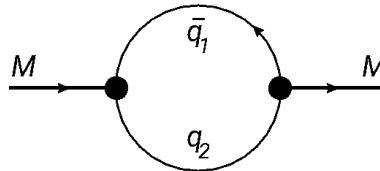

Figure 1. Meson mass function diagram.

To reach the equality (6) we profit from the up-to-now undetermined coupling constant g_M and tune its value so that (6) is satisfied. As consequence, the coupling g_M becomes the function of Λ_M. In this way we reduce the number of parameters of the model and increase its predictive power and stability. If the values Λ_M and g_M are unknown from previous studies, their determination is the first step in the application of the CCQM.

2.3. Infrared confinement

The CCQM was initially built without the quark confinement, but new data on heavy particles required its extension to situations where the hadron is heavier than the sum of its constituent quarks [37]. To prevent the decay into free quarks in such a scenario, we use a technique inspired by confined propagators. Here the propagators are written in the Schwinger representation and a cutoff is introduced in the upper integration limit. The propagator then becomes an entire function

$$\frac{S_i(k)}{(m_{q_i} + \gamma^\mu k_\mu)} = \int_0^\infty d\alpha\, e^{-\alpha(m_{q_i}^2 - k^2)} \rightarrow \int_0^{1/\lambda^2} d\alpha\, e^{-\alpha(m_{q_i}^2 - k^2)} = \frac{1 - e^{-(m_{q_i}^2 - p^2)/\lambda^2}}{m_{q_i}^2 - p^2}, \tag{9}$$

where the absence of singularities indicates the absence of a single quark asymptotic state. We adopt a modified version of this strategy and apply the cutoff to the whole structure F of the Feynman diagram. It can be formally written as

$$\Pi = \int_0^\infty d^n\alpha\, F(\alpha_1, \dots, \alpha_2) = \int_0^{\infty \to 1/\lambda^2} dt\, t^{n-1} \int_0^1 d^n\alpha\, \delta(1 - \sum_{i=1}^n \alpha_i) F(t\alpha_1, \dots, t\alpha_2) \tag{10}$$

and can be obtained by inserting the unity $1 = \int_0^\infty dt\, \delta(t - \sum_{i=1}^n \alpha_i)$ into the expression on the left hand side. The single cutoff (indicated by the arrow) in the t variable is done in the last step, the remaining integration variables are confined to an n dimensional simplex. After the cutoff is applied the integral becomes convergent for arbitrary values of the kinematic variables meaning that the quark thresholds are removed with quarks never being on the mass shell. The the cutoff value (5) is the same for all processes we study.

2.4. Electromagnetic interactions and gauge symmetry

Radiative decays represent another important class of processes measured at heavy meson factories. For their description one has to include the interactions with photons into the CCQM [37,49]. Because of the non-local interaction Lagrangian this is not straightforward and requires a dedicated

approach. Taking into the account quarks and scalar mesons, the free parts of the Lagrangian are treated in the usual way, i.e. the minimal substitution is used

$$\partial^\mu \psi \to (\partial^\mu - ie_\psi A^\mu)\psi, \quad \partial^\mu \bar\psi \to (\partial^\mu + ie_\psi A^\mu)\bar\psi, \tag{11}$$

where $\psi \in \{q, M\}$ and e_ψ is its electric charge in the units of the proton charge. One then gets

$$\mathcal{L}^{EM_1} = eA_\mu(x)J_M^\mu(x) + e^2 A^2(x)M^-(x)M^+(x) + \sum_q e_q A_\mu(x)J_q^\mu(x), \tag{12}$$

$$J_M^\mu(x) = i[M^-(x)\partial^\mu M^+(x) - M^+(x)\partial^\mu M^-(x)], \quad J_q^\mu(x) = \bar q(x)\gamma^\mu q(x). \tag{13}$$

The compositeness condition formulated above however prevents a direct interaction of the dressed particle, i.e. the meson, with photons: the contributions from the photon-meson tree level diagram and analogous diagrams with self-energy insertions into the external mesonic line determine the renormalization constant Z and $Z = 0$ implies they cancel. The interaction thus proceeds only through intermediate virtual states.

The gauging of the non-local interaction (2) is done in a manner similar to [50]. First one multiplies the quark fields in (2) by a gauge field exponential

$$q_i(x) \to e^{-ie_{q_i} I(x_i, x, P)} q_i(x), \quad I(x_i, x, P) = \int_x^{x_i} dz_\mu A^\mu(z), \tag{14}$$

where P is the path connecting x_i and x, the latter being the position of the meson. One can verify that the Lagrangian is invariant under the following gauge transformations

$$q_i(x) \to e^{ie_{q_i} f(x)} q_i(x), \quad \bar q_i(x) \to \bar q_i(x) e^{-ie_{q_i} f(x)}, \tag{15}$$

$$M(x) \to e^{ie_M f(x)} M(x), \quad A^\mu(x) \to A^\mu(x) + \partial^\mu f(x), \tag{16}$$

here $f(x)$ is some scalar function. The apparent path-dependence of the definition (14) is not an actual one: in the perturbative expansion only derivatives of the path integral appear and these are path independent

$$\frac{\partial}{\partial x^\mu} I(x, y, P) = A_\mu(x). \tag{17}$$

The individual terms of the Lagrangian are generated by expanding the gauge field exponential by orders in A^μ. At first order one has

$$\mathcal{L}^{EM_2}(x) = g_M M(x) \iiint dx_1\, dx_2\, dy\, E_M^\mu(x; x_1, x_2, y)\, A_\mu(y)\bar q_2(x_2)\, \Gamma_M q_1(x_1), \tag{18}$$

where E_M is defined through its Fourier transform $\widetilde E_M$: $(x_1 - x, x_2 - x, y - x) \overset{FT}{\leftrightarrow} (p_1, p_2, q)$

$$\widetilde E_M^\mu(p_1, p_2, q) = \sum_{i=1,2} \vartheta_i e_{q_i} w_i (w_i q^\mu + \vartheta_{i+1} 2l^\mu) \int_0^1 dt \widetilde\Phi_M' \left[-t(w_i q + \vartheta_{i+1} l)^2 - (1-t)l^2 \right], \tag{19}$$

$$l = w_1 p_1 + w_2 p_2, \quad \vartheta_i = (-1)^i. \tag{20}$$

Symbol $\widetilde\Phi_M'$ denotes the derivative with respect to the argument. In corresponding Feynman diagrams the photon is attached to the non-local vertex.

2.5. Computations

From the Lagrangian one derives the Feynman diagrams. Gaussian expressions in the vertex function (4) and in the Fock-Schwinger propagator (9) can be joined into a single exponent which takes

a quadratic form in the loop momenta k. It can be formally written as $\exp(ak^2 + 2rk + z)$, $a = a(\{\alpha\})$, $r = r(\{\alpha\}, \{p\})$, where $\{\alpha\}$ denotes the set of Schwinger parameters and $\{p\}$ external momenta. The exponential is preceded by a polynomial P in loop momenta which originates from the trace of Dirac matrices (numerators of propagators). Since the powers of k can be generated by differentiation with respect to r, the loop momenta integration is formally written as

$$\int d^4k \, P(k) \exp(ak^2 + 2rk + z) = \exp(z) P\left(\frac{1}{2}\frac{\partial}{\partial r}\right) \int d^4k \, \exp(ak^2 + 2rk). \tag{21}$$

Using the substitution $u = k + r/a$, the argument of the exponential is transformed

$$\int d^4k \, \exp(ak^2 + 2rk) = \int d^4u \, \exp(au^2 - r^2/a) = \exp(-r^2/a) \int d^4u \, \exp(au^2) \tag{22}$$

and the integration is performed in the Euclidean region as a simple Gaussian integral. Further, the differential operator and the r-dependent exponential can be interchanged

$$P\left(\frac{1}{2}\frac{\partial}{\partial r}\right) \exp\left(-\frac{r^2}{a}\right) = \exp\left(-\frac{r^2}{a}\right) P\left(-\frac{r}{a} + \frac{1}{2}\frac{\partial}{\partial r}\right) \tag{23}$$

which simplifies the action of the differential operator. One arrives to

$$\int_0^\infty d\alpha_1 \cdots \int_0^\infty d\alpha_n F(\alpha_1, \ldots, \alpha_n), \tag{24}$$

where F represents the whole structure of the Feynman diagram including (23). We use a FORM [51] code to treat symbolic expressions: besides computing traces we also us it to repeatedly perform chain rule application in (23) and arrive to an explicit formula with no differential operators appearing. The implementation of the infrared confinement as expressed by (10) is the last step before the numerical integration.

3. Leptonic decays of B mesons

3.1. Overview

Large mass difference between heavy mesons and leptons implies, by phase-space arguments, small branching fractions of pure and radiative leptonic decays. Some of these are further suppressed by CKM elements or helicity. Thus for most leptonic decays only limits have been measured.

At the usual 95% confidence level a branching fraction measurement is available only for $B_s^0 \to 2\mu$ [52–55] and $B^\pm \to \tau^\pm \nu_\tau$ [56–59]. If the criteria are loosened to (at least) one sigma significance, additional results can be cited: $B^0 \to 2\mu$ [52], $B^+ \to \mu^+\nu_\mu$ [60,61] and $B^+ \to \ell^+\nu_\ell\gamma$ [62]. The limits are settled [23] for $B^+ \to e^+\nu_e$, $B^+ \to e^+\nu_e\gamma$, $B^+ \to \mu^+\nu_\mu\gamma$, $B^+ \to \mu^+\mu^-\mu^+\nu_\mu$, $B^0 \to e^+e^-$, $B^0 \to e^+e^-\gamma$, $B^0 \to \mu^+\mu^-\gamma$, $B^0 \to \mu^+\mu^-\mu^+\mu^-$, $B^0 \to \tau^+\tau^-$, $B_s^0 \to e^+e^-$, $B_s^0 \to \tau^+\tau^-$ and $B_s^0 \to \mu^+\mu^-\mu^+\mu^-$.

These experimental results motivate various analyses. Pure leptonic decays are considered as theoretically clean with the main source of uncertainty represented by the hadronic effects of the initial state, which are contained in the leptonic decay constant of the hadron. The neutrino production process corresponds, in the leading order, to the annihilation of the constituent quarks into a virtual W meson which subsequently decays. The branching fraction is given by

$$\mathcal{B}(B^+ \to \ell^+\nu) = \frac{G_F^2 m_B m_l^2}{8\pi}\left(1 - \frac{m_l^2}{m_B^2}\right)^2 f_B^2 |V_{ub}|^2 \tau_{B^+}, \tag{25}$$

where G_F is the Fermi coupling constant, V_{ij} the CKM matrix element and τ_P the lifetime of the particle P.

A general information about *B* leptonic decays is contained in several reviews. Besides [26], a more specific focus on processes with charged pseudoscalar mesons is given in [63] and a summary concerning specifically *B* decays (leptonic and semileptonic) is provided in [64]. The existing theoretical approaches follow two directions. One focuses on the SM contributions at different precision levels, the other is concerned with NP beyond the SM.

Dilepton final states are produced at one loop through box and penguin diagrams. The cross section formula can be found e.g. in [65], Equation (4.10). The leptonic decays constants of *B* (and *D*) mesons where determined in a model-independent way using lattice calculations in [66]. The SM treatment of dilepton decays includes the computation of three-loop QCD corrections [67], the evaluation of the electroweak contributions at the two-loop level [68] and further improvements of theoretical predictions reached by combining additional EM and strong corrections [69]. The authors of [70] investigated the effect of the virtual photon exchange from scales below the bottom-quark mass and found a dynamical enhancement of the amplitude at the 1% level. The soft-collinear effective theory approach was used in [71] to evaluate the power-enhanced leading-logarithmic QED corrections.

The radiative processes have the advantage of not being helicity suppressed at the price of one additional α_{EM} factor. A larger number of results can be cited for radiative dilepton production. An evaluation within a constituent quark model was performed in [72] to estimate branching fractions, the same observables were predicted by the authors of [73,74] using the light-cone QCD sum rules and by those of [75] using the light-front model. Universal form factors related to the light cone wave function of the B_s meson allowed to make estimates in [76]. Interesting results were given in [77], where it was shown that the gauge invariance and other considerations allow to significantly constrain the form factor behavior, and also in [78] where the authors have demonstrated that the non-perturbative hadronic effects largely cancel in amplitude ratios of pure leptonic and radiative decays. The impact of the light meson resonances on long-distance QCD effects was studied in [79]. In [80] the authors have identified the effective $B \to \mu\mu\gamma$ lifetime and a related CP-phase sensitive observable as appropriate quantities to study the existing B decay discrepancies.

Also for decays $B \to \gamma l \nu_l$ several studies can be cited. The work [81] was concerned with photon spectrum and the decay rates of the process. The authors of [82] used the HQET to predict form factors and in [83] the heavy-quark expansion and soft-collinear effective theory were applied to evaluate the soft-overlap contribution to the photon. The process was also studied in [84]. Here, assuming an energetic photon, the authors aimed to quantify the leading power-suppressed corrections in $1/E_\gamma$ and $1/m_b$ from higher-twist B-meson light-cone distribution amplitudes. The soft-collinear effective theory was the approach adopted in [85,86].

The recent publication [87] focused on four-body leptonic B decays: off-shell photon form factors were computed within the QCD factorization formalism and predictions for differential distribution of various observables were presented. Similar processes are addressed also in [88–90].

Although the most tensions with the SM are seen in the semileptonic sector, the pure leptonic decays are of a concern too. The summary papers [29,91] mention two tensions. Fist is related to the combined likelihood for B^0 and B_s^0 decays to $\mu^+\mu^-$ where the theory-measurement difference reaches 2.3σ. The other concerns the branching fraction ratio for the $B_s^0 \to \mu^+\mu^-$ reaction $R = \mathcal{B}_{\exp}/\mathcal{B}_{\mathrm{SM}}$ which deviates from 1 by 2.4σ. In [92] is the difference between the theory and the experiment for the dimuon B_s decay quantified to be 2.2σ.

The possible NP contributions are usually assessed by introducing new, beyond SM four-fermion contact operators and the corresponding Wilson coefficients. Once evaluated in the appropriate NP approach, it is possible to conclude about their effect on the theory-experiment discrepancy, see e.g. [93].

An overview of various flavor-violating extensions of the SM also with relation to $B \to \ell\ell$ decay was presented in [94]. In [95] the B_s dimuon decay was considered and it was argued that the decay

width difference between the light and heavy B_s mass eigenstates is a well-suited observable for the detection of NP. The work [31] points to the ambiguity in choice of the NP operators that might play role in explaining the tensions in the B semileptonic decays. They show that this ambiguity can be lifted by analyzing the longitudinal polarization asymmetry of the muons in $B_s^* \to \mu\mu$. Various discrepancies in measured data are addressed in [96], among them also dimuon branching fractions. The attempt to explain them is based on lepton-flavored gauge extensions of the SM, a specific construction with a massive gauge boson X_μ and "muoquark" S_3 is presented. Several texts are interested in decays with tau lepton in the final state. In [97–99] these decays are studied in relation with various alternative scenarios of the Higgs boson model and in [100] they are analyzed in the context of non-universal left-right models.

3.2. Radiative leptonic decay $B_s \to \ell^+\ell^-\gamma$ in CCQM

Before reviewing other CCQM results on leptonic B decays we present in more details the evaluation of the branching fraction for $B_s \to \ell^+\ell^-\gamma$ [101]. The computations are in many ways similar to those of other cases and provide an insight of how leptonic and radiative decays are treated within the CCQM. Since B_s is the only hadron, we need to extend the set of parameters (5) only by one number, i.e. $\Lambda_{B_s} = 2.05$ GeV which was settled in previous works. Two explicit forms of the effective Hamiltonian (1) are considered

$$\mathcal{H}_{\text{eff.}}^{b\to s\ell^+\ell^-} = \frac{G_F\alpha_{\text{EM}}}{2\sqrt{2}\pi}V_{tb}V_{ts}^*\left[C_9^{\text{eff}}\{\bar{s}\gamma^\mu(1-\gamma^5)b\}(\bar{\ell}\gamma_\mu\ell) - \frac{2\tilde{m}_b}{q^2}C_7^{\text{eff}}\{\bar{s}i\sigma^{\mu\nu}q_\nu(1+\gamma_5)b\}(\bar{\ell}\gamma_\mu\ell)\right.$$

$$\left. + C_{10}\{\bar{s}\gamma^\mu(1-\gamma_5)b\}(\bar{\ell}\gamma_\mu\gamma_5\ell)\right], \tag{26}$$

$$\mathcal{H}_{\text{eff}}^{b\to s\gamma} = -\frac{G_F}{\sqrt{(2)}}V_{tb}V_{ts}^*C_7^{\text{eff}}\frac{e\tilde{m}_b}{8\pi^2}\left[\bar{s}\sigma_{\mu\nu}(1+\gamma_5)b\right]F^{\mu\nu}, \tag{27}$$

where $\sigma_{\mu\nu} = i[\gamma_\mu, \gamma_\nu]$ and $F^{\mu\nu}$ is the EM field tensor. In (26) the dilepton is produced from the weak b-s transition, Figure 2, in (27) the weak transition gives birth to a real photon, Figure 3. An additional set of diagrams depicted in Figure 4 is considered too, where the real photon is emitted as the final-state radiation (FSR).
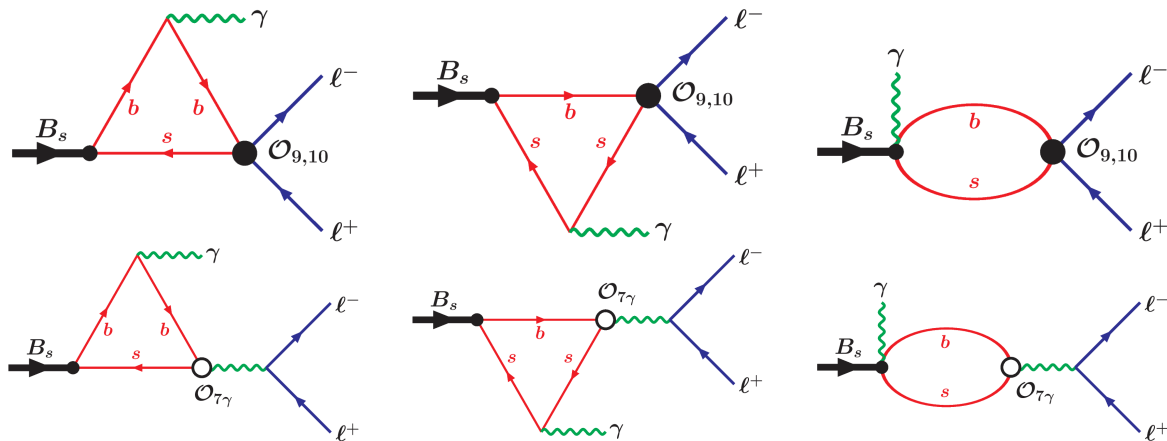

Figure 2. Diagrams with the dilepton produced from the b-s transition.
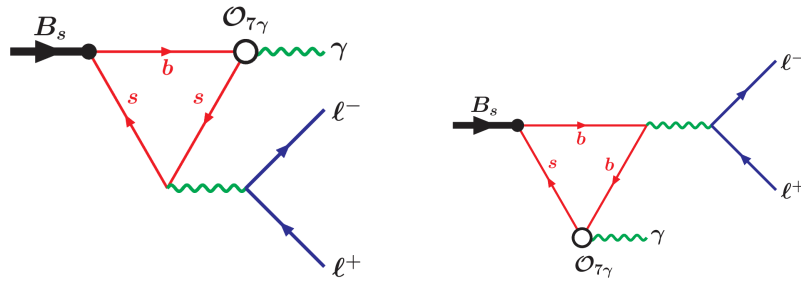
Figure 3. Diagrams with a real photon produced from the *b-s* transition.
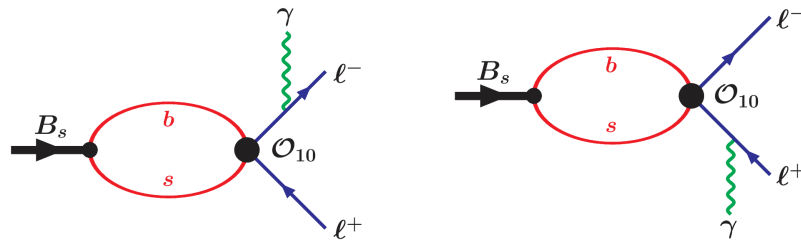

Figure 4. Final-state radiation diagrams.

The tilde notation in (26) (27) indicates the QCD quark mass (different from (5)) which is $\tilde{m}_b = 4.68 \pm 0.03$ GeV [102]. The values of scale-dependent Wilson coefficients were determined in [103] at the matching scale $\mu_0 = 2m_W$ and run to the hadronic scale $\mu_b = 4.8$ GeV. The effective operators are defined through the standard SM operators as follows

$$
\begin{aligned}
C_7^{\text{eff}} =& C_7 - C_5/3 - C_6, \\
C_9^{\text{eff}} =& C_9 + C_0[h(\hat{m}_c, s) + \Omega] - \frac{1}{2}h(1, s)(4C_3 + 4C_4 + 3C_5 + C_6) \\
& - \frac{1}{2}h(0, s)(C_3 + 3C_4) + \frac{2}{9}(3C_3 + C_4 + 3C_5 + C_6),
\end{aligned}
\tag{28}
$$

where

$$
\begin{aligned}
& C_0 = 3C_1 + C_2 + 3C_3 + C_4 + 3C_5 + C_6, \quad \Omega = \frac{3\pi}{\alpha^2}\kappa \sum_{V_i = \Psi(1s), \Psi(2s)} \frac{\Gamma(V_i \to \ell^+\ell^-)m_{V_i}}{m_{V_i}^2 - q^2 - im_{V_i}\Gamma_{V_i}}, \\
& \hat{m}_c = \tilde{m}_c/m_{B_s}, \quad \tilde{m}_c = 1.27 \pm 0.03 \text{GeV}, \quad s = q^2/m_{B_s}^2, \quad \kappa = 1/C_0, \\
& h(0, s) = \frac{8}{27} - \frac{8}{9}\ln\frac{\tilde{m}_b}{\mu} - \frac{4}{9}\ln s + \frac{4}{9}i\pi, \\
& h(\hat{m}_c, s) = -\frac{8}{9}\left[\ln\frac{\tilde{m}_b}{\mu} + \ln\hat{m}_c - \frac{1}{3} - \frac{x}{2}\right] - \frac{2}{9}(2 + x)\sqrt{|1 - x|}\,\Theta(x), \\
& \Theta(x)|_{x<1} = \ln\left|\frac{\sqrt{1-x}+1}{\sqrt{1-x}-1}\right| - i\pi, \quad \Theta(x)|_{x>1} = 2\arctan\frac{1}{\sqrt{x-1}}, \quad x = \frac{4\hat{m}_c^2}{s}.
\end{aligned}
\tag{29}
$$

The Ω function in C_9^{eff} parameterizes, in the standard Breit-Wigner form, the resonant contributions from $\Psi(1s)$ and $\Psi(2s)$ charmonia states.

Amplitudes given by the diagrams in Figures 2 and 3, where the photon originates from the intermediate QCD-generated states, are labeled as structure dependent and can be described by four

$B_s \to \gamma$ transition form factors (see e.g. [79]). Defining momenta as $B_s(p_1) \to \gamma(p_2)\, \ell^+(k_+)\, \ell^-(k_-)$, $q = p_1 - p_2$ with $p_1^2 = m_{B_s}^2$, $p_2^2 = 0$, $\epsilon_2^\dagger \cdot p_2 = 0$ and $k_\pm^2 = m_\ell^2$ one has

$$
\begin{aligned}
\langle \gamma(p_2, \epsilon_2) | \bar{s} \gamma^\mu b | B_s(p_1) \rangle &= e(\epsilon_2^\dagger)_\alpha \varepsilon^{\mu\alpha\beta\delta}(p_1)_\beta (p_2)_\delta F_V(q^2) / m_{B_s}, \\
\langle \gamma(p_2, \epsilon_2) | \bar{s} \gamma^\mu \gamma_5 b | B_s(p_1) \rangle &= i e(\epsilon_2^\dagger)_\alpha (g^{\mu\alpha} p_1 p_2 - p_1^\alpha p_2^\mu) F_A(q^2) / m_{B_s}, \\
\langle \gamma(p_2, \epsilon_2) | \bar{s} \sigma^{\mu\beta} q_\beta b | B_s(p_1) \rangle &= i e(\epsilon_2^\dagger)_\alpha \varepsilon^{\mu\alpha\beta\delta}(p_1)_\beta (p_2)_\delta F_{TV}(q^2), \\
\langle \gamma(p_2, \epsilon_2) | \bar{s} \sigma^{\mu\beta} q_\beta \gamma_5 b | B_s(p_1) \rangle &= e(\epsilon_2^\dagger)_\alpha (g^{\mu\alpha} p_1 p_2 - p_1^\alpha p_2^\mu) F_{TA}(q^2),
\end{aligned}
\tag{30}
$$

where ϵ is the polarization vector. Each of the four introduced form factors can be expressed as sum of contributions from particular Feynman graphs in Figures 2 and 3. We have

$$
\begin{aligned}
F_V &= m_{B_s}(e_b \tilde{F}_V^{b\gamma b} + e_s \tilde{F}_V^{s\gamma s}), \\
F_A &= m_{B_s}(e_b \tilde{F}_A^{b\gamma b} + e_s \tilde{F}_A^{s\gamma s} e_b \tilde{F}_A^{\text{bubble}-b} + e_s \tilde{F}_A^{\text{bubble}-s}), \\
F_{TV} &= e_b \tilde{F}_{TV}^{b\gamma b} + e_s \tilde{F}_{TV}^{s\gamma s} + e_b \tilde{F}_{TV}^{b(\bar{\ell}\ell)b} + e_s \tilde{F}_{TV}^{s(\bar{\ell}\ell)s}, \\
F_{TA} &= e_b \tilde{F}_{TA}^{b\gamma b} + e_s \tilde{F}_{TA}^{s\gamma s} + e_b \tilde{F}_{TA}^{\text{bubble}-b} + e_s \tilde{F}_{TA}^{\text{bubble}-s} + e_b \tilde{F}_{TA}^{b(\bar{\ell}\ell)b} + e_s \tilde{F}_{TA}^{s(\bar{\ell}\ell)s},
\end{aligned}
\tag{31}
$$

where "$q\gamma q$" superscript refers to a real photon emission from the quark line, "*bubble*" to the real photon emission from the non-local hadron-quark vertex and "$q(\bar{\ell}\ell)q$" corresponds to the virtual photon emission from the quark line.

The branch point at $q^2 = 4m_s^2$ corresponding to the virtual photon emission from the s quark (left in Figure 3) is situated well inside the accessible physical q^2 region. This leads to the appearance of light vector meson resonance which prevents us to compute the corresponding form factors within the CCQM. An approach inspired by [104] is adopted and a gauge-invariant vector-meson dominance model is used to express the form factors in question

$$
\tilde{F}_{TV,TA}^{s(\bar{\ell}\ell)s} = \tilde{F}_{TA}^{s(\bar{\ell}\ell)s}(0) - \sum_V 2 f_V^{EM} G_1^T(0) \frac{q^2 / M_V}{q^2 - M_V^2 + i M_V \Gamma_V},
\tag{32}
$$

$$
G_1^T: \quad \langle V(p_2, \epsilon_2) | \bar{s} \sigma^{\mu\nu} b | B_s(p_1) \rangle =
$$

$$
= (\epsilon_2^\dagger)_\alpha \left[\varepsilon^{\beta\mu\nu\alpha} P_\beta G_1^T(q^2) + \varepsilon^{\beta\mu\nu\alpha} q_\beta G_2^T(q^2) + \varepsilon^{\alpha\beta\mu\nu} P_\alpha q_\beta \frac{G_0^T(q^2)}{(m_{B_s} + M_V)^2} \right],
\tag{33}
$$

where $P = p_1 + p_2$. With all this objects defined, one can write down the amplitude for the structure dependent part

$$
\begin{aligned}
\mathcal{M}_{\text{SD}} = \frac{G_F}{\sqrt{2}} \frac{\alpha_{EM} V_{tb} V_{ts}^*}{2\pi} e(\epsilon_2^*)_\alpha \Bigg\{ &\left[\varepsilon^{\mu\alpha\nu\beta}(p_1)_\nu (p_2)_\beta \frac{F_V(q^2)}{m_{B_s}} - i T_1^{\mu\alpha} \frac{F_A(q^2)}{m_{B_s}} \right] \times (C_9^{\text{eff}} \bar{\ell} \gamma_\mu \ell \\
&+ C_{10} \bar{\ell} \gamma_\mu \gamma_5 \ell) + \left[\varepsilon^{\mu\alpha\nu\beta}(p_1)_\nu (p_2)_\beta F_{TV}(q^2) - i T_1^{\mu\alpha} F_{TA}(q^2) \right] \frac{3 \tilde{m}_b}{q^2} C_7^{\text{eff}} \bar{\ell} \gamma_\mu \ell,
\end{aligned}
\tag{34}
$$

where $T_1^{\mu\alpha} = [g^{\mu\alpha} p_1 p_2 - (p_1)^\alpha (p_2)^\mu]$. The structure-independent *bremsstrahlung* (Figure 4) amplitude takes the form

$$
\mathcal{M}_{\text{BR}} = -i \frac{G_F}{\sqrt{2}} \frac{\alpha_{EM} V_{tb} V_{ts}^*}{2\pi} e(\epsilon_2^*)_\alpha (2 m_\ell f_{B_s} C_{10}) \bar{u}(k_-) \left[\frac{\gamma^\alpha \slashed{p}_1}{t - m_\ell^2} - \frac{\slashed{p}_1 \gamma^\alpha}{u - m_\ell^2} \right] \gamma_5 v(k_+).
\tag{35}
$$

Here $t = (p_2 + k_-)^2$, $u = (p_2 + k_+)^2$. To avoid infrared divergences in (35) a lower boundary on the photon energy has to be introduced $E_\gamma > E_{\gamma\,\text{min}}$ set later, in numerical computations (Table 1), to 20 MeV.

The differential branching fraction in t and $s \equiv q^2$ has a general expression

$$\frac{d\Gamma}{ds\,dt} = \frac{1}{2^8\pi^3 m_{B_s}^3} \sum_{\text{pol.}} |\mathcal{M}_{\text{SD}} + \mathcal{M}_{\text{BR}}|^2, \tag{36}$$

where one sums over the polarization of photons and leptons, $4m_\ell^2 \le s \le m_{B_s}^2$, $t_- \le t \le t_+$ with $t_\pm = m_\ell^2 + (m_{B_s}^2 - s)[1 \pm \sqrt{1 - 4m_\ell^2/s}]/2$. The explicit formulas for double and single differential distributions we omit here because of their complexity, they are stated in Equations (32)-(38) of [101].

The form factors predicted by the CCQM model are shown in Figure 5. For $F_{TV/TA}$ form factors we present two scenarios: by including the VMD component (32) these form factors become complex and thus their norm is shown. Alternatively, they can be shown without the VMD component as real functions

$$\tilde{F}_{TV,TA} \equiv F_{TV} - e_s \tilde{F}_{TV,TA}^{s(\bar{\ell}\ell)s}. \tag{37}$$

Figure 5. Transition form factors $B_s \to \gamma$ as defined by (31) and (37).

The form factors were also compared to those determined in [104] with which they well agreed. The differential branching fractions shown as a function of dimensionless variable $\hat{s} = q^2/m_{B_s}$ are, together with the branching fraction ratio

$$r_\gamma(\hat{s}) \equiv \frac{d\mathcal{B}(B_s \to \gamma\mu^+\mu^-)/d\hat{s}}{d\mathcal{B}(B_s \to \gamma e^+ e^-)/d\hat{s}} \tag{38}$$

depicted in Figure 6.

Figure 6. Differential decay rates for $B_s \to \ell^+\ell^-\gamma$ and the ratio $\hat{r}$ (38) with long-distant contributions included (solid line) and excluded (dashed line).

The total branching fractions for the three lepton flavors are presented in Table 1.

Table 1. Branching fractions for the three lepton flavors. Values in brackets take into account long-distance contributions.
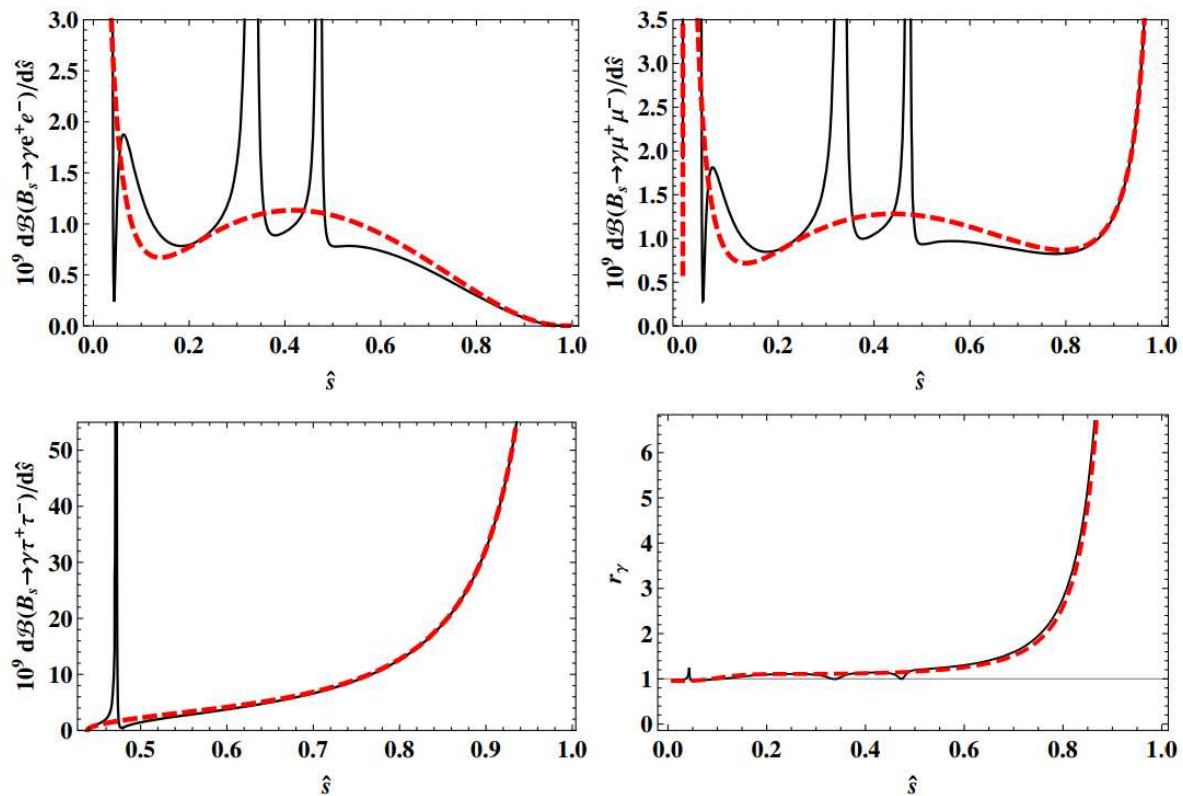
	Struct. Dep.	Bremst.	Interf.	Sum
$10^9\mathcal{B}(B_s \to \gamma e^+ e^-)$	3.05 (**15.9**)	3.2×10^{-5}	-4.8 (**-9.5**) $\times 10^{-6}$	3.05 (**15.9**)
$10^9\mathcal{B}(B_s \to \gamma \mu^+ \mu^-)$	1.16 (**10.0**)	0.53	-7.4 (**-14.4**) $\times 10^{-3}$	1.7 (**10.5**)
$10^9\mathcal{B}(B_s \to \gamma \tau^+ \tau^-)$	0.10 (**0.05**)	13.4	0.30 (**0.18**)	13.8 (**13.7**)

The numbers in brackets indicate the results of computations with long-distance contributions included (but we exclude the region of the two low lying charmonia $0.33 \leq \hat{s} \leq 0.55$), results without the long distance contributions correspond to $\kappa = 0$ in (29). The comparison with theoretical predictions of other authors is shown in Table 2.

Table 2. Comparison of branching fractions with other theoretical predictions.

	Our work	[72]	[73]	[74]	[75]	[76]	[79]	[105]	[106]
electron	15.9	6.2	2.35	-	7.1	20.0	24.6	18.4	17.4
muon	10.5	4.6	1.9	-	8.3	12.0	18.9	11.6	17.4
tau	13.7	-	-	15.2	15.7	-	11.6	-	-

We identify the dominant error source of our results to be the uncertainty of the hadronic form factors and estimate the error on the branching fractions to reach 30%. One should remark that the resonant peaks induced by light ϕ particles lead to significant enhancement of the branching fraction ($\approx$15%).

In summary, in our SM computations within the CCQM we evaluated the hadronic transition form factors and radiative leptonic branching fractions of the B_s meson. Our form factors are in a very good agreement with those presented in [104] and our branching fraction numbers for light leptons agree with [105]. For the tau lepton decay mode, where bremsstrahlung dominates, we agree with all other authors. Together, these results from various authors with us included, reflect our understanding of the SM description of the $B_s \to \ell^+\ell^-\gamma$ decay process and provide an estimate on the error of theoretical SM predictions, beyond which one can claim NP manifestations.

3.3. Other CCQM results on B leptonic decay

The CCQM was applied also to the leptonic decays $B \to \ell^-\bar{\nu}_\ell$ [107] and $B_c^- \to \tau\bar{\nu}$ [108].

The work [107] provides a SM analysis of pure leptonic and semileptonic decays. Most of the results presented there concern the semileptonic processes, which have richer structure and significant hints for the NP. Yet the results for purely leptonic branching fractions were presented too

$$
\begin{array}{c|ccc}
 & \ell & e & \mu & \tau \\
\mathcal{B}(B^- \to \ell^-\bar{\nu}_\ell) & 1.16 \times 10^{-11} & 0.49 \times 10^{-6} & 1.10 \times 10^{-4}
\end{array} \;.
$$

The numbers are in good agreement with the experimental values for the tau lepton $(1.090 \pm 0.24) \times 10^{-4}$ [23] and the muon $(0.53 \pm 0.22) \times 10^{-9}$ [61], which became more precisely measured since then, and also with the experimental limit for the electron. The agreement with several theoretical prediction of other authors was shown too. Since the leptonic decay constants are crucial in the description of purely leptonic decays and carry all of the necessary non-perturbavite information, their values have also been listed for $B_{(s,c)}^{(*)}$ and $D_{(s)}^{(*)}$ mesons, see Table I of [107] .

In [108] possible NP contributions were evaluated for chosen leptonic and semileptonic decays. It was assumed that these contributions affect only the third generation of leptons and all neutrinos were considered as left-handed. New, beyond-SM four-fermion operators were introduced in the Hamiltonian (1)

$$
Q_{V_i} = (\bar{q}\gamma^\mu P_i b)(\bar{\tau}\gamma_\mu P_L \nu_\tau), \quad Q_{S_i} = (\bar{q}P_i b)(\bar{\tau}P_L \nu_\tau), \quad Q_{T_L} = (\bar{q}\sigma^{\mu\nu}P_L b)(\bar{\tau}\sigma_{\mu\nu}P_L \nu_\tau) \tag{39}
$$

with $\sigma_{\mu\nu} = i[\gamma_\mu, \gamma_\nu]$, $P_{L,R} = (1 \mp \gamma_5)/2$ and $i \in \{L, R\}$ (left, right). The most of the text deals with semileptonic decays where the $R_{D^{(*)}}$ discrepancy is observed (41). The set of observables was extended to

$$
R_{\pi(\rho)} = \frac{\mathcal{B}(\bar{B}^0 \to \pi(\rho)\tau\bar{\nu})}{\mathcal{B}(\bar{B}^0 \to \pi(\rho)\mu\bar{\nu})}, \quad R_\tau^u = \frac{\tau_{\bar{B}^0}}{\tau_{\bar{B}^-}} \frac{\mathcal{B}(\bar{B}^- \to \tau\bar{\nu})}{\mathcal{B}(\bar{B}^0 \to \pi\mu\bar{\nu})}, \quad R_\tau^c = \frac{\tau_{\bar{B}^0}}{\tau_{B_c^-}} \frac{\mathcal{B}(\bar{B}_c^- \to \tau\bar{\nu})}{\mathcal{B}(\bar{B}^0 \to D\mu\bar{\nu})}, \tag{40}
$$

of which the first is meant to analyze the R anomaly also for the $b \to u$ transition and the two remaining concern the leptonic decays. The limits on the Wilson coefficients C_{V_i, S_i, T_l} were extracted assuming that only one of them is dominant at a time (besides the SM ones). Including into the analysis also the leptonic observable R_τ^u (together with $R_{D^{(*)}}$) it was found that no C_{S_R, S_L} values were allowed (within 2 σ) and for C_{V_L, V_R, T_L} allowed regions were identified in the complex plane (Figure 1 of [108]). Further, the leptonic $\bar{B}_c^-$ branching fractions were evaluated within the SM, $\mathcal{B}(\bar{B}_c^- \to \tau\bar{\nu}) = 2.85 \times 10^{-2}$, $\mathcal{B}(\bar{B}_c^- \to \mu\bar{\nu}) = 1.18 \times 10^{-4}$ and observables (40) were predicted for the SM and NP scenarios. In the latter case the corresponding Wilson coefficient C_i was varied (one at a time) in the allowed region of the complex plain and the impact on the observable was determined. For the leptonic R_τ^c variable the prediction stands

$$
\begin{array}{c|cccc}
 & SM & C_{V_L} & C_{V_R} & C_{T_L} \\
R_\tau^c = & 3.03 & 3.945 \pm 0.735 & 3.925 \pm 0.815 & 3.03.
\end{array}
$$

As summary one can say that, within the given scenario, the text translated existing experimental information into the constraints on NP Wilson coefficients. Contributions of some of them (C_{S_R, S_L}) were excluded and some (C_{V_L, V_R, T_L}) were constrained.

4. Semileptonic decays of B mesons

4.1. Overview

The experimental information on the semileptonic B decays is much larger than on the pure leptonic decays. The LHCb experiment alone published in the past 10 years more than 35 papers on this topic and the number further increases if other experiments (Belle, BaBar, Belle II) are taken into the account. The same is true for theoretical publications which are large in quantity. With the aim to provide an overview of the CCQM results, we restrain ourselves only to most significant experimental measurements and theoretical predictions of other authors.

The focus of the community is predominantly driven by the so-called flavor anomalies. They are often defined as ratios of branching fractions, the most prominent of them are

$$R_{K^{(*)}} = \frac{\mathcal{B}(B \to K^{(*)}\mu^+\mu^-)}{\mathcal{B}(B \to K^{(*)}e^+e^-)}, \quad R_{D^{(*)}} = \frac{\mathcal{B}(B \to D^{(*)}\tau\nu_\tau)}{\mathcal{B}(B \to D^{(*)}\ell\nu_\ell)}, \quad R_{J/\Psi} = \frac{\mathcal{B}(B \to J/\Psi\tau\nu_\tau)}{\mathcal{B}(B \to J/\Psi\mu\nu_\mu)}. \quad (41)$$

The first observable is sensitive to the $b \to s$ quark transition, the two remaining to $b \to c$. Other quantities measured in semileptonic decays of the B meson are listed for example in Section VII of [109]. In these and other observables deviations were seen (see e.g. Tab XVIII of [110] for a nice review) with some of them reaching up to 4σ, which is naturally interpreted as significant argument in favor of the NP (see e.g. [111]). The most recent LHCb measurements nevertheless weaken some of these observations and imply that the discrepancy with the SM may not be so pronounced after all. In [112] the deviation of a correlated observables R_D and R_{D^*} from the SM prediction is 1.9σ and the results for R_K and R_{K^*} given in [113] are in agreement with the SM. However, if one includes also older measurements and measurements of different experiments, the situation seem not to be yet solved and discrepancy is still close to 3σ [114].

The LHCb detector was specifically designed for b physics and the experiment successfully reaches its purpose by being the most important source of the experimental information on b decays. The measurements of $B \to K^*\ell^+\ell^-$ were presented in works [115–123]. Two of them [120,123] study the lepton-flavor universality by measuring R_{K^*}, but with no significant deviations from the SM. Most of the remaining works are concerned with angular distributions: the coefficients (noted for a p-wave process as F_L, A_{FB}, $S_{3,...,9}$) in front of angular terms which appear in the decay width formula are combined into so-called optimized observables $P_i^{(')}$, and here some significant tensions are seen (e.g. 3σ in P_2 for q^2 between 6 and 8 GeV^2 [122]).

The semileptonic B decays with the K meson in the final state are addressed in [124–126]. The first publication is concerned with the angular distribution and the differential branching fraction, the two others focus more specifically on the lepton flavor universality question, with an observation of a 2.5σ deviation from the SM in R_K. This was however, as mentioned earlier, undermined by the recent measurement [113] where no longer the deviation is seen.

The process $B \to D^*\ell^+\ell^-$ was analyzed in [112,127–129] and no deviation of R_{D^*} from the SM greater than 2σ was detected. The same is true for the $R_{J/\Psi}$ observable measured in [130]. The decay of the B_s^0 particle to $\phi\mu^+\mu^-$ was studied in [131–133], where, in the last analysis, a disagreement with the SM prediction is observed in the differential branching fraction for $1\text{GeV}^2 \le q^2 \le 6\text{GeV}^2$ at the level of 3.6σ.

Various other semileptonic B decays were measured at the LHCb which we do not mention here. An overview of the lepton flavor universality question in b decays at the LHCb was, as of 2022, given in [134].

An additional experimental information on the semileptonic B decays comes from BaBar measurements. Studies of the $B \to D^{(*)}\ell\nu_\ell$ process were presented in [135–141]. In the first three

references the question of the lepton flavor universality is addressed ($\ell = \tau$) and the measurement of R_D and R_{D^*} performed. The authors claim a deviation of 2.0σ for R_D, 2.7σ for R_{D^*} and 3.4σ for their combination. The four latter references present the measurement of the $|V_{cb}|$ element of the CKM matrix and the analysis of corresponding transition form factors.

The decays with the $K^{(*)}\ell^+\ell^-$ final state were addressed in [142–147]. The texts present the measurements of branching fractions, the $R_{K^{(*)}}$ observable, the isospin and CP asymmetries, the forward-backward angular asymmetry of the lepton pair and the K^* longitudinal polarization (and others). Overall, the results are in an agreement with the SM expectations, the anomaly observed for isospin asymmetries in both K and K^* channels in [144] was not later confirmed in [145].

The BaBar collaboration also published results on semileptonic B decays into light mesons π and ρ [148,149]. Here the branching fractions and the $|V_{ub}|$ element were determined and also transition form factors were discussed.

Further, BaBar published results on semileptonic decays where hadronic state X_s containing kaons was produced and measured corresponding branching fractions [150,151]. One can also mention the measurement of charmless semileptonic decays [152,153] and the measurement with the electron in the final state [154], all of which were used to establish the $|V_{ub}|$ value. In [155] the semileptonic decay with five particles in the final state $D^{(*)}\pi^+\pi^-\ell\nu_\ell$, was confirmed.

Important contribution to measurements of semileptonic B decays comes form the Belle and Belle II collaborations.

Analyses [156–160] investigate both D and D^* decay channels (with τ and ν_τ). They measure branching fractions and ratios $R_{D^{(*)}}$, where they do not see significant deviations from the SM expectations. The last work focuses also on the extraction of parameters for the Caprini-Lellouch-Neubert form factor parameterization.

Specifically D^*-containing final states are addressed in [161–166]. Also here the objects of interest are the branching fractions and the R_{D^*} observable and, again, no significant deviations from the SM are seen. Works [162,166] present, in addition, the measurement of the $|V_{cb}|$ matrix element and form factor analysis, in works [164,165] the τ lepton polarization is measured.

The references [167,168] focus on the $D\ell\nu_\ell$ final state. The first work is concerned with the branching fraction and form factors, in both works $|V_{cb}|$ is measured. Authors of [169] report on the first observation of $B \to \bar{D}_1\ell\nu_\ell$ decay and measure the branching fractions of $B \to \bar{D}^{(*)}\pi\ell^+\nu_\ell$ and $B \to \bar{D}^{(*)}\pi^+\pi^-\ell^+\nu_\ell$ processes.

Production of strange mesons in semileptonic B decays is studied in [170,171] for the K meson, in [172–174] for the K^* meson and in [175] for both, K and K^*. Besides branching fractions and $R_{K^{(*)}}$ ratios, some of the works present also measurements of angular and polarization variables and the isospin asymmetry. In general all measured values agree well with the SM predictions, some tensions for the subset of the optimized angular observables P_i were reported in [173].

Semileptonic decays to light mesons (π, ρ and η) were described in [176–179], the works are mostly concerned with the branching fractions and the determination of the $|V_{ub}|$ element of the CKM matrix.

The Belle(II) collaboration also published articles on semileptonic B decays to a general hadronic state X containing the s quark, X_s [180,181], the u quark, X_u [182–184] and the c quark, X_c [185,186]. The main objects of interest were branching fractions, CKM elements $|V_{ub}|$ and $|V_{cb}|$ and first four moments of the lepton mass squared (for X_c). The question of the lepton flavor universality in semileptonic decays to a general hadronic state X was addressed in [187].

Other results from different experiments could be cited in the domain of semileptonic B decays, yet the measurements of the above-mentioned B-factories represent the most important data from both, the quantity and quality perspective.

The large number of theoretical works implies strong selection criteria which we base on the impact of the work with some preference for review and pedagogical texts. We have already mentioned nice reviews [26,27,29,64,110] which cover (also) the semileptonic B decays. Further survey papers are [188], where the SM theory and appropriate observables are presented, a pedagogically-written article [189], which focuses on the charged lepton flavour violation and also a generally-oriented texts [190,191]. One can in addition mention [192], in which B flavor anomalies are discussed and also similarly oriented recent text [193].

Reliable SM predictions are the starting point for assessing various anomalies. Already decades ago a quark potential model was used to make predictions for semileptonic B and D decays [194] with an update several years later [195]. Decays to $D^{(*)}$ mesons were addressed in [196], the analyticity and dispersion relations were used to produce parametrizations of the QCD form factors with small model dependence. The same authors later published QCD two-loop level computations [197] including lepton mass effect, higher resonances and heavy quark symmetry, which further improved the theoretical precision. The heavy quark spin symmetry was used in [198] to derive dispersive constraints on $B \to D^{(*)}$ form factors and implications for the determination of $|V_{cb}|$. Semileptonic decays to light mesons ρ, ω, K^* and ϕ were discussed in [199] in the framework of light-cone sum rules, the authors claim 10% precision at zero momentum transfer. The angular analysis of the process $\bar{B} \to \bar{K} \ell^+ \ell^-$ was presented in [200]. The work is based on the QCD factorization and large recoil symmetry relations and besides angular coefficients it also gives a prediction of R_K and explores the potential of the introduced observables to reach the NP. Taking into the consideration also the excited state K^*, the publication [201] is dedicated to the charm-loop effect. The results are derived using QCD light-cone sum rules and hadronic dispersion relations and the evaluated charm loop effect, which is claimed to reach up to 20% , is represented as a contribution to the C_9 Wilson coefficient. Lattice QCD was used in [202–204] to predict form factors and matrix elements for processes with $D^{(*)}$ mesons. In [205] were the lattice form factors used as input and allowed to determine CKM matrix elements, or, alternatively, constrain the real part of the Wilson coefficients C_9 and C_{10}. The CKM matrix was also the subject of the work [206], where $|V_{cb}|$ was extracted using the OPE, the expansion in powers of the heavy quark mass and constraints derived from the experimental values on the normalized lepton energy moments. A process with a vector meson particle production $B \to V \ell^+ \ell^-$ was considered in [207] where the authors used light-cone sum rules to predict form factors. The paper [208] has a somewhat review character, it present three common form factor parameterizations, summarizes the data and the available lattice information (as of 2016) and gives a special emphasis on the unitarity constraints. Then it presents fits to experimental points and to the lattice numbers from which the results on R_D and $|V_{cb}|$ are extracted. Radiative corrections to the $R_{K^{(*)}}$ observables are of a concern to the authors of [209], their thorough analysis indicates that these observables are indeed well suited to be a probe of NP. Similar questions related to the same observables are addressed in [210]. Still the same observables are, together with the angular observables P_i, discussed in a pedagogical way in [211] with special emphasis on the hadronic uncertainties. Coming back to D particles and works published within few years after the first measurements indicating a possible lepton-flavor violation, one can mention [212], where the coefficients of the Boyd-Grinstein-Lebed form factor parametrization were constrained by analyzing the form factor ratios and their uncertainties in the heavy quark limit. With this knowledge fits to experimental data were performed and R_{D^*} computed. In [213] two different form factors parameterizations are used to predict R_{D^*} and $|V_{cb}|$. The approach uses, besides data, inputs from the light cone sum rules and lattice and the relations between form factors as given by HQET. To mention more recent theoretical works, one can point to e.g. [214,215], where QED corrections and non-local matrix elements are discussed for B decays to dilepton and a kaon. The status of the $b \to c \tau \nu$ anomalies as of 2022 is summarized in [216], where the models for global fits are based mostly on the HQET and lattice results. The latter are also reviewed the Section 8 of [18].

The number of NP papers progressively grew as the evidence for tensions and anomalies became more and more convincing, with the first hints appearing at the beginning of the new millennium.

Often, the NP is theoretically addressed by non-SM operators appearing in the effective Hamiltonian. So was done in [217], where the approach was applied to the $b \to s$ process. No strong claims were given there, but it was shown that the evaluated NP effects can reach up to 13% for R_{K^*}. The same effective-operator approach was applied in [218] to $b \to c$ transition and the impact of the NP to $B \to D^* \tau \bar{\nu}_\tau$ observables was evaluated. The authors demonstrated that it is significant, i.e. the sensitivity of the process is high enough for the NP to be detected. Effective operators were used also in [219], where, after the NP operator contributions were discussed, two leptoquark models were proposed to explain two out of three possible scenarios which lead to the observed R_K value. Leptoquarks (vector and scalar, respectively) are also considered in [220,221], both works claim that their theory allows to simultaneously resolve discrepancies appearing in $b \to s$ and $b \to c$ transitions. Still leptoquarks, the authors of [222] investigate single leptoquark extensions of the SM with $1 \, \text{TeV} \lesssim m_{LQ} \lesssim 2 \, \text{TeV}$ with conclusion that no such scalar leptoquark can be, a vector particle is the only option. The work [223] uses scenarios with light right-handed neutrinos appearing in low-scale seesaw models as the NP framework for analyzing the lepton flavor violation. Among other results the authors propose observables, i.e. properly chosen branching fraction ratios, which could discriminate between supersymmetric (SUSY) and non-SUSY NP realizations. Further works which analyze the R_K and R_{K^*} anomalies are [224] and [225], the former assumes a composite Higgs model, the latter uses a two-Higgs-doublet model. At last, let us mention a set of more generally-oriented works [91,92,226–229] which focus mainly on $b \to s \ell^+ \ell^-$ and which aim to provide model-independent or theoretically clean conclusions. By different approaches they investigate the space for NP parameters and most of them presents arguments in favor of some NP scenario.

4.2. Semileptonic and radiative decays $B_s \to \phi \ell^+ \ell^- \gamma$ and $B_s \to \phi \gamma$ in CCQM

The $B_s \to \phi \ell^+ \ell^- \gamma$ and $B_s \to \phi \gamma$ decays were within the CCQM analyzed in [230]. The analysis was done in the light of the LHCb measurements [131,132], where the second one was recent at that time. The measurement focused on angular observabes and the branching fraction distribution and reported on a deviation from the SM in the latter exceeding 3σ for $1 \, \text{GeV}^2 \leq q^2 \leq 6 \, \text{GeV}^2$. Several years later two new measurements were performed. The work [231] addressed the angular distribution where no significant tensions with the SM were observed, [133] however confirmed the discrepancy from the previous branching fraction measurement. One may put this observation in relation with R_K and R_{K^*} anomalies, which also happen for the $b \to s$ transition, from where the motivation to study this process in more details.

In [230] we analyze both, the angular coefficients and the differential decay rate distribution. In addition to (5), the necessary model inputs are

$$\Lambda_{B_s} = 2.05 \, \text{GeV} \quad \text{and} \quad \Lambda_\phi = 0.88 \, \text{GeV} \tag{42}$$

determined in prior works. The transition is expressed through two matrix elements

$$M_1^\mu = < \phi(p_2, \epsilon) | \bar{s} O^\mu b | B_s(p_1)) >, \quad M_2^\mu = < \phi(p_2, \epsilon) | \bar{s} [\sigma^{\mu\nu} q_\nu (1 + \gamma^5)] b | B_s(p_1)) >, \tag{43}$$

where $O^\mu = \gamma^\mu (1 - \gamma^5)$ and p_i are momenta with $q = p_1 - p_2$ and $P = p_1 + p_2$. The appearing variables satisfy $p_1^2 = m_{B_s}^2 \equiv m_1^2$, $p_2^2 = m_\phi^2 \equiv m_2^2$ and $\epsilon_2^\dagger \cdot p_2 = 0$. In total seven invariant form factors, defined as coefficient functions in front of the Lorentz structures, are necessary to parameterize them

$$M_1^\mu = \frac{\epsilon_\nu^\dagger}{m_1 + m_2} \left[-g^{\mu\nu} P \cdot q A_0(q^2) + P^\mu P^\nu A_+(q^2) + q^\mu P^\nu A_-(q^2) + i\varepsilon^{\mu\nu\alpha\beta} P_\alpha q_\beta V(q^2) \right], \tag{44}$$

$$M_2^\mu = \epsilon_\nu^\dagger \left[-\left(g^{\mu\nu} - \frac{q^\mu q^\nu}{q^2} \right) P \cdot q \, a_0(q^2) + \left(P^\mu P^\nu - q^\mu P^\nu \frac{P \cdot q}{q^2} \right) a_+(q^2) + i\varepsilon^{\mu\nu\alpha\beta} P_\alpha q_\beta \, g(q^2) \right]. \tag{45}$$

The same amplitudes can be expressed in the CCQM

$$M^{\mu}_{1,2} = N_c g_{B_s} g_{\phi} \int \frac{d^4 k}{i(2\pi)^4} \tilde{\Phi}_{B_s}(-[k + w_{13}p_1]^2) \tilde{\Phi}_{\phi}(-[k + w_{23}p_2]^2) \times T_{1,2}, \tag{46}$$

$$T_1 = \text{tr}[O^{\mu} S_b(k_1 + p_1)\gamma^5 S_s(k)\not{\epsilon}_2^{\dagger} S_s(k + p_2)], \tag{47}$$

$$T_2 = \text{tr}[\sigma^{\mu\nu} q_{\nu}(1 + \gamma^5) S_b(k_1 + p_1)\gamma^5 S_s(k)\not{\epsilon}_2^{\dagger} S_s(k + p_2)], \tag{48}$$

with S_i being quark propagators and N_c the number of colors. The origin of various terms in (46)-(48) is schematically represented in Figure 7. Once the model expression (46) is evaluated to the level of invariant Lorentz structures, it can be compared to (44) and (45) and form factor expressions read out. Their behavior is shown in Figure 8, it determines the necessary model input and completes the model-dependent part of the calculation.
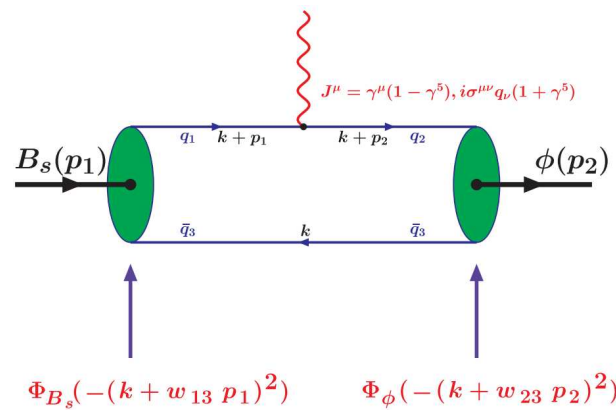

Figure 7. $B_s \to \phi$ transition in the CCQM.

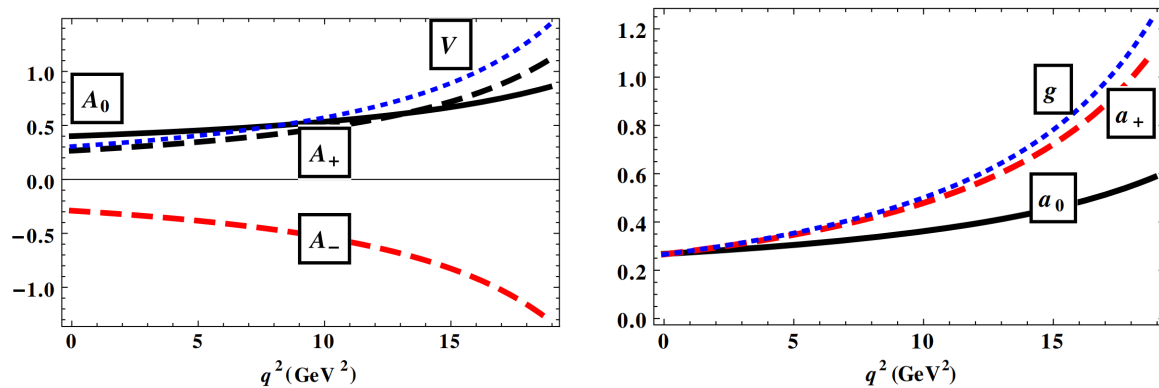**Figure 8.** Vector and tensor form factors for the $B_s \to \phi$ transition as predicted by the CCQM.

Let us briefly review also the remaining steps to reach observable quantities. The set of the SM four-fermion operators is written as

$$
\begin{aligned}
\mathcal{O}_1 &= (\bar{s}_{a_1}\gamma^\mu P_L c_{a_2})(\bar{c}_{a_2}\gamma_\mu P_L b_{a_1}), & \mathcal{O}_2 &= (\bar{s}\gamma^\mu P_L c)(\bar{c}\gamma_\mu P_L b), \\
\mathcal{O}_3 &= (\bar{s}\gamma^\mu P_L b)\sum_q(\bar{q}\gamma_\mu P_L q), & \mathcal{O}_4 &= (\bar{s}_{a_1}\gamma^\mu P_L b_{a_2})\sum_q(\bar{q}_{a_2}\gamma_\mu P_L q_{a_1}), \\
\mathcal{O}_5 &= (\bar{s}\gamma^\mu P_L b)\sum_q(\bar{q}\gamma_\mu P_R q), & \mathcal{O}_6 &= (\bar{s}_{a_1}\gamma^\mu P_L b_{a_2})\sum_q(\bar{q}_{a_2}\gamma_\mu P_R q_{a_1}), \\
\mathcal{O}_7 &= \frac{e}{8\pi^2}\tilde{m}_b(\bar{s}\sigma^{\mu\nu}P_R b)F_{\mu\nu}, & \mathcal{O}_8 &= \frac{g_s}{8\pi^2}\tilde{m}_b(\bar{s}_{a_1}\sigma^{\mu\nu}P_R \mathbf{T}_{a_1 a_2}b_{a_2})\mathbf{G}_{\mu\nu}, \\
\mathcal{O}_9 &= \frac{e^2}{8\pi^2}(\bar{s}\gamma^\mu P_L b)(\bar{\ell}\gamma_\mu\ell), & \mathcal{O}_{10} &= \frac{e^2}{8\pi^2}(\bar{s}\gamma^\mu P_L b)(\bar{\ell}\gamma_\mu\gamma_5\ell),
\end{aligned}
\tag{49}
$$

where $P_{L,R} = (1 \mp \gamma^5)$, a_i are color indices (implicit for color singlet currents), $\mathbf{T}_{a_1 a_2}$ are generators of the $SU(3)$ color group, $\mathbf{G}_{\mu\nu}$ is the gluonic field strength and g_s is the QCD coupling (other symbols have meaning as defined before). Operators $\mathcal{O}_1$ and $\mathcal{O}_2$ are referred to as current-current operators, $\mathcal{O}_3 - \mathcal{O}_6$ are QCD penguin operators, $\mathcal{O}_{7,8}$ are so-called magnetic penguin operators and $\mathcal{O}_8$ and $\mathcal{O}_9$ operators correspond to semileptonic electroweak penguin diagrams. The transition amplitude takes the form

$$
\mathcal{M} = \frac{G_F}{2\sqrt{2}}\frac{\alpha|V_{tb}V_{ts}^*|}{\pi}\left[C_9^{\text{eff}}\langle\phi|\bar{s}\gamma^\mu P_L b|B_s\rangle(\bar{\ell}\gamma_\mu\ell) - \frac{2\tilde{m}_b}{q^2}C_7^{\text{eff}}\langle\phi|\bar{s}i\sigma^{\mu\nu}q_\nu P_R b|B_s\rangle(\bar{\ell}\gamma_\mu\ell) \right.
$$
$$
\left. + C_{10}\langle\phi|\bar{s}\gamma^\mu P_L b|B_s\rangle(\bar{\ell}\gamma_\mu\gamma_5\ell)\right].
\tag{50}
$$

The Wilson coefficients $C_1 - C_6$ are absorbed into the effective coefficients C_7^{eff} and C_9^{eff}, $C_7^{\text{eff}} = C^7 - C_5/3 - C_6$ and C_9^{eff} is defined by (28) (29), where, again, the $\bar{c}c$ resonances appear in the Breit-Wigner form and we drop them by setting $\kappa = 0$. The renormalization scale is set to $\mu = \bar{m}_{b,\text{pole}}$. Numerical values of Wilson coefficients were taken from [103], as we described it already in Section 3.2. Also the QCD quark masses are the same as in the leptonic-decay section. In addition to the charm loop contribution, we take into the consideration the two loop effects as computed in [232,233]. They modify the effective coefficients

$$
C_7^{\text{eff}} \to C_7^{\text{eff}} - \frac{\alpha_s}{4\pi}(C_1 F_1^{(7)} + C_2 F_2^{(7)}), \quad C_9^{\text{eff}} \to C_9^{\text{eff}} - \frac{\alpha_s}{4\pi}(C_1 F_1^{(9)} + C_2 F_2^{(9)}),
\tag{51}
$$

where the functions $F_{1,2}^{(7,9)}$ were made publicly available by authors of [233] as *Wolfram Mathematica* code.

The differential decay rate is then expressed as

$$
\frac{d\Gamma(B_s \to \phi\ell\ell)}{dq^2} = \frac{G_F^2}{(2\pi)^3}\left(\frac{\alpha|V_{tb}V_{ts}^*|}{2\pi}\right)^2\frac{|\mathbf{p_2}|q^2\beta_\ell}{12m_1^2}\mathcal{H}_{\text{tot}},
\tag{52}
$$

$$
\mathcal{H}_{\text{tot}} = \frac{1}{2}\left(\mathcal{H}_U^{11} + \mathcal{H}_U^{22} + \mathcal{H}_L^{11} + \mathcal{H}_L^{22}\right) + \delta_{\ell\ell}\left(\frac{\mathcal{H}_U^{11}}{2} - \mathcal{H}_U^{22} + \frac{\mathcal{H}_L^{11}}{2} - \mathcal{H}_L^{22} + \frac{3\mathcal{H}_S^{22}}{2}\right),
\tag{53}
$$

where $\delta_{\ell\ell} = 2m_\ell^2/q^2$, $\beta_\ell = \sqrt{1 - 2\delta_{\ell\ell}}$ and $|\mathbf{p_2}| = \sqrt{\lambda^{\text{Källén}}(m_1^2, m_2^2, q^2)}/(2m_1)$ is the momentum of the ϕ meson in the B_s rest frame. The objects $\mathcal{H}_X^{ii}$ represent bilinear combinations of the helicity amplitudes

$$
\mathcal{H}_U^{ii} = |H_{++}^i|^2 + |H_{--}^i|^2, \quad \mathcal{H}_L^{ii} = |H_{00}^i|^2, \quad \mathcal{H}_S^{ii} = |H_{t0}^i|^2,
\tag{54}
$$

which are related to the invariant form factors through intermediate functions $A^i_{+,-,0}$ and V^i

$$H^i_{t0} = \frac{1}{m_1 + m_2} \frac{m_1 |\mathbf{p_2}|}{m_2 \sqrt{q^2}} \{Pq(-A^i_0 + A^i_+) + q^2 A^i_-\}, \tag{55}$$

$$H^i_{\pm\pm} = \frac{1}{m_1 + m_2}(-PqA^i_0 \pm 2m_1|\mathbf{p_2}|V^i), \tag{56}$$

$$H^i_{00} = \frac{1}{m_1 + m_2} \frac{1}{2m_2\sqrt{q^2}}\{-Pq(m_1^2 - m_2^2 - q^2)A^i_0 + 4m_1^2|\mathbf{p_2}|^2 A^i_+\}, \tag{57}$$

with

$$V^1 = C_9^{\text{eff}}V + C_7^{\text{eff}}\chi g, \qquad\qquad V^2 = C_{10}V, \tag{58}$$

$$A^1_+ = C_9^{\text{eff}}A_+ + C_7^{\text{eff}}\chi a_+, \qquad\qquad A^2_\pm = C_{10}A_\pm \tag{59}$$

$$A^1_- = C_9^{\text{eff}}A_- + C_7^{\text{eff}}\chi Pq\,(a_0 - a_+)/q^2, \qquad A^1_0 = C_9^{\text{eff}}A_0 + C_7^{\text{eff}}\chi a_0, \tag{60}$$

$$A^2_0 = C_{10}A_0, \qquad\qquad \text{where} \qquad \chi = 2\tilde{m}_b(m_1 + m_2)/q^2. \tag{61}$$

The full description of the $B_s \to \phi\ell\ell$ decay requires, besides the q^2, three additional angles, see for example Eq. (2.1) in [234], where completely analogous formula is written for fully differential decay rate of $B_d \to K^*\mu^+\mu^-$. The advantage of the helicity formalism is that the angular observables, i.e. the coefficients in front of various angular terms, have simple expressions. For the longitudinal polarization fraction F_L and the forward-backward asymmetry A_{FB} they stand

$$F_L = \frac{1}{2}\beta_\ell^2 \frac{\mathcal{H}_L^{11} + \mathcal{H}_L^{22}}{\mathcal{H}_{\text{tot}}}, \qquad A_{\text{FB}} = -\frac{3}{4}\beta_\ell \frac{\mathcal{H}_P^{12}}{\mathcal{H}_{\text{tot}}}, \tag{62}$$

$$\text{where } \mathcal{H}_P^{12} = \text{Re}\left[H^1_{++}(H^2_{++})^\dagger\right] - \text{Re}\left[H^1_{--}(H^2_{--})^\dagger\right]. \tag{63}$$

The CCQM-predicted behavior of the branching fraction and of the two angular observables F_L and A_{FB} is, as function of q^2, show in Figure 9.
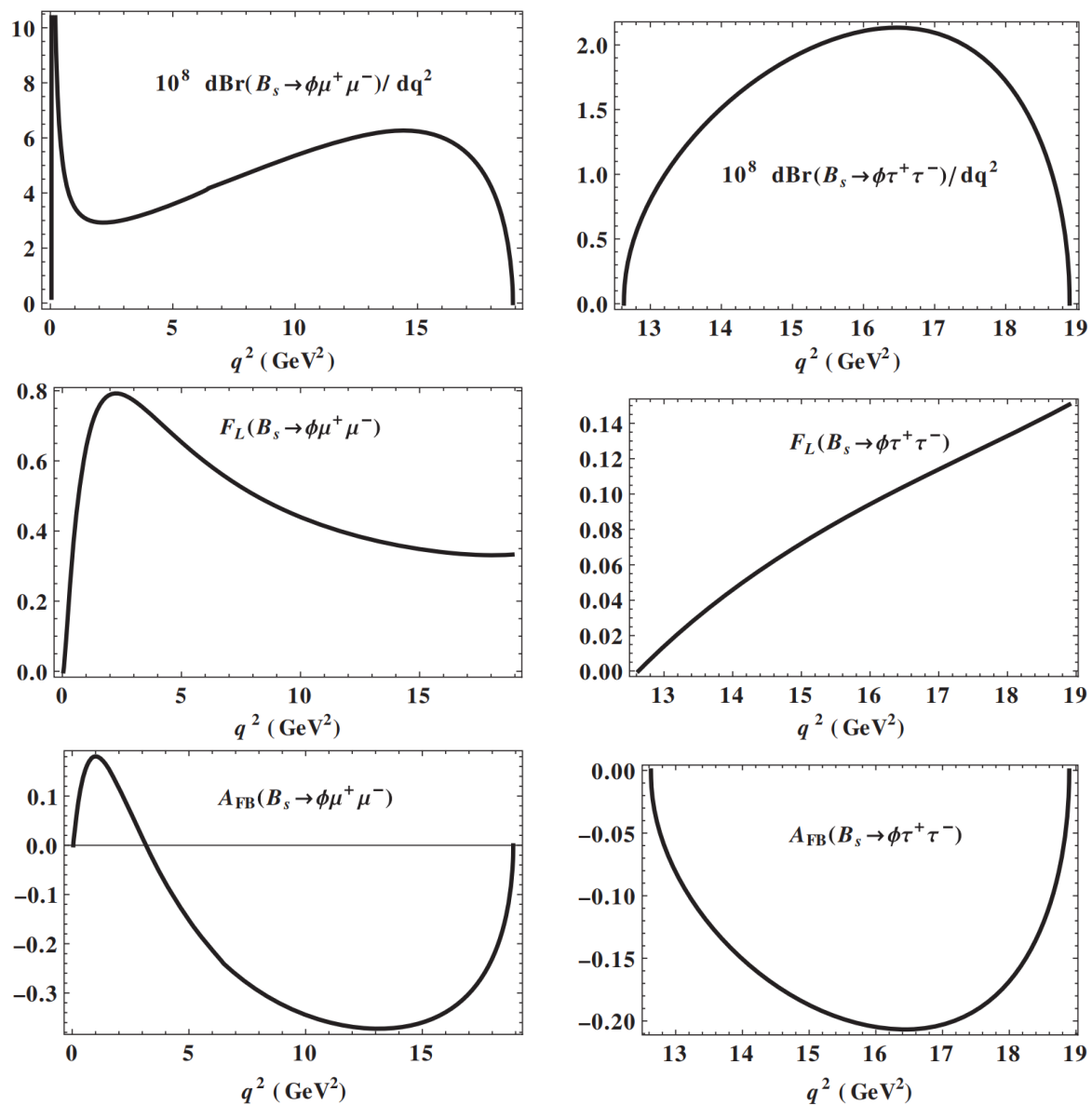
Figure 9. Branching fraction, F_L and A_{FB} as function of q^2 for μ and τ in the final state.

The q^2-averaged numbers were computed for F_L, A_{FB}, additional angular observables S_3, S_4 and also for optimized observables P_1 and P_4' which are derived from them, $P_1 = 2S_3/(1 - F_L)$, $P_4' = S_4/\sqrt{F_L(1 - F_L)}$. The results are presented in Table 3.

Table 3. Total branching fractions and averaged angular observables of selected decay channels for the whole kinematic region.

	$B_s \to \phi\mu^+\mu^-$	$B_s \to \phi\tau^+\tau^-$	$B_s \to \phi\nu\bar{\nu}$
$\mathcal{B}_{tot}$	$(9.11 \pm 1.82) \times 10^{-7}$	$(1.03 \pm 0.20) \times 10^{-7}$	$(0.84 \pm 0.16) \times 10^{-5}$
$\langle A_{FB}\rangle$	-0.24 ± 0.05	-0.18 ± 0.04	$\cdot$
$\langle F_L\rangle$	0.45 ± 0.09	0.09 ± 0.02	$\cdot$
$\langle P_1\rangle$	-0.52 ± 0.1	-0.76 ± 0.15	$\cdot$
$\langle P_4'\rangle$	1.05 ± 0.21	1.33 ± 0.27	$\cdot$
$\langle S_3\rangle$	-0.14 ± 0.03	-0.067 ± 0.013	$\cdot$
$\langle S_4\rangle$	0.26 ± 0.05	0.083 ± 0.017	$\cdot$

The table shows the branching fraction also for $B_s \to \phi \nu \bar{\nu}$, the corresponding decay formula is indicated in Equations (34)-(36) of [230]. The text [230] also contains predictions for the radiative decay to $\phi \gamma$ and non-leptonic decay to $\phi J/\Psi$ (Formulas (38) and (37) there)

$$\mathcal{B}(B_s \to \phi \gamma) = (2.39 \pm 0.48) \times 10^{-5}, \quad \mathcal{B}(B_s \to \phi J/\Psi) = (1.6 \pm 0.3) \times 10^{-3}. \tag{64}$$

The results can be compared to the actual experimental numbers [23].

$$\mathcal{B}(B_s \to \phi \mu^+ \mu^-) = (8.4 \pm 0.4) \times 10^{-7}, \quad \mathcal{B}(B_s \to \phi \nu \bar{\nu}) < 540 \times 10^{-5}, \tag{65}$$

$$\mathcal{B}(B_s \to \phi \gamma) = (3.4 \pm 0.4) \times 10^{-5}, \quad \mathcal{B}(B_s \to \phi J/\Psi) = (1.04 \pm 0.04) \times 10^{-3}. \tag{66}$$

The branching fraction to $\phi \mu^+ \mu^-$ is in good agreement with the SM, in fact the experimental numbers measured after the publication moved closer to the published CCQM value. The same is also true for the two non-leptonic decay channels, yet, here a discrepancy of the order of 2σ remains.

Coming back to the semileptonic decays, a detailed interval values were presented in Table VI of [230] for $B_s \to \phi \mu^+ \mu^-$. They mimic the way the experimental measurements are done and they are of the interest because the largest discrepancy observed by [132,133] is the branching fraction on the q^2 interval[1] $1 - 6\,\text{GeV}^2$. Also, the table presents the effect of the two-loop contributions by giving the numbers with and without them. We do not reproduce here all of them but focus only on the interval $1\,\text{GeV}^2 \le q^2 \le 6\,\text{GeV}^2$ and observables measured on this interval, see Table 4.

Table 4. Branching fraction and selected angular observables on the interval $1\,\text{GeV}^2 \le q^2 \le 6\,\text{GeV}^2$ for $B_s \to \phi \mu^+ \mu^-$. Indicated are the CCQM predictions with and without 2-loop contributions and the experimental value.

	CCQM, 2 loop	*CCQM*, 1 loop	Experiment [133,231] ([132])
$10^7 \mathcal{B}_{\text{tot.}}$	1.56 ± 0.31	1.64 ± 0.33	1.41 ± 0.11 (1.29)
F_L	0.69 ± 0.14	0.71 ± 0.14	0.715 ± 0.036 (0.63)
S_3	-0.034 ± 0.007	-0.039 ± 0.008	-0.083 ± 0.047 (-0.02)
S_4	0.17 ± 0.03	0.19 ± 0.04	0.155 ± 0.058 (0.19)
S_7	0.0065 ± 0.0013	0	0.020 ± 0.059 (-0.03)

In the table we indicate also older measurements in brackets and one sees that for all indicated observables except S_3 the new measurement bring the experimental value closer to the theoretical one. The large error of the S_3 measurement implies that both CCQM predictions (1-loop and 2-loop) do not much exceed 1σ deviation. Considering the 2-loop results one observes that no significant deviations from the experiment are observed, especially in the branching fraction case they bring the value closer to the measurement (w.r.t. one-loop calculations).

As summary we can conclude that we addressed the interesting decay channel $B_s \to \phi \ell^+ \ell^-$ in the framework of the CCQM. Already at the time of the publication the comparison with the LHCb numbers did not allow us to claim NP presence, the major discrepancy in the branching fraction on the $1 - 6\,\text{GeV}^2$ interval was reduced significantly by our prediction. This was true also for other discrepancies (F_L, S_4) seen on other intervals. The new data further decreased the branching fraction discrepancy and with results of our model we cannot talk about a discrepancy any longer.

---

[1] In [133,231] the lower interval limit is $1.1\,\text{GeV}^2$. We consider this effect as negligible because the measured quantities are intensive (not additive), e.g. the branching fraction measurement is q^2-averaged (the number of entries in the interval is divided by the integral length).

4.3. Other CCQM results on semileptonic B decays.

Quite a few papers were dedicated to the study of semileptonic *B* decays in the framework of the CCQM. We will not include into the overview older texts, where an earlier version of the model was used [235–243].

The first text we mention [37] was already cited several times here. It is a generally oriented text focusing mostly on the model itself and presenting its various aspects, including, for the first time, also the infrared confinement of quarks. A global fit on basic experimental quantities, such as weak leptonic decay constants, was performed in order to determine universal and hadron-specific model parameters. These parameters were used in the same text to predict weak leptonic decay constants (including for *B* mesons) and Dalitz dacays of several light mesons. The results were encouraging, most of predictions were in a quite good agreement with measured data.

The paper [244] is dedicated to various $B_{(s)}$ decays with, however, emphasis on the nonleptonic processes. In the first part of the text the global fits are refined and the model parameters are updated. Then, the semileptonic decays are addressed, but only in the context of the universal transition form factors to several final-state mesons (pseudoscalar and vector). The results on form factors are given in form of plots and the comparison with seven other authors based on the value at $q^2 = 0$ is shown in Table III.

Somewhat similar treatment of the semileptonic decays is given in [245]. Here again the emphasis is on exotic and nonleptonic decays. The semileptonic decays are addressed in the context of transition form factors, similarly to the previous text.

The publication [246] focuses on the semileptonic decays of $B_{(s)}$ to scalar mesons with light masses (below 1 GeV) in the context of the $B \to K^*(\to K\pi)\mu^+\mu^-$ decay. The CCQM form factors $F_\pm$ and F_T are predicted for the range $0.8\,\text{GeV} \le \Lambda_S \le 1.5\,\text{GeV}$ of scalar vector model parameters for the $b \to u$, $b \to d$ and $b \to s$ transitions. The predictions are approximated for $\Lambda_S = 0.8\,\text{GeV}$ and $\Lambda_S = 1.5\,\text{GeV}$ by a simplified parameterization which depends on three numbers. They are given in Table II of the text, so as to make our results available to other authors. Branching fractions ($\Lambda_S = 1.5\,\text{GeV}$) for various semileptonic decays $B_{(s)} \to S\ell\ell$, $B_{(s)} \to S\ell\nu_\ell$ are shown in Table IV of the work. The text then briefly discusses the role of the scalar $K_0^*(800)$ particle in the cascade decay of the *B* meson pointing out the fact that the narrow-width approximation is not appropriate and estimating the *S*-wave pollution in the $B \to K^*\ell^+\ell^-$ decay to 6%.

The leptonic and semileptonic processes $B \to \ell\bar\nu$ and $B \to D^{(*)}\ell^-\bar\nu$ are investigated in [107] to address the question of the lepton flavor universality. We have already commented before on the leptonic results, they are entirely linked to the weak decay constant which is for various *B* and *D* mesons computed in Table I. Semileptonic decay are more demanding and the usual steps are taken: the SM CCQM form factors are determined (also the simplified parameterization is provided) and are used in a helicity formulation to predict the full four-dimensional differential distribution for the decay rate and various q^2-dependent distributions for angular and polarization observables. By integration one gets total branching fractions, shown in Tables III and IV of the publication, and their ratios R_D and R_{D^*} (Table V). The results are favorable to the NP presence, the deviation in $R_{D^{(*)}}$ is not smaller than seen by other authors at that time.

An analogous process with the K^* meson in the final state is the subject of the analysis in [44]. The text follows the same logic as the previous one: the model is used to predict form factors and then the helicity formalism is employed to derive various differential distributions. Besides the branching fraction, the empasis is on the angular coefficients A_{FB}, F_L and $P_i^{(')}$, $i = 1 - 5, 8$ depicted in Figures 7–11 of the publication. The numbers are given for integrated or averaged variables over the whole kinematical range (Tables 5 and 6) but also for various intervals (i.e. bins, Tables 7,8). The predicted branching fraction exceed the measured values, for what concerns the angular observables reliable conclusions require more precise experimental data.

The article [247] analyses possible NP scenarios for $\bar B^0 \to D^{(*)}\tau^-\bar\nu_\tau$ and in this way differs from the previous ones. The analysis relies on the usual effective Hamiltonian approach where beyond-SM

four-fermion operators are introduced with the definition analogous to (39) where $q \to c$. It is assumed that the NP affects only the leptons of the third generation and the effect of each NP operator is studied separately, with no other NP operator interfering. The form factors are computed in the CCQM framework from where observables quantities are obtained. By the fit to the $R_{D^{(*)}}$ ratios, allowed regions of the complex plane for the Wilson coefficients $V_{L,R}$, S_L and T_L are identified (Figure 2 of the text). No room was found for the S_R coefficient to explain the observed ratio and thus the corresponding operator was removed from further considerations. Next, full four-fold differential distribution was derived and various q^2-differential distributions analyzed: the NP Wilson coefficient was perturbed on the 2σ level from the central value and the effect on a given distribution depicted as a gray band around the central line (Figures 4-9). Depending on what distributions will future measurements provide, the presented results can serve us to identify which NP Wilson coefficients play a role.

The same process is also considered in [248], once again in the NP scenario based on the SM-extended effective Hamiltonian. Here the main topic are the longitudinal, transverse, and normal polarization components of the tau lepton and it is argued about their high sensitivity to NP effects. Using a model independent approach and the experimental data, constraints for various NP scenarios are derived and their effect on the polarization observables is investigated. To get numerical results the CCQM form factors are used. The acquired knowledge about the dependence of polarization observables on the NP Wilson coefficients may be useful in future data analysis as a guiding rule to differentiate between various NP scenarios.

Very similar analysis is performed in [108] but for different decays. The text focuses on the processes with light mesons in the final state $\bar{B}^0 \to \pi\tau\bar{\nu}$, $\bar{B}^0 \to \rho\tau\bar{\nu}$ and on the leptonic decay $B_c \to \tau\bar{\nu}$ assuming an SM-extended set of four-fermion operators. It uses the observables (40) defined already in the leptonic section and the CCQM-predicted form factors to constrain the introduced NP Wilson coefficients. The effect of their variation on (40) and on selected angular observables is analyzed.

Yet another publication which follows the same logic is [249], focusing this time on the decays $B_c \to J/\psi\tau\nu$ and $B_c \to \eta_c\tau\nu$. The observables used to constrain the NP Wilson coefficients are R_D, R_{D^*}, $R_{J/\psi}$ and $\mathcal{B}(B_c \to \tau\nu)$. With form factors derived in the CCQM assuming the NP, the impact of variation of these coefficients on other branching fraction ratios and angular observables is evaluated. The work provides a detailed comparison of the CCQM form factors with form factors from different approaches.

The work [250] is interested in $B_c \to J/\psi\bar{\ell}\nu_\ell$ and in the hadronic decay $B_c \to J/\psi\pi(K)$. This time a SM calculation is presented, the agreement with the SM is assessed through comparison of measured and predicted values for $R_{J/\psi}$ and two additional observables

$$R_{\pi^+/\mu^+\nu} = \mathcal{B}(B_c^+ \to J/\psi\pi^+)/\mathcal{B}(B_c^+ \to J/\psi\mu^+\nu_\mu), \tag{67}$$

$$R_{K^+/\pi^+} = \mathcal{B}(B_c^+ \to J/\psi K^+)/\mathcal{B}(B_c^+ \to J/\psi\pi^+). \tag{68}$$

The form factors are evaluated in the CCQM framework and results for a set of semileptonic decays with J/ψ or η in the final state are presented (Table 2 there). The conclusion regarding the ratios is that an agreement with the SM is reached for $R_{\pi^+/\mu^+\nu}$ and R_{K^+/π^+}, but the theoretical prediction for $R_{J/\psi}$ is too low with respect to data.

The semileptonic decays $B \to K^*\mu\mu$, $B_s^0 \to \phi\mu\mu$ and the leptonic decay $B_s \to \mu^+\mu^-$ are addressed in [251]. This brief text summarizes selected results and refers to previous papers.

The next paper dedicated to semileptonic decays is [252]. It analyzes the $B \to K^{(*)}\nu\bar{\nu}$ process, where the current experimental limits on the branching fraction are expected not to be very far from the central value predicted by theory (i.e. the central value may be measured in the future). The CCQM is used to predict hadronic form factors which are then used in the helicity framework to predict branching fractions. The results agree with the experimental limits and also wit most of other authors.

Approximately, the value of limits are only four times higher than the central values predicted by the theory.

5. Nonleptonic decays of B mesons

5.1. Overview

The number of experimental measurements concerning nonleptonic (or hadronic) B decays is even larger than for semileptonic ones. Again, we briefly review the LHCb results and the results of the two B factories, BaBar and Belle(II), as the most representative. Nevertheless, we do not provide an exhaustive list but mention only works with larger impact.

The question of NP is for hadronic decays less pronounced than for the semileptonic ones, since these are theoretically less clean. Yet, the NP is often mentioned and treated together with some of the usual topics such as (exotic) multiquark states, observations of new decay channels, CP-related measurements, fragmentation fractions or branching fractions determination. In what follows we will try to observe this classification.

The LHCb published several papers reporting the observation of a specific decay channel, some being observed for the first time. This comprises the first observations of $B_s^0 \to J/\psi f_0(980)$ [253], $B_c^+ \to J/\psi D_s^+$ and $B_c^+ \to J/\psi D_s^{*+}$ [254], $B_c^+ \to B_s^0 \pi^+$ [255], $B^+ \to D_s^+ D_s^- K^+$ [256], $B_s^0 \to D^{*+} D^{*-}$ [257], $B^+ \to J/\psi \eta' K^+$ [258] or $B_s^0 \to \chi_{c1}(3872)\pi^+\pi^-$ [259]. For the most of these observations some quantitative numbers are given, usually branching fraction ratios to a different decay mode (normalization channel).

A special interest is given to the observation of "resonant structures", i.e. observation of possible exotic multiquark states which are sometimes seen in invariant mass distributions of particles originating from the B disintegration. An important contribution to the exotic physics was done in 2013 when the LHCb measured, in the B decay channel, the quantum numbers of the $X(3872)$ resonance [260], previously discovered by Belle. Contemporary texts [261–263] analyze the $\bar{B}_s^0 \to J/\psi\pi^+\pi^-$ and $\bar{B}^0 \to J/\psi\pi^+\pi^-$ spectra, and identify various resonant structures; here only the usual SM resonances are seen. The possible tetraquark character of the $f_0(980)$ invoked in the last text is rejected as inconsistent with data. The situation becomes different in [264], where four resonant structures, possibly tetraquarks, are observed and their quantum numbers are determined. The work [265] reports on two exotic particles having $c\bar{c}u\bar{s}$ quark content determined with high significance and also confirms four previously reported states. The authors of [266] perform an amplitude analysis of the $B^- \to J/\psi\Lambda\bar{p}$ process, where the $J/\psi\Lambda$ mass spectrum contains a narrow resonance, possibly a strange pentaquark; its quantum numbers are measured. A resonant structure, referred to as $X(3960)$, is also observed in the $B^+ \to D_s^+ D_s^- K^+$ decay mode close to the $D_s^+ D_s^-$ production threshold [267]. It is established to be consistent with a four-quark state $c\bar{c}s\bar{s}$ having quantum numbers $J^{PC} = 0^{++}$. The text [268] analyses the spectrum of $B^+ \to D^+ D^- K^+$ and advances a hypothesis of new charm-strange resonances. Another recent text, [269], also sees a new resonance of mass 4337 MeV in the $J/\psi p$ ($J/\psi\bar{p}$) spectrum of the $B_s^0 \to J/\psi p\bar{p}$ decay. A very recent analysis [270] is concerned with decays of the B mesons to $J/\psi\phi K_S^0$ and presents evidence for $T_{\psi s1}^\theta$ state in the $J/\psi K_S^0$ invariant spectrum, presumably a tetraquark.

Besides direct investigations of the invariant mass spectrum, many LHCb publications rely, to identify resonant components, on the Dalitz plot and amplitude analysis where further resonances are identified, see [271–277]. The hadronic B decays are also often studied in the context of the CP analysis and weak parameter determination [278–291]. Various topics are addressed in these works: observation of the CP violation in a specific decay, measurement of the CP-violating phase, $B_{(s)}^0$-$\bar{B}_{(s)}^0$ oscillations and determination of the CKM angles. The B decay measurements are also used to determine basic particle quantities, such as production cross sections, branching ratios or fragmentation fractions [292–301].

The publications of the BaBar experiment fall into similar categories. We choose to mention in more detail the CP-related results which had, in the domain of nonleptonic B decays, the most significant impact. Namely, the violation of the CP symmetry was before the BaBar measurement [302] only observed for kaons. The measurement was done for several decay modes of the B^0 particle, for each decay the CP asymmetry A_{CP} was measured. The latter was defined in terms of a decay-time distribution $f_{\pm}(\Delta t)$ for B and $\bar{B}$ decaying into the common final state. The results were derived for the $\sin(2\beta)$ quantity, where β is an angle of the unitarity triangle constructed from the CKM matrix elements and its deviation from zero measures the CP violation. The significance of the measurement reached 4σ level. The CP-violation topic was then discussed in further publications for the neutral [303–311] and also charged B meson [312–315]. Both, indirect (i.e. involving particle-antiparticle oscillations) and direct CP violation was seen with relevant significance. Several texts present measurements were the branching fraction and the CP asymmetries were addressed at the same time [316–321]. Besides the direct CP violation measurements, the closely related measurements of the CKM angles α and γ were presented in [322–325].

The BaBar collaboration also investigated, in a variety of publications [326–337], the usual quantities which characterize decays, i.e. branching fractions, angular observables and branching fractions. The related topic of resonances and exotic states were subject to numerous analysis. The resonances were investigated by invariant mass spectra or the Dalitz-plot method, as presented in [338–340]. Concerning exotic states, most of the BaBar results are related to the $X(3872)$ particle [341–349] and present related searches, observations and measurements in various decay modes. The state $Y(3940)$, first discovered at Belle, was observed also (as a product of a B decay) and its mass and width were determined.

The Belle experiment was very successful in search for various exotic states, tetraquarks and pentaquarks. Not all were related to hadronic decays of the B meson, but the most cited result [350] was. It presents the discovery of the $X(3872)$ particle seen in the $\pi^+\pi^- J/\psi$ spectrum of $B^{\pm} \to K^{\pm}\pi^+\pi^- J/\psi$. Another achievements were the detection of tetraquark candidates $Z(4430)$ [351] and $Y(3940)$ [352], both among the decay products of B. In addition to these, further publications on this topic were issued [353–362], all related to nonleptonic B decays. The physic program regarding the CP violation and the weak physics in general is also very present at Belle. The collaboration published the B^0 CP-violation paper [363] only a short time after BaBar did. Yet, it drew a lot of attention as an independent measurement of the $\sin(2\beta)$ parameter. The measurement was updated later in [364], direct CP violation was reported in [365,366]. Many additional papers were published by Belle where various CP parameters (CKM angles) and weak-physics related processes were studied [367–387].

Naturally, the research at Belle is devoted also to branching fraction measurements of different B decay modes [388–397], observation and analysis of new decay channels [398–406], polarization studies [407,408] and photon energy spectra analysis in radiative events [409,410].

The large amount of data on hadronic B decays motivates the theorists to describe observations and prove our understanding of the underlying physics to be correct. The exotic multiquark states have a specific character from the perspective of b physics: as a matter of fact many of them originate from nonleptonic B decays, yet, these decays seen as exotic production processes, are not addressed very frequently. They often have a larger number of hadrons in the final state (three or more) and thus large phase space and technically complicated description. The exotic particles are usually treated in the scenario where they represent the initial state (for the CCQM model see [43]) and thus are not in the scope of this text (are not B mesons). The emphasis of the theoretical overview is therefore on the remaining topics: branching fractions and weak-interaction physics.

The theoretical grounds to describe (not only) hadronic B decays were laid decades ago. The CP violation in the SM stems from the flavor mixing through the CKM matrix which has an irreducible complex phase, as formulated in the pioneering works [411,412]. This rapidly lead to first theoretical

predictions. In [413] the expectation of a small but measurable CP non-invariance in B meson decays was expressed. The authors of [414] argued, studying the on-shell transitions in heavy meson cascade decays, that the effect may not be so small after all and propose methods to detect the CP violation in the B sector. The latter topic is also discussed in [415], where mainly the non-leptonic decay modes are addressed.

In parallel the issues related to the asymptotic behavior and quark interactions were considered. The nice review [416] addressed the question of the power behavior of amplitudes and its relation to mesonic wave functions and quantum numbers. As results quantitative conclusions are made for hadronic form factors, large angle scattering processes and other related quantities. The highly cited paper [417] presents a relativistic extension of the quark model based on one-gluon exchange and a linear confining quark potential. It is used to describe mesons, their spectroscopy and decays, and succeeds to large extent. The work [418] studies (among others also) B decays in the framework of the valence quark model; the model assumes factorization and good results are obtained especially for nonleptonic processes. Following works further sharpen the QCD SM prediction; the next-to-leading QCD corrections are computed in [419], the implications of the heavy quark symmetry are analyzed in [420], the generalized factorization hypothesis and its impact on the structure of non-factorizable corrections are presented in [421] and three-loop anomalous dimensions at the next-to-leading order in α_s for weak radiative B decays are computed in [422]. The role of the charm penguin diagrams in the B decay to pions was evaluated by the authors of [423] and a next-to-leading order evaluation of the branching fraction and photon spectrum of the $B \to X_s + \gamma$ process was presented in [424].

Coming back to the CP symmetry, one can mention the publication [425], where large time-dependent CP asymmetries in the $B^0 - \bar{B}^0$ system are predicted or [426] where it is shown that the theoretical uncertainty associated with penguin diagrams in the $B^0 \to \pi\pi$ decay can be reduced by considering isospin relations.

An important issue addressed by various authors is the factorization validity, often assumed for hadronic matrix elements of the four-fermion operators. In [427] a theoretical investigation of B branching fractions is undertaken and branching fraction ratios of selected two-body hadronic B decays are proposed as factorization experimental tests. The article [428] is focused on the factorization for heavy-light final states. Such decays are treated in the heavy quark limit and the validity of the factorization ansatz is in this scenario proven at the two-loop order. In the similar context the authors of [429] study processes with two light mesons (K, π) in the final state. They argue that in the heavy quark limit the hadronic matrix elements of nonleptonic B meson decays can be computed from first principles which helps to reduce the errors on the weak phases α and γ. Very similarly is oriented the paper [430], where the proof of the factorization is provided for $B^- \to D^0\pi^-$ and $B^0 \to D^+\pi^-$. The topic of the factorization is further treated in [431], where decays $B \to PP$ and $B \to PV$ are addressed, and also in [432], where soft-collinear effective theory is used to prove factorization for B decaying to two light particles (π, K, ρ, K^*).

One should also mention new physics searches. The paper [433] studies the $B \to \pi\pi$ process from which it extracts relevant hadronic parameters. These are then used, under plausible assumptions, to predict $B \to \pi K$. Those observables (for the latter process) which have small EW penguin contributions seem to agree with the experiment, those with significant contributions do not. This might indicate NP in the W penguin sector. Similar ideas are developed also in [434]. A related topic, the final state interactions in hadronic B decays, is treated in [435]. Indeed, when considering the B decays to light mesons, there are, generally speaking, some difficulties to describe the data. To disentangle possible NP, all SM effects need to be considered, rescattering included. The latter is here treated in a phenomenological way in terms of off-shell meson exchange.

Let us briefly mention other works of interest: papers [199,436] apply the light-cone sum rules to tackle B decays to light vector and pseudoscalar mesons respectively, the authors of [437] compute, at next-to-next-to-leading order of QCD, the effective Hamiltonian for non-leptonic $|\Delta F| = 1$ decays, and the text [438] focuses on the B decays to two vector particles in the framework of the QCD factorization.

At last we can mention the paper [439] which summarizes the status of our CKM matrix knowledge based on a global fit to various (leptonic, semileptonic, hadronic) data.

5.2. Nonleptonic B decays in CCQM

Decay $B_s \to J/\psi \eta^{(')}$

We have chosen to demonstrate the CCQM approach on two hadronic processes to point out various aspects of the model application. The first one is $B_s \to J/\psi \eta^{(')}$ [440], were a fit to the data was performed so as to determine the model input parameters. The $\eta^{(')}$ mesons are described as a superposition of light ($q = u, d$) and strange components, $\eta = -\sin\delta(\bar{q}q) - \cos\delta(\bar{s}s)$ and $\eta' = \cos\delta(\bar{q}q) - \sin\delta(\bar{s}s)$ where $\delta = \varphi_P - \pi/2$, $\varphi_P = 41.4°$ [441]. We treat the considered decay within the naïve factorization picture in the leading order, meaning we describe it as a $B_s \to \eta^{(')}$ transition where only the $\bar{s}s$ component of the latter is taken into the account, see Figure 10.

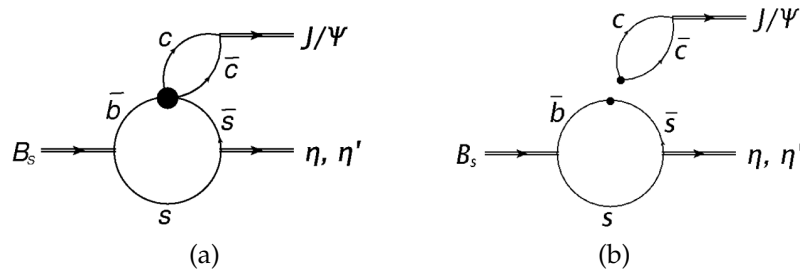(a)   (b)

Figure 10. The $B_s \to \eta^{(')} J/\psi$ decay as a B_s transition to the $\bar{s}s$ component of $\eta^{(')}$ (a) in the factorization picture (b).

The necessary inputs for the decay width formula ($P = \eta, \eta'$)

$$\Gamma(B_s \to J/\Psi + P) = \frac{G_F^2}{4\pi}|V_{cb}V_{cs}^\dagger|C_W^2 f_{J/\Psi}^2 |\mathbf{q}_P|^3 \zeta_P^2 [F_+^{B_s\eta^{(')}}(m_{J/\Psi}^2)]^2, \quad \zeta_\eta = \cos\delta, \quad \zeta_{\eta'} = \sin\delta \qquad (69)$$

are the leptonic decay constants $f_{J/\Psi} \equiv f_V$ and the transition form factor F_+

$$m_V f_V \epsilon_V^\mu = N_c g_V \int \frac{d^4k}{(2\pi)^4 i} \tilde{\Phi}(-k^2)\mathrm{tr}[O^\mu S_1(k + w_1 p)\not{\epsilon}_V S_2(k - w_2 p)], \quad p^2 = m_V^2, \qquad (70)$$

$$\langle P_{q_1,q_3}(p_2)|\bar{q}_2 O^\mu q_1|B_{\bar{q}_3,q_2}(p_1)\rangle = F_+(q^2)P^\mu + F_-(q^2)q^\mu, \qquad (71)$$

$$= N_c g_B g_P \int \frac{d^4}{(2\pi)^4 i}\tilde{\Phi}_B(-[k + w_{13}p_1]^2)\tilde{\Phi}_P(-[k + w_{23}p_2]^2)$$

$$\times \mathrm{tr}[O^\mu S_1(k + p_1)\gamma^5 S_3(k)\gamma^5 S_2(k + p_2)],$$

where the Wilson coefficient is given by $C_W = C_1 + C_2/N_c + C_3 + C_4/N_c + C_5 + C_6/N_c$ and the meaning of other symbols is analogous to Sections 3.2 and 4.2. The results are derived in the large N_c limit $N_c \to \infty$. To get to the form factor and the decay constants one needs to know the model Λ parameters $\Lambda_\eta^{\bar{q}q}$, $\Lambda_\eta^{\bar{s}s}$, $\Lambda_{\eta'}^{\bar{q}q}$ and $\Lambda_{\eta'}^{\bar{s}s}$, four in total if we treat q and s components as independent. They can be derived from various processes where they play a role, so, in addition to the two studied decay channels, we have chosen also $\eta \to \gamma\gamma$, $\eta' \to \gamma\gamma$, $\varphi \to \eta\gamma$, $\varphi \to \eta'\gamma$, $\rho^0 \to \eta\gamma$, $\omega \to \eta\gamma$, $\eta' \to \omega\gamma$,

$B_d \to J/\Psi + \eta$ and $B_d \to J/\Psi + \eta'$. Fitting all together 11 processes, the optimal-fit parameters were determined

$$\Lambda_\eta^{\bar{q}q} = 0.881\,\text{GeV}, \quad \Lambda_\eta^{\bar{s}s} = 1.973\,\text{GeV}, \quad \Lambda_{\eta'}^{\bar{q}q} = 0.257\,\text{GeV}, \quad \Lambda_{\eta'}^{\bar{s}s} = 2.797\,\text{GeV}, \tag{72}$$

other model parameters were taken from our previous works. With these in hand one computes results, see Table 5.

Table 5. Decay widths and branching fractions for various processes with η and η' mesons as predicted by the CCQM.

Observable	CCQM	Exp.[23]
$\Gamma(\eta \to \gamma\gamma)$	0.380 keV	0.515 ± 0.020 keV
$\Gamma(\eta' \to \gamma\gamma)$	3.74 keV	4.34 ± 0.14 keV
$\Gamma(\eta' \to \omega\gamma)$	9.49 keV	4.74 ± 0.15 keV
$\Gamma(\rho \to \eta\gamma)$	53.07 keV	44.22 ± 0.24 keV
$\Gamma(\omega \to \eta\gamma)$	6.21 keV	3.91 ± 0.06 keV
$\Gamma(\varphi \to \eta\gamma)$	42.59 keV	55.28 ± 0.17 keV
$\Gamma(\varphi \to \eta'\gamma)$	0.276 keV	0.26 ± 0.001 keV
$\mathcal{B}(B_d \to J/\Psi + \eta)$	16.5×10^{-6}	$(10.8 \pm 2.3) \times 10^{-6}$
$\mathcal{B}(B_d \to J/\Psi + \eta')$	12.2×10^{-6}	$(7.6 \pm 2.4) \times 10^{-6}$
$\mathcal{B}(B_s \to J/\Psi + \eta)$	4.67×10^{-4}	$(4.0 \pm 0.7) \times 10^{-4}$
$\mathcal{B}(B_s \to J/\Psi + \eta')$	4.04×10^{-4}	$(3.3 \pm 0.4) \times 10^{-4}$

Generally speaking the discrepancies in terms of standard deviations are rather large, yet the model roughly (within the factor 2) reproduces the data. There might be reasons to the differences one needs to understand, e.g. a gluoniun contribution to the η' state [441] could weaken the largest disagreement for $\Gamma(\eta' \to \omega\gamma)$. As pointed out in [440], other models on the market do not seem to perform better than us.

The Belle and LHCb collaborations also measured the ratio

$$R = \frac{\mathcal{B}(B_s \to J/\Psi + \eta')}{\mathcal{B}(B_s \to J/\Psi + \eta)} = \begin{cases} 0.73 \pm 0.14, & \text{Belle [442]} \\ 0.90 \pm 0.1, & \text{LHCb [443]}\,. \\ 0.86, & \text{CCQM} \end{cases} \tag{73}$$

Here the CCQM number reproduces well the measurements and through the predicted form factors adds a non-trivial factor 0.83 to the model-independent part of the calculation

$$R^{\text{theor}} = \left(\frac{|\mathbf{q}_{\eta'}|^3}{|\mathbf{q}_\eta|^3} \tan^2(\delta) \right) \times \left(\frac{F_+^{B_s\eta'}}{F_+^{B_s\eta}} \right)^2 = 1.04... \times 0.83... \approx 0.86. \tag{74}$$

The overall precision of results is not fully satisfactory and further efforts may be done to investigate the discrepancies. Yet, besides the results themselves we wanted, in this subsection, also to point to the methodology we adopt in the CCQM for determining the model inputs.

Decay $B \to D_{(s)}^{(*)} h$, $(h = \pi, \rho)$

The second process we want to review is the B_d decay to a D meson and a light particle [444]. The interest here comes form the observation confirmed by other authors too, that the predictions systematically overshoot the data, which might indicate the NP.

We describe the processes in the leading order and naïve factorization framework. These decays correspond to rich set of various spin states and diagram topologies, as is summarized in Figure 11 and

Table 6. We label by $D_{1,2,3}$ the diagram structure (color favored, color suppressed and their interference), where within each group, various spin configurations are present (labeled $A, \ldots, D$).
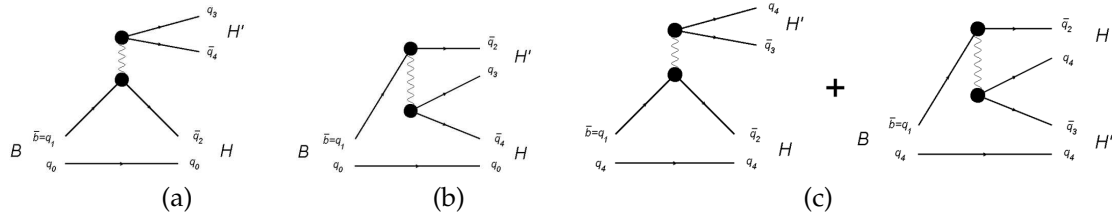

Figure 11. B decays to two hadrons: color favored D_1 (a), color suppressed D_2 (b) and their interference D_3 (c).

Table 6. Studied decays arranged with respect to the spin structure and diagram topology. Underlined parts correspond to the transition of the spectator quark (in case of D_3 to the first diagram of Figure 11(c).

Spin structure	D_1 diagram	D_2 diagram	D_3 diagram
(A)	$\underline{B^0} \to D^- + \pi^+$	$\underline{B^0} \to \pi^0 + \bar{D}^0$	$\underline{B^+} \to \bar{D}^0 + \pi^+$
$\underline{PS} \to PS + PS$	$\underline{B^0} \to \pi^- + D^+$		
	$\underline{B^0} \to \pi^- + D_s^+$		
	$\underline{B^+} \to \pi^0 + D_s^+$		
(B)	$\underline{B^0} \to D^- + \rho^+$	$\underline{B^0} \to \pi^0 + \bar{D}^{*0}$	$\underline{B^+} \to \bar{D}^0 + \rho^+$
$\underline{PS} \to PS + V$	$\underline{B^0} \to \pi^- + D_s^{*+}$		
	$\underline{B^+} \to \pi^0 + D^{*+}$		
	$\underline{B^+} \to \pi^0 + D_s^{*+}$		
(C)	$\underline{B^0} \to D^{*-} + \pi^+$	$\underline{B^0} \to \rho^0 + \bar{D}^0$	$\underline{B^+} \to \bar{D}^{*0} + \pi^+$
$\underline{PS} \to V + PS$	$\underline{B^0} \to \rho^- + D_s^+$		
	$\underline{B^+} \to \rho^0 + D_s^+$		
(D)	$\underline{B^0} \to D^{*-} + \rho^+$	$\underline{B^0} \to \rho^0 + \bar{D}^{*0}$	$\underline{B^+} \to \bar{D}^{*0} + \rho^+$
$\underline{PS} \to V + V$	$\underline{B^0} \to \rho^- + D_s^{*+}$		
	$\underline{B^+} \to \rho^0 + D_s^{*+}$		

Using the leading order operators

$$Q_1 = [(\bar{q}_1)_{i_1}(q_2)_{i_2}]_{V-A}[(\bar{q}_3)_{i_2}(q_4)_{i_1}]_{V-A}, \quad Q_2 = [(\bar{q}_1)_{i_1}(q_2)_{i_1}]_{V-A}[(\bar{q}_3)_{i_2}(q_4)_{i_2}]_{V-A}, \tag{75}$$

where i_j are color indices and $[q_1 q_2]_{V-A} = \bar{q}_1 \gamma^\mu (1 - \gamma^5) q_2$, one can derive form factors. They are in the case of the scalar-to-scalar transition given by (71), for the scalar-to-vector form factor the expression stands

$$\langle V_{q_3,q_2}(p_2, \epsilon) | \bar{q}_1 O^\mu q_2 | B_{q_3,q_1}(p_1) \rangle = \tag{76}$$
$$= \frac{\epsilon_\nu^\dagger}{m_B + m_V} \left[-g^{\mu\nu} P \cdot q A_0(q^2) + P^\mu P^\nu A_+(q^2) + q^\mu P^\nu A_-(q^2) + \epsilon^{\mu\nu\alpha\beta} P_\alpha q_\beta V(q^2) \right].$$

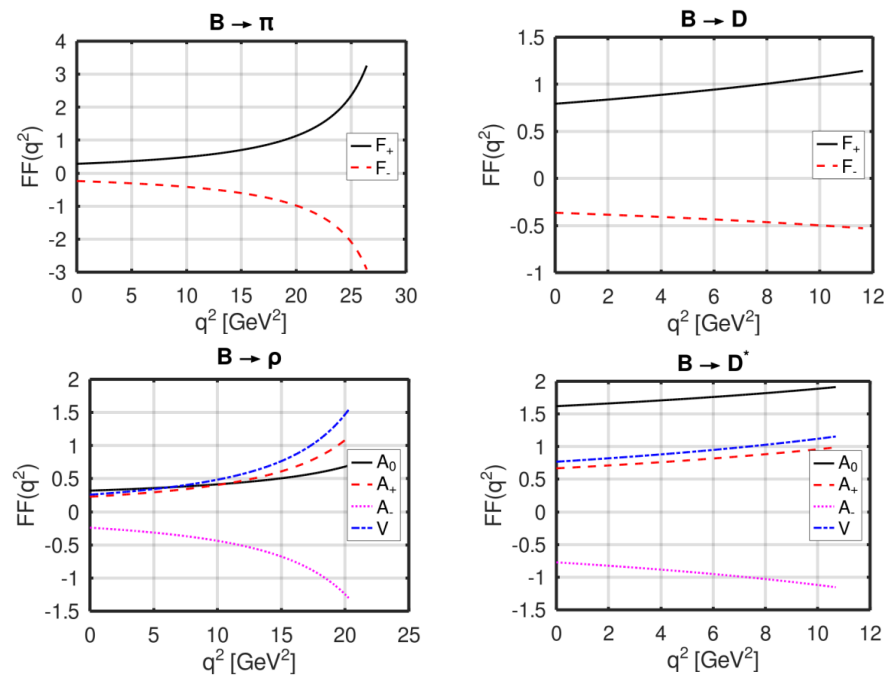The obtained form factors are shown in Figure 12.

Figure 12. Transition form factors as predicted by the CCQM.

The corresponding decay-width formulas (see [444], page 3) then allow one to get results summarized in Table 7.

Table 7. CCQM branching fractions compared to data.

	Process	Diagram	$\mathcal{B}_{\text{CCQM}}/E$	$\mathcal{B}_{\text{PDG}}/E$	E
1	$B^0 \to D^- + \pi^+$	D_1	5.34 ± 0.27	2.52 ± 0.13	10^{-3}
2	$B^0 \to \pi^- + D^+$	D_1	11.19 ± 0.56	7.4 ± 1.3	10^{-7}
3	$B^0 \to \pi^- + D_s^+$	D_1	3.48 ± 0.17	2.16 ± 0.26	10^{-5}
4	$B^+ \to \pi^0 + D_s^+$	D_1	1.88 ± 0.09	1.6 ± 0.5	10^{-5}
5	$B^0 \to D^- + \rho^+$	D_1	14.06 ± 0.70	7.6 ± 1.2	10^{-3}
6	$B^0 \to \pi^- + D_s^{*+}$	D_1	3.66 ± 0.18	2.1 ± 0.4	10^{-5}
7	$B^+ \to \pi^0 + D^{*+}$	D_1	0.804 ± 0.04	< 3.6	10^{-6}
8	$B^+ \to \pi^0 + D_s^{*+}$	D_1	0.197 ± 0.01	< 2.6	10^{-4}
9	$B^0 \to D^{*-} + \pi^+$	D_1	4.74 ± 0.24	2.74 ± 0.13	10^{-3}
10	$B^0 \to \rho^- + D_s^+$	D_1	2.76 ± 0.14	< 2.4	10^{-5}
11	$B^+ \to \rho^0 + D_s^+$	D_1	0.149 ± 0.01	< 3.0	10^{-4}
12	$B^0 \to D^{*-} + \rho^+$	D_1	14.58 ± 0.73	6.8 ± 0.9	10^{-3}
13	$B^0 \to \rho^- + D_s^{*+}$	D_1	5.09 ± 0.25	4.1 ± 1.3	10^{-5}
14	$B^+ \to \rho^0 + D_s^{*+}$	D_1	0.275 ± 0.01	< 4.0	10^{-4}
15	$B^0 \to \pi^0 + \overline{D}^0$	D_2	0.085 ± 0.00	2.63 ± 0.14	10^{-4}
16	$B^0 \to \pi^0 + \overline{D}^{*0}$	D_2	1.13 ± 0.06	2.2 ± 0.6	10^{-4}
17	$B^0 \to \rho^0 + \overline{D}^0$	D_2	0.675 ± 0.03	3.21 ± 0.21	10^{-4}
18	$B^0 \to \rho^0 + \overline{D}^{*0}$	D_2	1.50 ± 0.08	< 5.1	10^{-4}
19	$B^+ \to \overline{D}^0 + \pi^+$	D_3	3.89 ± 0.19	4.68 ± 0.13	10^{-3}
20	$B^+ \to \overline{D}^0 + \rho^+$	D_3	1.83 ± 0.09	1.34 ± 0.18	10^{-2}
21	$B^+ \to \overline{D}^{*0} + \pi^+$	D_3	7.60 ± 0.38	4.9 ± 0.17	10^{-3}
22	$B^+ \to \overline{D}^{*0} + \rho^+$	D_3	11.75 ± 0.59	9.8 ± 1.7	10^{-3}

The level of agreement between the model and the data can be visually estimated by looking at Figure 13.
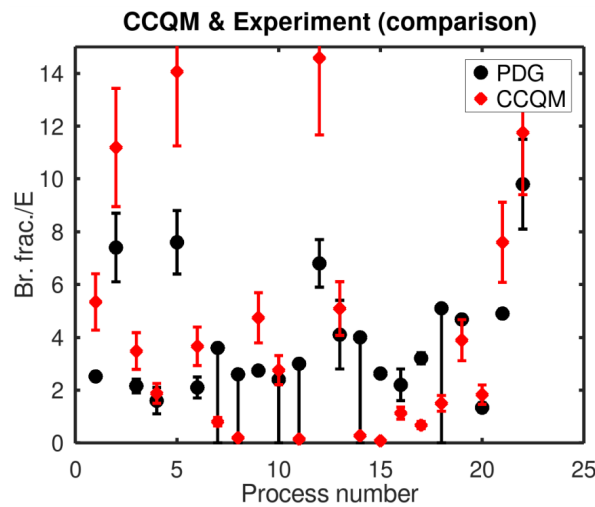

Figure 13. The comparison of CCQM predictions and data. Processes are numbered as in Table 7.

Generally speaking, the description of data is not satisfactory. The agreement within errors is reached for measurements where only limits are given and for few other cases. This might be expected for a subset of the processes since the factorization assumption is not supposed to hold in the scenario where the spectator quark enters the light meson, see [428]. Yet we see an overall overestimation including decays with the spectator quark entering the D meson. This observation joins similar observations made by other authors [36,445–447], i.e. it is seen across various approaches which naturally rises the question about the NP. The authors of [447] talk about "novel puzzle" and NP scenarios are advanced to explain it in [36,447].

5.3. Other CCQM results on nonleptonic B decays.

The CCQM was also applied to other hadronic decay processes of B mesons. Skipping older publications [243,448] with an earlier version of the model, we can mention again the generally oriented text [244] where decay width for B_s going to $D_s^- + D_s^{(*)+}$, $D_s^{*-} + D_s^{(*)+}$ and $J/\Psi + \Phi$ are computed. They are determined within the effective Hamiltonian approach using the helicity formalism from the CCQM-predicted form factors. The numbers are in fair agreement with experimental measurements. The same results are reviewed in paper [245], which, in addition, treats the exotic state $X(3872)$ as a tetraquark and evaluates its selected branching fractions.

The work [449] deals with double-heavy B_c particles and their decays to charmonia and various D mesons. Two diagrams contribute in the leading order, in one the B_c spectator quark $\bar{c}$ goes to the charmonium state, in the other it forms the D meson. One thus needs to evaluate form factors of six transitions $B_c \to D, D_s, \eta_c, D^*, D_s^*, J/\Psi$, their behavior is shown in Figure 2 of the work and their values at zero are also presented. Next, helicity amplitudes are constructed and branching fractions calculated for in total 8 processes $B_s \to \eta_c + D_{(s)}^{(*)}$ and $B_s \to J/\Psi + D_{(s)}^{(*)}$ (all combinations of brackets). Comparison with the experiment is based on branching fraction ratios $\mathcal{R}(D_s^+/\pi^+)$, $\mathcal{R}(D_s^{*+}/\pi^+)$, $\mathcal{R}(D_s^+/D_s^+)$ and also Γ_{++}/Γ measured by Atlas [450] and LHCb [254]. Here

$$\mathcal{R}(A/B) = \frac{\mathcal{B}(B_c^+ \to J/\Psi A)}{\mathcal{B}(B_c^+ \to J/\Psi B)} \tag{77}$$

and Γ_{++}/Γ is the transverse polarization fraction in the $B_c^+ \rightarrow J/\Psi + D_s^{*+}$ decay. The results are presented in the Table VIII of [449] with no significant deviations from the SM. Yet, as two different sets of Wilson coefficients were investigated, it turned out that the results are quite sensitive to their choice.

Similar processes are addressed in [250], however with π or K in the final state instead of D. Consequently only one diagram contributes which is the one corresponding to the transition to charmonium, since all other π/K production diagrams from B_c are of a higher order. Also the semileptonic mode to $J/\Psi\mu^+\nu_\mu$ is investigated so as to define observables $\mathcal{R}(\pi^+/\mu^+\nu)$, $\mathcal{R}(K^+/\pi^+)$, $\mathcal{R}(J/\Psi)$ and $\mathcal{R}(\eta_c)$, see (41), (77). With the CCQM transition form factors identical to those mentioned previously one gets in total eight decay widths $B_c^+ \rightarrow \eta_c + h$, $B_c^+ \rightarrow J/\Psi + h$, $h \in \{\pi^+, \rho^+, K^+, K^{*+}\}$ (Table 3 of the publication) and branching fraction ratios which can be compared to the LHCb numbers (Table 5 of [250]) and also to other theoretical works. The ratios are in an agreement with measurements except for $\mathcal{R}(J/\Psi)$, which deviates more than 2σ.

Let us, at last, mention the paper [451] dedicated to vector particles B^* and B_s^* and their transition to $B_{(s)}\gamma$ and $D_{(s)}^* + V$, $V \in \{\rho, K^*, D^*, D_s^*\}$. The radiative deexitation processes use the formalism presented in Section 2.4 to describe the decay: a photon can be radiated from one of the valence quarks or from the non-local quark-hadron vertex. In the latter case, however, it can be shown that the contribution vanishes due to the anomalous nature of the $V \rightarrow P\gamma$ process and so the calculation is simplified. The results on decay widths of B^+, B^0 and B_s^{*0}, presented in Table V of the work, depend on radiative decay constants of the particles given in Table IV. For what concerns the decays to two vector particles, the computation proceeds in a usual way, where the CCQM invariant form factors are combined to helicity amplitudes to give branching fractions. Due to small cross sections of the studied processes the experimental numbers are not available and so our results are compared to other theoretical approaches (Table XII of [451]).

6. Summary and outlook

We provided in this text a review of the results of the confined covariant quark model for B decays presented together with a survey of selected experimental and theoretical results. Unlike for other physics models and their achievements mentioned here, we explained in depth the principles of the CCQM (Section 2) and presented computational details for chosen processes, namely $B_s \rightarrow \ell^+\ell^-\gamma$ (Section 3.2), $B_s \rightarrow \phi\ell^+\ell^-\gamma$ (Section 4.2), $B \rightarrow D_{(s)}^{(*)}h$, $(h = \pi, \rho)$ and $B_s \rightarrow J/\psi\eta^{(')}$ (Section 5.2). For the sake of the review the decays were divided into three groups: leptonic, semileptonic and non-leptonic. Although somewhat arbitrary, this division allowed us to demonstrate the application of the CCQM in various situations. Generally speaking, despite some studies on NP contributions, the CCQM results do not provide strong indications for NP and suggest that further efforts within the SM may be needed.

One should also recall that we presented only a small section of what the CCQM can provide: it was, in many papers, successfully applied to describe baryon, tetraquark and other (than B) mesonic states. The quality of the CCQM is also confirmed by the interest of other authors. Narrowing the large number of citations to those related to B decays and referring to the recent version of the model (2010 and later, without conference papers) one sees that the model was noticed by large collaborations (LHCb [52,452], ATLAS [453]).

The ongoing physics program on existing and future high-luminosity machines implies that the CCQM may also in the future be an appropriate theoretical tool which will contribute to unraveling the questions brought by experiments about the presence of NP or the nature of various (exotic) states. Together with other approaches, it may help to understand model-related uncertainties beyond which new physics observations can be claimed.

References

1. Weinberg, S. Phenomenological Lagrangians. *Physica A* **1979**, *96*, 327–340. doi:10.1016/0378-4371(79)90223-1.
2. Gasser, J.; Leutwyler, H. Chiral Perturbation Theory to One Loop. *Annals Phys.* **1984**, *158*, 142. doi:10.1016/0003-4916(84)90242-2.
3. Gasser, J.; Leutwyler, H. Chiral Perturbation Theory: Expansions in the Mass of the Strange Quark. *Nucl. Phys. B* **1985**, *250*, 465–516. doi:10.1016/0550-3213(85)90492-4.
4. Scherer, S. Chiral perturbation theory: Success and challenge. *Eur. Phys. J. A* **2006**, *28*, 59–70, [hep-ph/0512291]. doi:10.1140/epja/i2006-09-007-4.
5. MacHleidt, R.; Sammarruca, F. Chiral EFT based nuclear forces: Achievements and challenges. *Physica Scripta* **2016**, *91*. doi:10.1088/0031-8949/91/8/083007.
6. Dyson, F.J. The *S* Matrix in Quantum Electrodynamics. *Phys. Rev.* **1949**, *75*, 1736–1755. doi:10.1103/PhysRev.75.1736.
7. Schwinger, J.S. On the Green's functions of quantized fields. 1. *Proc. Nat. Acad. Sci.* **1951**, *37*, 452–455. doi:10.1073/pnas.37.7.452.
8. Schwinger, J.S. On the Green's functions of quantized fields. 2. *Proc. Nat. Acad. Sci.* **1951**, *37*, 455–459. doi:10.1073/pnas.37.7.455.
9. Roberts, C.D.; Williams, A.G. Dyson-Schwinger equations and their application to hadronic physics. *Prog. Part. Nucl. Phys.* **1994**, *33*, 477–575, [hep-ph/9403224]. doi:10.1016/0146-6410(94)90049-3.
10. Ivanov, M.A.; Kalinovsky, Y.L.; Roberts, C.D. Survey of heavy meson observables. *Phys. Rev. D* **1999**, *60*, 034018, [nucl-th/9812063]. doi:10.1103/PhysRevD.60.034018.
11. Shifman, M.A.; Vainshtein, A.I.; Zakharov, V.I. QCD and Resonance Physics. Theoretical Foundations. *Nucl. Phys. B* **1979**, *147*, 385–447. doi:10.1016/0550-3213(79)90022-1.
12. Shifman, M.A.; Vainshtein, A.I.; Zakharov, V.I. QCD and Resonance Physics: Applications. *Nucl. Phys. B* **1979**, *147*, 448–518. doi:10.1016/0550-3213(79)90023-3.
13. de Rafael, E. An Introduction to sum rules in QCD: Course. Les Houches Summer School in Theoretical Physics, Session 68: Probing the Standard Model of Particle Interactions, 1997, pp. 1171–1218, [hep-ph/9802448].
14. Colangelo, P.; Khodjamirian, A. QCD sum rules, a modern perspective **2000**. pp. 1495–1576, [hep-ph/0010175]. doi:10.1142/9789812810458_0033.
15. Isgur, N.; Wise, M.B. Weak Decays of Heavy Mesons in the Static Quark Approximation. *Phys. Lett. B* **1989**, *232*, 113–117. doi:10.1016/0370-2693(89)90566-2.
16. Isgur, N.; Wise, M.B. WEAK TRANSITION FORM-FACTORS BETWEEN HEAVY MESONS. *Phys. Lett. B* **1990**, *237*, 527–530. doi:10.1016/0370-2693(90)91219-2.
17. Neubert, M. Heavy quark symmetry. *Phys. Rept.* **1994**, *245*, 259–396, [hep-ph/9306320]. doi:10.1016/0370-1573(94)90091-4.
18. Aoki, Y.; others. FLAG Review 2021. *Eur. Phys. J. C* **2022**, *82*, 869, [arXiv:hep-lat/2111.09849]. doi:10.1140/epjc/s10052-022-10536-1.
19. Gambino, P.; Hashimoto, S. Inclusive Semileptonic Decays from Lattice QCD. *Phys. Rev. Lett.* **2020**, *125*, 032001, [arXiv:hep-lat/2005.13730]. doi:10.1103/PhysRevLett.125.032001.
20. Desiderio, A.; others. First lattice calculation of radiative leptonic decay rates of pseudoscalar mesons. *Phys. Rev. D* **2021**, *103*, 014502, [arXiv:hep-lat/2006.05358]. doi:10.1103/PhysRevD.103.014502.
21. Boyle, P.A.; others. A lattice QCD perspective on weak decays of *b* and *c* quarks Snowmass 2022 White Paper. 2022 Snowmass Summer Study, 2022, [arXiv:hep-lat/2205.15373].
22. Gambino, P.; Hashimoto, S.; Mächler, S.; Panero, M.; Sanfilippo, F.; Simula, S.; Smecca, A.; Tantalo, N. Lattice QCD study of inclusive semileptonic decays of heavy mesons. *JHEP* **2022**, *07*, 083, [arXiv:hep-lat/2203.11762]. doi:10.1007/JHEP07(2022)083.
23. Workman, R.L.; Others. Review of Particle Physics. *PTEP* **2022**, *2022*, 083C01. doi:10.1093/ptep/ptac097.
24. Ebert, D.; Galkin, V.O.; Faustov, R.N. Mass spectrum of orbitally and radially excited heavy - light mesons in the relativistic quark model. *Phys. Rev. D* **1998**, *57*, 5663–5669, [hep-ph/9712318]. [Erratum: Phys.Rev.D 59, 019902 (1999)], doi:10.1103/PhysRevD.59.019902.

25. Ebert, D.; Faustov, R.N.; Galkin, V.O. Properties of heavy quarkonia and B_c mesons in the relativistic quark model. *Phys. Rev. D* **2003**, *67*, 014027, [hep-ph/0210381]. doi:10.1103/PhysRevD.67.014027.

26. Buchalla, G.; Buras, A.J.; Lautenbacher, M.E. Weak decays beyond leading logarithms. *Rev. Mod. Phys.* **1996**, *68*, 1125–1144, [hep-ph/9512380]. doi:10.1103/RevModPhys.68.1125.

27. Bevan, A.J.; others. The Physics of the B Factories. *Eur. Phys. J. C* **2014**, *74*, 3026, [arXiv:hep-ex/1406.6311]. doi:10.1140/epjc/s10052-014-3026-9.

28. Artuso, M.; Isidori, G.; Stone, S. *New Physics in b Decays*; WORLD SCIENTIFIC, 2022; [https://www.worldscientific.com/doi/pdf/10.1142/12696]. doi:10.1142/12696.

29. Altmannshofer, W.; Stangl, P. New physics in rare B decays after Moriond 2021. *Eur. Phys. J. C* **2021**, *81*, 952, [arXiv:hep-ph/2103.13370]. doi:10.1140/epjc/s10052-021-09725-1.

30. Jäger, S.; Kirk, M.; Lenz, A.; Leslie, K. Charming new physics in rare B-decays and mixing? *Phys. Rev. D* **2018**, *97*, 015021, [arXiv:hep-ph/1701.09183]. doi:10.1103/PhysRevD.97.015021.

31. Kumbhakar, S.; Saini, J. New physics effects in purely leptonic B_s^* decays. *Eur. Phys. J. C* **2019**, *79*, 394, [arXiv:hep-ph/1807.04055]. doi:10.1140/epjc/s10052-019-6901-6.

32. Chala, M.; Egede, U.; Spannowsky, M. Searching new physics in rare *B*-meson decays into multiple muons. *Eur. Phys. J. C* **2019**, *79*, 431, [arXiv:hep-ph/1902.10156]. doi:10.1140/epjc/s10052-019-6946-6.

33. Coy, R.; Frigerio, M.; Mescia, F.; Sumensari, O. New physics in $b \to s\ell\ell$ transitions at one loop. *Eur. Phys. J. C* **2020**, *80*, 52, [arXiv:hep-ph/1909.08567]. doi:10.1140/epjc/s10052-019-7581-y.

34. Charles, J.; Descotes-Genon, S.; Ligeti, Z.; Monteil, S.; Papucci, M.; Trabelsi, K.; Vale Silva, L. New physics in *B* meson mixing: future sensitivity and limitations. *Phys. Rev. D* **2020**, *102*, 056023, [arXiv:hep-ph/2006.04824]. doi:10.1103/PhysRevD.102.056023.

35. Bhutta, F.M.; Huang, Z.R.; Lü, C.D.; Ali Paracha, M.; Wang, W. New physics in b → sll anomalies and its implications for the complementary neutral current decays. *Nuclear Physics B* **2022**, *979*, 115763. doi:https://doi.org/10.1016/j.nuclphysb.2022.115763.

36. Cai, F.M.; Deng, W.J.; Li, X.Q.; Yang, Y.D. Probing new physics in class-I B-meson decays into heavy-light final states. *JHEP* **2021**, *10*, 235, [arXiv:hep-ph/2103.04138]. doi:10.1007/JHEP10(2021)235.

37. Branz, T.; Faessler, A.; Gutsche, T.; Ivanov, M.A.; Korner, J.G.; Lyubovitskij, V.E. Relativistic constituent quark model with infrared confinement. *Phys. Rev. D* **2010**, *81*, 034010, [arXiv:hep-ph/0912.3710]. doi:10.1103/PhysRevD.81.034010.

38. Anikin, I.V.; Ivanov, M.A.; Kulimanova, N.B.; Lyubovitskij, V.E. The Extended Nambu-Jona-Lasinio model with separable interaction: Low-energy pion physics and pion nucleon form-factor. *Z. Phys. C* **1995**, *65*, 681–690. doi:10.1007/BF01578675.

39. Ganbold, G.; Gutsche, T.; Ivanov, M.A.; Lyubovitskij, V.E. On the meson mass spectrum in the covariant confined quark model. *J. Phys. G* **2015**, *42*, 075002, [arXiv:hep-ph/1410.3741]. doi:10.1088/0954-3899/42/7/075002.

40. Gutsche, T.; Ivanov, M.A.; Körner, J.G.; Lyubovitskij, V.E.; Santorelli, P.; Habyl, N. Semileptonic decay $\Lambda_b \to \Lambda_c + \tau^- + \bar{\nu}_\tau$ in the covariant confined quark model. *Phys. Rev. D* **2015**, *91*, 074001, [arXiv:hep-ph/1502.04864]. [Erratum: Phys.Rev.D 91, 119907 (2015)], doi:10.1103/PhysRevD.91.074001.

41. Gutsche, T.; Ivanov, M.A.; Körner, J.G.; Lyubovitskij, V.E.; Santorelli, P. Heavy-to-light semileptonic decays of Λ_b and Λ_c baryons in the covariant confined quark model. *Phys. Rev. D* **2014**, *90*, 114033, [arXiv:hep-ph/1410.6043]. [Erratum: Phys.Rev.D 94, 059902 (2016)], doi:10.1103/PhysRevD.90.114033.

42. Ivanov, M.A. Nonleptonic Decays of Doubly Charmed Baryons. *Particles* **2020**, *3*, 123–144. doi:10.3390/particles3010011.

43. Dubnička, S.; Dubničková, A.Z.; Ivanov, M.A.; Liptaj, A. Dynamical Approach to Decays of XYZ States. *Symmetry* **2020**, *12*, 884. doi:10.3390/sym12060884.

44. Dubnička, S.; Dubničková, A.Z.; Habyl, N.; Ivanov, M.A.; Liptaj, A.; Nurbakova, G.S. Decay $B \to K^*(\to K\pi)\ell^+\ell^-$ in covariant quark model. *Few Body Syst.* **2016**, *57*, 121–143, [arXiv:hep-ph/1511.04887]. doi:10.1007/s00601-015-1034-4.

45. Jouvet, B. On the meaning of Fermi coupling. *Nuovo Cim.* **1956**, *3*, 1133–1135. doi:10.1007/BF02823510.

46. Salam, A. Lagrangian theory of composite particles. *Nuovo Cim.* **1962**, *25*, 224–227. doi:10.1007/BF02733330.

47. Weinberg, S. Elementary particle theory of composite particles. *Phys. Rev.* **1963**, *130*, 776–783. doi:10.1103/PhysRev.130.776.

48.   Hayashi, K.; Hirayama, M.; Muta, T.; Seto, N.; Shirafuji, T. Compositeness criteria of particles in quantum field theory and S-matrix theory. *Fortsch. Phys.* **1967**, *15*, 625–660. doi:10.1002/prop.19670151002.

49.   Branz, T.; Faessler, A.; Gutsche, T.; Ivanov, M.A.; Korner, J.G.; Lyubovitskij, V.E.; Oexl, B. Radiative decays of double heavy baryons in a relativistic constituent three–quark model including hyperfine mixing. *Phys. Rev. D* **2010**, *81*, 114036, [arXiv:hep-ph/1005.1850]. doi:10.1103/PhysRevD.81.114036.

50.   Terning, J. Gauging nonlocal Lagrangians. *Phys. Rev. D* **1991**, *44*, 887–897. doi:10.1103/PhysRevD.44.887.

51.   Ruijl, B.; Ueda, T.; Vermaseren, J.A.M. Forcer, a FORM program for the parametric reduction of four-loop massless propagator diagrams. *Comput. Phys. Commun.* **2020**, *253*, 107198, [arXiv:hep-ph/1704.06650]. doi:10.1016/j.cpc.2020.107198.

52.   Aaij, R.; others. Analysis of Neutral B-Meson Decays into Two Muons. *Phys. Rev. Lett.* **2022**, *128*, 041801, [arXiv:hep-ex/2108.09284]. doi:10.1103/PhysRevLett.128.041801.

53.   Aaboud, M.; others. Study of the rare decays of B_s^0 and B^0 mesons into muon pairs using data collected during 2015 and 2016 with the ATLAS detector. *JHEP* **2019**, *04*, 098, [arXiv:hep-ex/1812.03017]. doi:10.1007/JHEP04(2019)098.

54.   Sirunyan, A.M.; others. Measurement of properties of $B_s^0 \to \mu^+\mu^-$ decays and search for $B^0 \to \mu^+\mu^-$ with the CMS experiment. *JHEP* **2020**, *04*, 188, [arXiv:hep-ex/1910.12127]. doi:10.1007/JHEP04(2020)188.

55.   Langenegger, U. Recent results on $B \to \mu^+\mu^-$ decays with the CMS experiment. *Mod. Phys. Lett. A* **2020**, *35*, 2030017, [arXiv:hep-ex/2006.14849]. doi:10.1142/S0217732320300177.

56.   Kronenbitter, B.; others. Measurement of the branching fraction of $B^+ \to \tau^+\nu_\tau$ decays with the semileptonic tagging method. *Phys. Rev. D* **2015**, *92*, 051102, [arXiv:hep-ex/1503.05613]. doi:10.1103/PhysRevD.92.051102.

57.   Adachi, I.; others. Evidence for $B^- \to \tau^-\bar{\nu}_\tau$ with a Hadronic Tagging Method Using the Full Data Sample of Belle. *Phys. Rev. Lett.* **2013**, *110*, 131801, [arXiv:hep-ex/1208.4678]. doi:10.1103/PhysRevLett.110.131801.

58.   Lees, J.P.; others. Evidence of $B^+ \to \tau^+\nu$ decays with hadronic B tags. *Phys. Rev. D* **2013**, *88*, 031102, [arXiv:hep-ex/1207.0698]. doi:10.1103/PhysRevD.88.031102.

59.   Aubert, B.; others. A Search for $B^+ \to \ell^+\nu_\ell$ Recoiling Against $B^- \to D^0\ell^-\bar{\nu}X$. *Phys. Rev. D* **2010**, *81*, 051101, [arXiv:hep-ex/0912.2453]. doi:10.1103/PhysRevD.81.051101.

60.   Sibidanov, A.; others. Search for $B^- \to \mu^-\bar{\nu}_\mu$ Decays at the Belle Experiment. *Phys. Rev. Lett.* **2018**, *121*, 031801, [arXiv:hep-ex/1712.04123]. doi:10.1103/PhysRevLett.121.031801.

61.   Prim, M.T.; others. Search for $B^+ \to \mu^+\nu_\mu$ and $B^+ \to \mu^+ N$ with inclusive tagging. *Phys. Rev. D* **2020**, *101*, 032007, [arXiv:hep-ex/1911.03186]. doi:10.1103/PhysRevD.101.032007.

62.   Gelb, M.; others. Search for the rare decay of $B^+ \to \ell^+\nu_\ell\gamma$ with improved hadronic tagging. *Phys. Rev. D* **2018**, *98*, 112016, [arXiv:hep-ex/1810.12976]. doi:10.1103/PhysRevD.98.112016.

63.   Rosner, J.L.; Stone, S.; Van de Water, R.S. Leptonic Decays of Charged Pseudoscalar Mesons - 2015 **2015**. [arXiv:hep-ph/1509.02220].

64.   Dingfelder, J.; Mannel, T. Leptonic and semileptonic decays of B mesons. *Rev. Mod. Phys.* **2016**, *88*, 035008. doi:10.1103/RevModPhys.88.035008.

65.   Buchalla, G.; Buras, A.J. QCD corrections to rare K and B decays for arbitrary top quark mass. *Nucl. Phys. B* **1993**, *400*, 225–239. doi:10.1016/0550-3213(93)90405-E.

66.   Bazavov, A.; others. B- and D-meson leptonic decay constants from four-flavor lattice QCD. *Phys. Rev. D* **2018**, *98*, 074512, [arXiv:hep-lat/1712.09262]. doi:10.1103/PhysRevD.98.074512.

67.   Hermann, T.; Misiak, M.; Steinhauser, M. Three-loop QCD corrections to $B_s \to \mu^+\mu^-$. *JHEP* **2013**, *12*, 097, [arXiv:hep-ph/1311.1347]. doi:10.1007/JHEP12(2013)097.

68.   Bobeth, C.; Gorbahn, M.; Stamou, E. Electroweak Corrections to $B_{s,d} \to \ell^+\ell^-$. *Phys. Rev. D* **2014**, *89*, 034023, [arXiv:hep-ph/1311.1348]. doi:10.1103/PhysRevD.89.034023.

69.   Bobeth, C.; Gorbahn, M.; Hermann, T.; Misiak, M.; Stamou, E.; Steinhauser, M. $B_{s,d} \to l^+l^-$ in the Standard Model with Reduced Theoretical Uncertainty. *Phys. Rev. Lett.* **2014**, *112*, 101801, [arXiv:hep-ph/1311.0903]. doi:10.1103/PhysRevLett.112.101801.

70.   Beneke, M.; Bobeth, C.; Szafron, R. Enhanced electromagnetic correction to the rare B-meson decay $B_{s,d} \to \mu^+\mu^-$. *Phys. Rev. Lett.* **2018**, *120*, 011801, [arXiv:hep-ph/1708.09152]. doi:10.1103/PhysRevLett.120.011801.

71.   Beneke, M.; Bobeth, C.; Szafron, R. Power-enhanced leading-logarithmic QED corrections to $B_q \to \mu^+\mu^-$. *JHEP* **2019**, *10*, 232, [arXiv:hep-ph/1908.07011]. [Erratum: JHEP 11, 099 (2022)], doi:10.1007/JHEP10(2019)232.

72. Eilam, G.; Lu, C.D.; Zhang, D.X. Radiative dileptonic decays of B mesons. *Phys. Lett. B* **1997**, *391*, 461–464, [hep-ph/9606444]. doi:10.1016/S0370-2693(96)01491-8.

73. Aliev, T.M.; Ozpineci, A.; Savci, M. B(q) —> lepton+ lepton- gamma decays in light cone QCD. *Phys. Rev. D* **1997**, *55*, 7059–7066, [hep-ph/9611393]. doi:10.1103/PhysRevD.55.7059.

74. Aliev, T.M.; Pak, N.K.; Savci, M. Rare radiative B —> tau+ tau- gamma decay. *Phys. Lett. B* **1998**, *424*, 175–184, [hep-ph/9710304]. doi:10.1016/S0370-2693(98)00126-9.

75. Geng, C.Q.; Lih, C.C.; Zhang, W.M. Study of B(s,d) —> l+ l- gamma decays. *Phys. Rev. D* **2000**, *62*, 074017, [hep-ph/0007252]. doi:10.1103/PhysRevD.62.074017.

76. Dincer, Y.; Sehgal, L.M. Charge asymmetry and photon energy spectrum in the decay B(s) —> l+ l- gamma. *Phys. Lett. B* **2001**, *521*, 7–14, [hep-ph/0108144]. doi:10.1016/S0370-2693(01)01203-5.

77. Kruger, F.; Melikhov, D. Gauge invariance and form-factors for the decay B —> gamma l+ l-. *Phys. Rev. D* **2003**, *67*, 034002, [hep-ph/0208256]. doi:10.1103/PhysRevD.67.034002.

78. Descotes-Genon, S.; Sachrajda, C.T. Universality of nonperturbative QCD effects in radiative B decays. *Phys. Lett. B* **2003**, *557*, 213–223, [hep-ph/0212162]. doi:10.1016/S0370-2693(03)00173-4.

79. Melikhov, D.; Nikitin, N. Rare radiative leptonic decays B(d,s) —> l+l- gamma. *Phys. Rev. D* **2004**, *70*, 114028, [hep-ph/0410146]. doi:10.1103/PhysRevD.70.114028.

80. Carvunis, A.; Dettori, F.; Gangal, S.; Guadagnoli, D.; Normand, C. On the effective lifetime of $B_s \to \mu\mu\gamma$. *JHEP* **2021**, *12*, 078, [arXiv:hep-ph/2102.13390]. doi:10.1007/JHEP12(2021)078.

81. Burdman, G.; Goldman, J.T.; Wyler, D. Radiative leptonic decays of heavy mesons. *Phys. Rev. D* **1995**, *51*, 111–117, [hep-ph/9405425]. doi:10.1103/PhysRevD.51.111.

82. Korchemsky, G.P.; Pirjol, D.; Yan, T.M. Radiative leptonic decays of B mesons in QCD. *Phys. Rev. D* **2000**, *61*, 114510, [hep-ph/9911427]. doi:10.1103/PhysRevD.61.114510.

83. Braun, V.M.; Khodjamirian, A. Soft contribution to $B \to \gamma \ell \nu_\ell$ and the *B*-meson distribution amplitude. *Phys. Lett. B* **2013**, *718*, 1014–1019, [arXiv:hep-ph/1210.4453]. doi:10.1016/j.physletb.2012.11.047.

84. Beneke, M.; Braun, V.M.; Ji, Y.; Wei, Y.B. Radiative leptonic decay $B \to \gamma \ell \nu_\ell$ with subleading power corrections. *JHEP* **2018**, *07*, 154, [arXiv:hep-ph/1804.04962]. doi:10.1007/JHEP07(2018)154.

85. Lunghi, E.; Pirjol, D.; Wyler, D. Factorization in leptonic radiative $B \to \gamma e \nu$ decays. *Nucl. Phys. B* **2003**, *649*, 349–364, [hep-ph/0210091]. doi:10.1016/S0550-3213(02)01032-5.

86. Bosch, S.W.; Hill, R.J.; Lange, B.O.; Neubert, M. Factorization and Sudakov resummation in leptonic radiative B decay. *Phys. Rev. D* **2003**, *67*, 094014, [hep-ph/0301123]. doi:10.1103/PhysRevD.67.094014.

87. Wang, C.; Wang, Y.M.; Wei, Y.B. QCD factorization for the four-body leptonic B-meson decays. *JHEP* **2022**, *02*, 141, [arXiv:hep-ph/2111.11811]. doi:10.1007/JHEP02(2022)141.

88. Danilina, A.; Nikitin, N.; Toms, K. Decays of charged *B*-mesons into three charged leptons and a neutrino. *Phys. Rev. D* **2020**, *101*, 096007, [arXiv:hep-ph/1911.03670]. doi:10.1103/PhysRevD.101.096007.

89. Ivanov, M.A.; Melikhov, D. Theoretical analysis of the leptonic decays $B \to \ell\ell\nu\ell$: Identical leptons in the final state. *Phys. Rev. D* **2022**, *105*, 094038, [arXiv:hep-ph/2204.02792]. doi:10.1103/PhysRevD.105.094038.

90. Ivanov, M.A.; Melikhov, D. Theoretical analysis of the leptonic decays $B \to \ell\ell\ell'\bar{\nu}_{\ell'}$. *Phys. Rev. D* **2022**, *105*, 014028, [arXiv:hep-ph/2107.07247]. [Erratum: Phys.Rev.D 106, 119901 (2022)], doi:10.1103/PhysRevD.105.014028.

91. Geng, L.S.; Grinstein, B.; Jäger, S.; Li, S.Y.; Martin Camalich, J.; Shi, R.X. Implications of new evidence for lepton-universality violation in $b \to s\ell + \ell-$ decays. *Phys. Rev. D* **2021**, *104*, 035029, [arXiv:hep-ph/2103.12738]. doi:10.1103/PhysRevD.104.035029.

92. Algueró, M.; Capdevila, B.; Descotes-Genon, S.; Matias, J.; Novoa-Brunet, M. $b \to s\ell^+\ell^-$ global fits after R_{K_S} and $R_{K^{*+}}$. *Eur. Phys. J. C* **2022**, *82*, 326, [arXiv:hep-ph/2104.08921]. doi:10.1140/epjc/s10052-022-10231-1.

93. Fleischer, R.; Jaarsma, R.; Tetlalmatzi-Xolocotzi, G. Mapping out the space for new physics with leptonic and semileptonic $B_{(c)}$ decays. *Eur. Phys. J. C* **2021**, *81*, 658, [arXiv:hep-ph/2104.04023]. doi:10.1140/epjc/s10052-021-09419-8.

94. D'Ambrosio, G.; Giudice, G.F.; Isidori, G.; Strumia, A. Minimal flavor violation: An Effective field theory approach. *Nucl. Phys. B* **2002**, *645*, 155–187, [hep-ph/0207036]. doi:10.1016/S0550-3213(02)00836-2.

95. De Bruyn, K.; Fleischer, R.; Knegjens, R.; Koppenburg, P.; Merk, M.; Pellegrino, A.; Tuning, N. Probing New Physics via the $B_s^0 \to \mu^+\mu^-$ Effective Lifetime. *Phys. Rev. Lett.* **2012**, *109*, 041801, [arXiv:hep-ph/1204.1737]. doi:10.1103/PhysRevLett.109.041801.

96. Greljo, A.; Soreq, Y.; Stangl, P.; Thomsen, A.E.; Zupan, J. Muonic force behind flavor anomalies. *JHEP* **2022**, *04*, 151, [arXiv:hep-ph/2107.07518]. doi:10.1007/JHEP04(2022)151.

97. Hou, W.S. Enhanced charged Higgs boson effects in B- —> tau anti-neutrino, mu anti-neutrino and b —> tau anti-neutrino + X. *Phys. Rev. D* **1993**, *48*, 2342–2344. doi:10.1103/PhysRevD.48.2342.

98. Akeroyd, A.G.; Recksiegel, S. The Effect of H+- on B+- —> tau+- nu(tau) and B+- —> mu+- muon neutrino. *J. Phys. G* **2003**, *29*, 2311–2317, [hep-ph/0306037]. doi:10.1088/0954-3899/29/10/301.

99. Crivellin, A.; Greub, C.; Kokulu, A. Explaining $B \to D\tau\nu$, $B \to D^*\tau\nu$ and $B \to \tau\nu$ in a 2HDM of type III. *Phys. Rev. D* **2012**, *86*, 054014, [arXiv:hep-ph/1206.2634]. doi:10.1103/PhysRevD.86.054014.

100. He, X.G.; Valencia, G. *B* decays with τ leptons in nonuniversal left-right models. *Phys. Rev. D* **2013**, *87*, 014014, [arXiv:hep-ph/1211.0348]. doi:10.1103/PhysRevD.87.014014.

101. Dubnička, S.; Dubničková, A.Z.; Ivanov, M.A.; Liptaj, A.; Santorelli, P.; Tran, C.T. Study of $B_s \to \ell^+\ell^-\gamma$ decays in covariant quark model. *Phys. Rev. D* **2019**, *99*, 014042, [arXiv:hep-ph/1808.06261]. doi:10.1103/PhysRevD.99.014042.

102. Bauer, C.W.; Ligeti, Z.; Luke, M.; Manohar, A.V.; Trott, M. Global analysis of inclusive B decays. *Phys. Rev. D* **2004**, *70*, 094017, [hep-ph/0408002]. doi:10.1103/PhysRevD.70.094017.

103. Descotes-Genon, S.; Hurth, T.; Matias, J.; Virto, J. Optimizing the basis of $B \to K^* ll$ observables in the full kinematic range. *JHEP* **2013**, *05*, 137, [arXiv:hep-ph/1303.5794]. doi:10.1007/JHEP05(2013)137.

104. Kozachuk, A.; Melikhov, D.; Nikitin, N. Rare FCNC radiative leptonic $B_{s,d} \to \gamma l^+ l^-$ decays in the standard model. *Phys. Rev. D* **2018**, *97*, 053007, [arXiv:hep-ph/1712.07926]. doi:10.1103/PhysRevD.97.053007.

105. Melikhov, D.; Kozachuk, A.; Nikitin, N. Rare FCNF radiative leptonic decays $B \to \gamma\ell^+\ell^-$. *PoS* **2017**, *EPS-HEP2017*, 228, [arXiv:hep-ph/1710.02719]. doi:10.22323/1.314.0228.

106. Wang, W.Y.; Xiong, Z.H.; Zhou, S.H. Complete Analyses on the Short-Distance Contribution of $B_s \to \ell^+\ell^-\gamma$ in the Standard Model. *Chin. Phys. Lett.* **2013**, *30*, 111202, [arXiv:hep-ph/1303.0660]. doi:10.1088/0256-307X/30/11/111202.

107. Ivanov, M.A.; Körner, J.G.; Tran, C.T. Exclusive decays $B \to \ell^-\bar{\nu}$ and $B \to D^{(*)}\ell^-\bar{\nu}$ in the covariant quark model. *Phys. Rev. D* **2015**, *92*, 114022, [arXiv:hep-ph/1508.02678]. doi:10.1103/PhysRevD.92.114022.

108. Ivanov, M.A.; Körner, J.G.; Tran, C.T. Looking for new physics in leptonic and semileptonic decays of B-meson. *Phys. Part. Nucl. Lett.* **2017**, *14*, 669–676. doi:10.1134/S1547477117050053.

109. Amhis, Y.S.; others. Averages of b-hadron, c-hadron, and τ-lepton properties as of 2021. *Phys. Rev. D* **2023**, *107*, 052008, [arXiv:hep-ex/2206.07501]. doi:10.1103/PhysRevD.107.052008.

110. Bernlochner, F.U.; Sevilla, M.F.; Robinson, D.J.; Wormser, G. Semitauonic b-hadron decays: A lepton flavor universality laboratory. *Rev. Mod. Phys.* **2022**, *94*, 015003, [arXiv:hep-ex/2101.08326]. doi:10.1103/RevModPhys.94.015003.

111. Crivellin, A.; Greub, C.; Müller, D.; Saturnino, F. Importance of Loop Effects in Explaining the Accumulated Evidence for New Physics in B Decays with a Vector Leptoquark. *Phys. Rev. Lett.* **2019**, *122*, 011805, [arXiv:hep-ph/1807.02068]. doi:10.1103/PhysRevLett.122.011805.

112. Measurement of the ratios of branching fractions $\mathcal{R}(D^*)$ and $\mathcal{R}(D^0)$ **2023**. [arXiv:hep-ex/2302.02886].

113. Test of lepton universality in $b \to s\ell^+\ell^-$ decays **2022**. [arXiv:hep-ex/2212.09152].

114. Puthumanaillam, R. Measurement of $R(D^*)$ with hadronic τ^+ decays at $\sqrt{s} = 13$TeV TeV by the LHCb collaboration (CERN seminar, Mar 21, 2023). Available at https://indico.cern.ch/event/1231797/.

115. Aaij, R.; others. Differential branching fraction and angular analysis of the decay $B^0 \to K^{*0}\mu^+\mu^-$. *JHEP* **2013**, *08*, 131, [arXiv:hep-ex/1304.6325]. doi:10.1007/JHEP08(2013)131.

116. Aaij, R.; others. Measurement of Form-Factor-Independent Observables in the Decay $B^0 \to K^{*0}\mu^+\mu^-$. *Phys. Rev. Lett.* **2013**, *111*, 191801, [arXiv:hep-ex/1308.1707]. doi:10.1103/PhysRevLett.111.191801.

117. Aaij, R.; others. Differential branching fractions and isospin asymmetries of $B \to K^{(*)}\mu^+\mu^-$ decays. *JHEP* **2014**, *06*, 133, [arXiv:hep-ex/1403.8044]. doi:10.1007/JHEP06(2014)133.

118. Aaij, R.; others. Angular analysis of the $B^0 \to K^{*0}e^+e^-$ decay in the low-q^2 region. *JHEP* **2015**, *04*, 064, [arXiv:hep-ex/1501.03038]. doi:10.1007/JHEP04(2015)064.

119. Aaij, R.; others. Angular analysis of the $B^0 \to K^{*0}\mu^+\mu^-$ decay using 3 fb^{-1} of integrated luminosity. *JHEP* **2016**, *02*, 104, [arXiv:hep-ex/1512.04442]. doi:10.1007/JHEP02(2016)104.

120. Aaij, R.; others. Test of lepton universality with $B^0 \to K^{*0}\ell^+\ell^-$ decays. *JHEP* **2017**, *08*, 055, [arXiv:hep-ex/1705.05802]. doi:10.1007/JHEP08(2017)055.

121.   Aaij, R.; others. Measurement of *CP*-Averaged Observables in the $B^0 \to K^{*0}\mu^+\mu^-$ Decay. *Phys. Rev. Lett.* **2020**, *125*, 011802, [arXiv:hep-ex/2003.04831]. doi:10.1103/PhysRevLett.125.011802.

122.   Aaij, R.; others. Angular Analysis of the $B^+ \to K^{*+}\mu^+\mu^-$ Decay. *Phys. Rev. Lett.* **2021**, *126*, 161802, [arXiv:hep-ex/2012.13241]. doi:10.1103/PhysRevLett.126.161802.

123.   Aaij, R.; others. Tests of lepton universality using $B^0 \to K^0_S\ell^+\ell^-$ and $B^+ \to K^{*+}\ell^+\ell^-$ decays. *Phys. Rev. Lett.* **2022**, *128*, 191802, [arXiv:hep-ex/2110.09501]. doi:10.1103/PhysRevLett.128.191802.

124.   Aaij, R.; others. Differential branching fraction and angular analysis of the $B^+ \to K^+\mu^+\mu^-$ decay. *JHEP* **2013**, *02*, 105, [arXiv:hep-ex/1209.4284]. doi:10.1007/JHEP02(2013)105.

125.   Aaij, R.; others. Test of lepton universality using $B^+ \to K^+\ell^+\ell^-$ decays. *Phys. Rev. Lett.* **2014**, *113*, 151601, [arXiv:hep-ex/1406.6482]. doi:10.1103/PhysRevLett.113.151601.

126.   Aaij, R.; others. Search for lepton-universality violation in $B^+ \to K^+\ell^+\ell^-$ decays. *Phys. Rev. Lett.* **2019**, *122*, 191801, [arXiv:hep-ex/1903.09252]. doi:10.1103/PhysRevLett.122.191801.

127.   Aaij, R.; others. Measurement of the ratio of branching fractions $\mathcal{B}(\bar{B}^0 \to D^{*+}\tau^-\bar{\nu}_\tau)/\mathcal{B}(\bar{B}^0 \to D^{*+}\mu^-\bar{\nu}_\mu)$. *Phys. Rev. Lett.* **2015**, *115*, 111803, [arXiv:hep-ex/1506.08614]. [Erratum: Phys.Rev.Lett. 115, 159901 (2015)], doi:10.1103/PhysRevLett.115.111803.

128.   Aaij, R.; others. Measurement of the ratio of the $B^0 \to D^{*-}\tau^+\nu_\tau$ and $B^0 \to D^{*-}\mu^+\nu_\mu$ branching fractions using three-prong τ-lepton decays. *Phys. Rev. Lett.* **2018**, *120*, 171802, [arXiv:hep-ex/1708.08856]. doi:10.1103/PhysRevLett.120.171802.

129.   Aaij, R.; others. Test of Lepton Flavor Universality by the measurement of the $B^0 \to D^{*-}\tau^+\nu_\tau$ branching fraction using three-prong τ decays. *Phys. Rev. D* **2018**, *97*, 072013, [arXiv:hep-ex/1711.02505]. doi:10.1103/PhysRevD.97.072013.

130.   Aaij, R.; others. Measurement of the ratio of branching fractions $\mathcal{B}(B_c^+ \to J/\psi\tau^+\nu_\tau)/\mathcal{B}(B_c^+ \to J/\psi\mu^+\nu_\mu)$. *Phys. Rev. Lett.* **2018**, *120*, 121801, [arXiv:hep-ex/1711.05623]. doi:10.1103/PhysRevLett.120.121801.

131.   Aaij, R.; others. Differential branching fraction and angular analysis of the decay $B_s^0 \to \phi\mu^+\mu^-$. *JHEP* **2013**, *07*, 084, [arXiv:hep-ex/1305.2168]. doi:10.1007/JHEP07(2013)084.

132.   Aaij, R.; others. Angular analysis and differential branching fraction of the decay $B_s^0 \to \phi\mu^+\mu^-$. *JHEP* **2015**, *09*, 179, [arXiv:hep-ex/1506.08777]. doi:10.1007/JHEP09(2015)179.

133.   Aaij, R.; others. Branching Fraction Measurements of the Rare $B_s^0 \to \phi\mu^+\mu^-$ and $B_s^0 \to f_2'(1525)\mu^+\mu^-$-Decays. *Phys. Rev. Lett.* **2021**, *127*, 151801, [arXiv:hep-ex/2105.14007]. doi:10.1103/PhysRevLett.127.151801.

134.   Aaij, R.; others. Test of lepton universality in beauty-quark decays. *Nature Phys.* **2022**, *18*, 277–282, [arXiv:hep-ex/2103.11769]. doi:10.1038/s41567-021-01478-8.

135.   Aubert, B.; others. Observation of the semileptonic decays $B \to D^*\tau^-\bar{\nu}(\tau)$ and evidence for $B \to D\tau^-\bar{\nu}(\tau)$. *Phys. Rev. Lett.* **2008**, *100*, 021801, [arXiv:hep-ex/0709.1698]. doi:10.1103/PhysRevLett.100.021801.

136.   Lees, J.P.; others. Evidence for an excess of $\bar{B} \to D^{(*)}\tau^-\bar{\nu}_\tau$ decays. *Phys. Rev. Lett.* **2012**, *109*, 101802, [arXiv:hep-ex/1205.5442]. doi:10.1103/PhysRevLett.109.101802.

137.   Lees, J.P.; others. Measurement of an Excess of $\bar{B} \to D^{(*)}\tau^-\bar{\nu}_\tau$ Decays and Implications for Charged Higgs Bosons. *Phys. Rev. D* **2013**, *88*, 072012, [arXiv:hep-ex/1303.0571]. doi:10.1103/PhysRevD.88.072012.

138.   Aubert, B.; others. Measurement of |V(cb)| and the Form-Factor Slope in anti-B —> D l- anti-nu Decays in Events Tagged by a Fully Reconstructed B Meson. *Phys. Rev. Lett.* **2010**, *104*, 011802, [arXiv:hep-ex/0904.4063]. doi:10.1103/PhysRevLett.104.011802.

139.   Aubert, B.; others. Determination of the form-factors for the decay $B^0 \to D^{*-}\ell^+\nu_l$ and of the CKM matrix element $|V_{cb}|$. *Phys. Rev. D* **2008**, *77*, 032002, [arXiv:hep-ex/0705.4008]. doi:10.1103/PhysRevD.77.032002.

140.   Aubert, B.; others. Measurements of the Semileptonic Decays anti-B —> D l anti-nu and anti-B —> D* l anti-nu Using a Global Fit to D X l anti-nu Final States. *Phys. Rev. D* **2009**, *79*, 012002, [arXiv:hep-ex/0809.0828]. doi:10.1103/PhysRevD.79.012002.

141.   Lees, J.P.; others. Extraction of form Factors from a Four-Dimensional Angular Analysis of $\overline{B} \to D^*\ell^-\overline{\nu}_\ell$. *Phys. Rev. Lett.* **2019**, *123*, 091801, [arXiv:hep-ex/1903.10002]. doi:10.1103/PhysRevLett.123.091801.

142.   Aubert, B.; others. Evidence for the rare decay $B \to K^*\ell^+\ell^-$ and measurement of the $B \to K\ell^+\ell^-$ branching fraction. *Phys. Rev. Lett.* **2003**, *91*, 221802, [hep-ex/0308042]. doi:10.1103/PhysRevLett.91.221802.

143.   Aubert, B.; others. Measurements of branching fractions, rate asymmetries, and angular distributions in the rare decays $B \to K\ell^+\ell^-$ and $B \to K^*\ell^+\ell^-$. *Phys. Rev. D* **2006**, *73*, 092001, [hep-ex/0604007]. doi:10.1103/PhysRevD.73.092001.

144. Aubert, B.; others. Direct CP, Lepton Flavor and Isospin Asymmetries in the Decays $B \to K^{(*)}\ell^+\ell^-$. *Phys. Rev. Lett.* **2009**, *102*, 091803, [arXiv:hep-ex/0807.4119]. doi:10.1103/PhysRevLett.102.091803.

145. Lees, J.P.; others. Measurement of Branching Fractions and Rate Asymmetries in the Rare Decays $B \to K^{(*)}l^+l^-$. *Phys. Rev. D* **2012**, *86*, 032012, [arXiv:hep-ex/1204.3933]. doi:10.1103/PhysRevD.86.032012.

146. Aubert, B.; others. Angular Distributions in the Decays B —> K* l+ l-. *Phys. Rev. D* **2009**, *79*, 031102, [arXiv:hep-ex/0804.4412]. doi:10.1103/PhysRevD.79.031102.

147. Lees, J.P.; others. Measurement of angular asymmetries in the decays $B \to K^*\ell^+\ell^-$. *Phys. Rev. D* **2016**, *93*, 052015, [arXiv:hep-ex/1508.07960]. doi:10.1103/PhysRevD.93.052015.

148. Aubert, B.; others. Measurement of the $B^0 \to \pi^-\ell^+\nu$ form-factor shape and branching fraction, and determination of $|V_{ub}|$ with a loose neutrino reconstruction technique. *Phys. Rev. Lett.* **2007**, *98*, 091801, [hep-ex/0612020]. doi:10.1103/PhysRevLett.98.091801.

149. del Amo Sanchez, P.; others. Study of $B \to \pi\ell\nu$ and $B \to \rho\ell\nu$ Decays and Determination of $|V_{ub}|$. *Phys. Rev. D* **2011**, *83*, 032007, [arXiv:hep-ex/1005.3288]. doi:10.1103/PhysRevD.83.032007.

150. Aubert, B.; others. Measurement of the $B \to X_s\ell^+\ell^-$ branching fraction with a sum over exclusive modes. *Phys. Rev. Lett.* **2004**, *93*, 081802, [hep-ex/0404006]. doi:10.1103/PhysRevLett.93.081802.

151. Lees, J.P.; others. Measurement of the $B \to X_s l^+l^-$ branching fraction and search for direct CP violation from a sum of exclusive final states. *Phys. Rev. Lett.* **2014**, *112*, 211802, [arXiv:hep-ex/1312.5364]. doi:10.1103/PhysRevLett.112.211802.

152. Aubert, B.; others. Measurement of the inclusive charmless semileptonic branching ratio of B mesons and determination of $|V_{ub}|$. *Phys. Rev. Lett.* **2004**, *92*, 071802, [hep-ex/0307062]. doi:10.1103/PhysRevLett.92.071802.

153. Lees, J.P.; others. Branching fraction and form-factor shape measurements of exclusive charmless semileptonic B decays, and determination of $|V_{ub}|$. *Phys. Rev. D* **2012**, *86*, 092004, [arXiv:hep-ex/1208.1253]. doi:10.1103/PhysRevD.86.092004.

154. Lees, J.P.; others. Measurement of the inclusive electron spectrum from B meson decays and determination of |Vub|. *Phys. Rev. D* **2017**, *95*, 072001, [arXiv:hep-ex/1611.05624]. doi:10.1103/PhysRevD.95.072001.

155. Lees, J.P.; others. Observation of $\bar{B} \to D^{(*)}\pi^+\pi^-\ell^-\bar{\nu}$ decays in e^+e^- collisions at the Y(4S) resonance. *Phys. Rev. Lett.* **2016**, *116*, 041801, [arXiv:hep-ex/1507.08303]. doi:10.1103/PhysRevLett.116.041801.

156. Bozek, A.; others. Observation of $B^+ \to \bar{D}^{*0}\tau^+\nu_\tau$ and Evidence for $B^+ \to \bar{D}^0\tau^+\nu_\tau$ at Belle. *Phys. Rev. D* **2010**, *82*, 072005, [arXiv:hep-ex/1005.2302]. doi:10.1103/PhysRevD.82.072005.

157. Huschle, M.; others. Measurement of the branching ratio of $\bar{B} \to D^{(*)}\tau^-\bar{\nu}_\tau$ relative to $\bar{B} \to D^{(*)}\ell^-\bar{\nu}_\ell$ decays with hadronic tagging at Belle. *Phys. Rev. D* **2015**, *92*, 072014, [arXiv:hep-ex/1507.03233]. doi:10.1103/PhysRevD.92.072014.

158. Abdesselam, A.; others. Measurement of $\mathcal{R}(D)$ and $\mathcal{R}(D^*)$ with a semileptonic tagging method **2019**. [arXiv:hep-ex/1904.08794].

159. Caria, G.; others. Measurement of $\mathcal{R}(D)$ and $\mathcal{R}(D^*)$ with a semileptonic tagging method. *Phys. Rev. Lett.* **2020**, *124*, 161803, [arXiv:hep-ex/1910.05864]. doi:10.1103/PhysRevLett.124.161803.

160. Abudinén, F.; others. Measurement of the $B^0 \to D^{*-}\ell^+\nu_\ell$ branching ratio and $|V_{cb}|$ with a fully reconstructed accompanying B meson in 2019-2021 Belle II data **2023**. [arXiv:hep-ex/2301.04716].

161. Matyja, A.; others. Observation of B0 —> D*- tau+ nu(tau) decay at Belle. *Phys. Rev. Lett.* **2007**, *99*, 191807, [arXiv:hep-ex/0706.4429]. doi:10.1103/PhysRevLett.99.191807.

162. Dungel, W.; others. Measurement of the form factors of the decay B0 -> D*- ell+ nu and determination of the CKM matrix element |Vcb|. *Phys. Rev. D* **2010**, *82*, 112007, [arXiv:hep-ex/1010.5620]. doi:10.1103/PhysRevD.82.112007.

163. Sato, Y.; others. Measurement of the branching ratio of $\bar{B}^0 \to D^{*+}\tau^-\bar{\nu}_\tau$ relative to $\bar{B}^0 \to D^{*+}\ell^-\bar{\nu}_\ell$ decays with a semileptonic tagging method. *Phys. Rev. D* **2016**, *94*, 072007, [arXiv:hep-ex/1607.07923]. doi:10.1103/PhysRevD.94.072007.

164. Hirose, S.; others. Measurement of the τ lepton polarization and $R(D^*)$ in the decay $\bar{B} \to D^*\tau^-\bar{\nu}_\tau$. *Phys. Rev. Lett.* **2017**, *118*, 211801, [arXiv:hep-ex/1612.00529]. doi:10.1103/PhysRevLett.118.211801.

165. Hirose, S.; others. Measurement of the τ lepton polarization and $R(D^*)$ in the decay $\bar{B} \to D^*\tau^-\bar{\nu}_\tau$ with one-prong hadronic τ decays at Belle. *Phys. Rev. D* **2018**, *97*, 012004, [arXiv:hep-ex/1709.00129]. doi:10.1103/PhysRevD.97.012004.

166. Waheed, E.; others. Measurement of the CKM matrix element $|V_{cb}|$ from $B^0 \to D^{*-}\ell^+\nu_\ell$ at Belle. *Phys. Rev. D* **2019**, *100*, 052007, [arXiv:hep-ex/1809.03290]. [Erratum: Phys.Rev.D 103, 079901 (2021)], doi:10.1103/PhysRevD.100.052007.

167. Glattauer, R.; others. Measurement of the decay $B \to D\ell\nu_\ell$ in fully reconstructed events and determination of the Cabibbo-Kobayashi-Maskawa matrix element $|V_{cb}|$. *Phys. Rev. D* **2016**, *93*, 032006, [arXiv:hep-ex/1510.03657]. doi:10.1103/PhysRevD.93.032006.

168. Abudinén, F.; others. Determination of $|V_{cb}|$ from $B \to D\ell\nu$ decays using 2019-2021 Belle II data **2022**. [arXiv:hep-ex/2210.13143].

169. Meier, F.; others. First observation of $B \to \bar{D}_1(\to \bar{D}\pi^+\pi^-)\ell^+\nu_\ell$ and measurement of the $B \to \bar{D}^{(*)}\pi\ell^+\nu_\ell$ and $B \to \bar{D}^{(*)}\pi^+\pi^-\ell^+\nu_\ell$ branching fractions with hadronic tagging at Belle **2022**. [arXiv:hep-ex/2211.09833].

170. Abe, K.; others. Observation of the decay $B \to K\ell^+\ell^-$. *Phys. Rev. Lett.* **2002**, *88*, 021801, [hep-ex/0109026]. doi:10.1103/PhysRevLett.88.021801.

171. Choudhury, S.; others. Test of lepton flavor universality and search for lepton flavor violation in $B \to K\ell\ell$ decays. *JHEP* **2021**, *03*, 105, [arXiv:hep-ex/1908.01848]. doi:10.1007/JHEP03(2021)105.

172. Ishikawa, A.; others. Measurement of Forward-Backward Asymmetry and Wilson Coefficients in B —> K* l+ l-. *Phys. Rev. Lett.* **2006**, *96*, 251801, [hep-ex/0603018]. doi:10.1103/PhysRevLett.96.251801.

173. Wehle, S.; others. Lepton-Flavor-Dependent Angular Analysis of $B \to K^*\ell^+\ell^-$. *Phys. Rev. Lett.* **2017**, *118*, 111801, [arXiv:hep-ex/1612.05014]. doi:10.1103/PhysRevLett.118.111801.

174. Abdesselam, A.; others. Test of Lepton-Flavor Universality in $B \to K^*\ell^+\ell^-$ Decays at Belle. *Phys. Rev. Lett.* **2021**, *126*, 161801, [arXiv:hep-ex/1904.02440]. doi:10.1103/PhysRevLett.126.161801.

175. Wei, J.T.; others. Measurement of the Differential Branching Fraction and Forward-Backward Asymmetry for $B \to K^{(*)}\ell^+\ell^-$. *Phys. Rev. Lett.* **2009**, *103*, 171801, [arXiv:hep-ex/0904.0770]. doi:10.1103/PhysRevLett.103.171801.

176. Ha, H.; others. Measurement of the decay $B^0 \to \pi^-\ell^+\nu$ and determination of $|V_{ub}|$. *Phys. Rev. D* **2011**, *83*, 071101, [arXiv:hep-ex/1012.0090]. doi:10.1103/PhysRevD.83.071101.

177. Adamczyk, K.; others. Determination of $|V_{ub}|$ from untagged $B^0 \to \pi^-\ell^+\nu_\ell$ decays using 2019-2021 Belle II data **2022**. [arXiv:hep-ex/2210.04224].

178. Abudinén, F.; others. Reconstruction of $B \to \rho\ell\nu_\ell$ decays identified using hadronic decays of the recoil B meson in 2019 – 2021 Belle II data **2022**. [arXiv:hep-ex/2211.15270].

179. Gebauer, U.; others. Measurement of the branching fractions of the $B^+ \to \eta\ell^+\nu_\ell$ and $B^+ \to \eta'\ell^+\nu_\ell$ decays with signal-side only reconstruction in the full q2 range. *Phys. Rev. D* **2022**, *106*, 032013, [arXiv:hep-ex/2104.13354]. doi:10.1103/PhysRevD.106.032013.

180. Kaneko, J.; others. Measurement of the electroweak penguin process B —> X(s) l+ l-. *Phys. Rev. Lett.* **2003**, *90*, 021801, [hep-ex/0208029]. doi:10.1103/PhysRevLett.90.021801.

181. Iwasaki, M.; others. Improved measurement of the electroweak penguin process $B \to X_s l^+ l^-$. *Phys. Rev. D* **2005**, *72*, 092005, [hep-ex/0503044]. doi:10.1103/PhysRevD.72.092005.

182. Cao, L.; others. Measurement of Differential Branching Fractions of Inclusive $B \to X_u\,\ell^+\,\nu_\ell$ Decays. *Phys. Rev. Lett.* **2021**, *127*, 261801, [arXiv:hep-ex/2107.13855]. doi:10.1103/PhysRevLett.127.261801.

183. Cao, L.; others. Measurements of Partial Branching Fractions of Inclusive $B \to X_u\,\ell^+\,\nu_\ell$ Decays with Hadronic Tagging. *Phys. Rev. D* **2021**, *104*, 012008, [arXiv:hep-ex/2102.00020]. doi:10.1103/PhysRevD.104.012008.

184. Sibidanov, A.; others. Study of Exclusive $B \to X_u\ell\nu$ Decays and Extraction of $\|V_{ub}\|$ using Full Reconstruction Tagging at the Belle Experiment. *Phys. Rev. D* **2013**, *88*, 032005, [arXiv:hep-ex/1306.2781]. doi:10.1103/PhysRevD.88.032005.

185. van Tonder, R.; others. Measurements of q^2 Moments of Inclusive $B \to X_c\ell^+\nu_\ell$ Decays with Hadronic Tagging. *Phys. Rev. D* **2021**, *104*, 112011, [arXiv:hep-ex/2109.01685]. doi:10.1103/PhysRevD.104.112011.

186. Abudinén, F.; others. Measurement of lepton mass squared moments in $B\,to X_c\ell\nu\ell$ decays with the Belle II experiment. *Phys. Rev. D* **2023**, *107*, 072002. doi:10.1103/PhysRevD.107.072002.

187. Aggarwal, L.; others. A test of light-lepton universality in the rates of inclusive semileptonic B-meson decays at Belle II **2023**. [arXiv:hep-ex/2301.08266].

188. Altmannshofer, W.; Ball, P.; Bharucha, A.; Buras, A.J.; Straub, D.M.; Wick, M. Symmetries and Asymmetries of $B \to K^* \mu^+ \mu^-$ Decays in the Standard Model and Beyond. *JHEP* **2009**, *01*, 019, [arXiv:hep-ph/0811.1214]. doi:10.1088/1126-6708/2009/01/019.

189. Calibbi, L.; Signorelli, G. Charged Lepton Flavour Violation: An Experimental and Theoretical Introduction. *Riv. Nuovo Cim.* **2018**, *41*, 71–174, [arXiv:hep-ph/1709.00294]. doi:10.1393/ncr/i2018-10144-0.

190. Blake, T.; Lanfranchi, G.; Straub, D.M. Rare *B* Decays as Tests of the Standard Model. *Prog. Part. Nucl. Phys.* **2017**, *92*, 50–91, [arXiv:hep-ph/1606.00916]. doi:10.1016/j.ppnp.2016.10.001.

191. Bifani, S.; Descotes-Genon, S.; Romero Vidal, A.; Schune, M.H. Review of Lepton Universality tests in *B* decays. *J. Phys. G* **2019**, *46*, 023001, [arXiv:hep-ex/1809.06229]. doi:10.1088/1361-6471/aaf5de.

192. Cornella, C.; Faroughy, D.A.; Fuentes-Martin, J.; Isidori, G.; Neubert, M. Reading the footprints of the B-meson flavor anomalies. *JHEP* **2021**, *08*, 050, [arXiv:hep-ph/2103.16558]. doi:10.1007/JHEP08(2021)050.

193. London, D.; Matias, J. *B* Flavour Anomalies: 2021 Theoretical Status Report. *Ann. Rev. Nucl. Part. Sci.* **2022**, *72*, 37–68, [arXiv:hep-ph/2110.13270]. doi:10.1146/annurev-nucl-102020-090209.

194. Isgur, N.; Scora, D.; Grinstein, B.; Wise, M.B. Semileptonic B and D Decays in the Quark Model. *Phys. Rev. D* **1989**, *39*, 799–818. doi:10.1103/PhysRevD.39.799.

195. Scora, D.; Isgur, N. Semileptonic meson decays in the quark model: An update. *Phys. Rev. D* **1995**, *52*, 2783–2812, [hep-ph/9503486]. doi:10.1103/PhysRevD.52.2783.

196. Boyd, C.G.; Grinstein, B.; Lebed, R.F. Model independent determinations of anti-B —> D (lepton), D* (lepton) anti-neutrino form-factors. *Nucl. Phys. B* **1996**, *461*, 493–511, [hep-ph/9508211]. doi:10.1016/0550-3213(95)00653-2.

197. Boyd, C.G.; Grinstein, B.; Lebed, R.F. Precision corrections to dispersive bounds on form-factors. *Phys. Rev. D* **1997**, *56*, 6895–6911, [hep-ph/9705252]. doi:10.1103/PhysRevD.56.6895.

198. Caprini, I.; Lellouch, L.; Neubert, M. Dispersive bounds on the shape of anti-B —> D(*) lepton anti-neutrino form-factors. *Nucl. Phys. B* **1998**, *530*, 153–181, [hep-ph/9712417]. doi:10.1016/S0550-3213(98)00350-2.

199. Ball, P.; Zwicky, R. $B_{d,s} \to \rho, \omega, K^*, \phi$ decay form-factors from light-cone sum rules revisited. *Phys. Rev. D* **2005**, *71*, 014029, [hep-ph/0412079]. doi:10.1103/PhysRevD.71.014029.

200. Bobeth, C.; Hiller, G.; Piranishvili, G. Angular distributions of $\bar{B} \to \bar{K} \ell^+ \ell^-$ decays. *JHEP* **2007**, *12*, 040, [arXiv:hep-ph/0709.4174]. doi:10.1088/1126-6708/2007/12/040.

201. Khodjamirian, A.; Mannel, T.; Pivovarov, A.A.; Wang, Y.M. Charm-loop effect in $B \to K^{(*)} \ell^+ \ell^-$ and $B \to K^* \gamma$. *JHEP* **2010**, *09*, 089, [arXiv:hep-ph/1006.4945]. doi:10.1007/JHEP09(2010)089.

202. Bailey, J.A.; others. Update of $|V_{cb}|$ from the $\bar{B} \to D^* \ell \bar{\nu}$ form factor at zero recoil with three-flavor lattice QCD. *Phys. Rev. D* **2014**, *89*, 114504, [arXiv:hep-lat/1403.0635]. doi:10.1103/PhysRevD.89.114504.

203. Na, H.; Bouchard, C.M.; Lepage, G.P.; Monahan, C.; Shigemitsu, J. $B \to D l \nu$ form factors at nonzero recoil and extraction of $|V_{cb}|$. *Phys. Rev. D* **2015**, *92*, 054510, [arXiv:hep-lat/1505.03925]. [Erratum: Phys.Rev.D 93, 119906 (2016)], doi:10.1103/PhysRevD.93.119906.

204. Harrison, J.; Davies, C.; Wingate, M. Lattice QCD calculation of the $B_{(s)} \to D^*_{(s)} \ell \nu$ form factors at zero recoil and implications for $|V_{cb}|$. *Phys. Rev. D* **2018**, *97*, 054502, [arXiv:hep-lat/1711.11013]. doi:10.1103/PhysRevD.97.054502.

205. Du, D.; El-Khadra, A.X.; Gottlieb, S.; Kronfeld, A.S.; Laiho, J.; Lunghi, E.; Van de Water, R.S.; Zhou, R. Phenomenology of semileptonic B-meson decays with form factors from lattice QCD. *Phys. Rev. D* **2016**, *93*, 034005, [arXiv:hep-ph/1510.02349]. doi:10.1103/PhysRevD.93.034005.

206. Alberti, A.; Gambino, P.; Healey, K.J.; Nandi, S. Precision Determination of the Cabibbo-Kobayashi-Maskawa Element V_{cb}. *Phys. Rev. Lett.* **2015**, *114*, 061802, [arXiv:hep-ph/1411.6560]. doi:10.1103/PhysRevLett.114.061802.

207. Bharucha, A.; Straub, D.M.; Zwicky, R. $B \to V \ell^+ \ell^-$ in the Standard Model from light-cone sum rules. *JHEP* **2016**, *08*, 098, [arXiv:hep-ph/1503.05534]. doi:10.1007/JHEP08(2016)098.

208. Bigi, D.; Gambino, P. Revisiting $B \to D \ell \nu$. *Phys. Rev. D* **2016**, *94*, 094008, [arXiv:hep-ph/1606.08030]. doi:10.1103/PhysRevD.94.094008.

209. Bordone, M.; Isidori, G.; Pattori, A. On the Standard Model predictions for R_K and R_{K^*}. *Eur. Phys. J. C* **2016**, *76*, 440, [arXiv:hep-ph/1605.07633]. doi:10.1140/epjc/s10052-016-4274-7.

210. Jäger, S.; Martin Camalich, J. Reassessing the discovery potential of the $B \to K^* \ell^+ \ell^-$ decays in the large-recoil region: SM challenges and BSM opportunities. *Phys. Rev. D* **2016**, *93*, 014028, [arXiv:hep-ph/1412.3183]. doi:10.1103/PhysRevD.93.014028.

211. Capdevila, B.; Descotes-Genon, S.; Hofer, L.; Matias, J. Hadronic uncertainties in $B \to K^* \mu^+ \mu^-$: a state-of-the-art analysis. *JHEP* **2017**, *04*, 016, [arXiv:hep-ph/1701.08672]. doi:10.1007/JHEP04(2017)016.

212. Bigi, D.; Gambino, P.; Schacht, S. $R(D^*)$, $|V_{cb}|$, and the Heavy Quark Symmetry relations between form factors. *JHEP* **2017**, *11*, 061, [arXiv:hep-ph/1707.09509]. doi:10.1007/JHEP11(2017)061.

213. Jaiswal, S.; Nandi, S.; Patra, S.K. Extraction of $|V_{cb}|$ from $B \to D^{(*)}\ell\nu_\ell$ and the Standard Model predictions of $R(D^{(*)})$. *JHEP* **2017**, *12*, 060, [arXiv:hep-ph/1707.09977]. doi:10.1007/JHEP12(2017)060.

214. Isidori, G.; Nabeebaccus, S.; Zwicky, R. QED corrections in $\overline{B} \to \overline{K}\ell^+\ell^-$ at the double-differential level. *JHEP* **2020**, *12*, 104, [arXiv:hep-ph/2009.00929]. doi:10.1007/JHEP12(2020)104.

215. Gubernari, N.; van Dyk, D.; Virto, J. Non-local matrix elements in $B_{(s)} \to \{K^{(*)}, \phi\}\ell^+\ell^-$. *JHEP* **2021**, *02*, 088, [arXiv:hep-ph/2011.09813]. doi:10.1007/JHEP02(2021)088.

216. Iguro, S.; Kitahara, T.; Watanabe, R. Global fit to $b \to c\tau\nu$ anomalies 2022 mid-autumn **2022**. [arXiv:hep-ph/2210.10751].

217. Hiller, G.; Kruger, F. More model-independent analysis of $b \to s$ processes. *Phys. Rev. D* **2004**, *69*, 074020, [hep-ph/0310219]. doi:10.1103/PhysRevD.69.074020.

218. Fajfer, S.; Kamenik, J.F.; Nisandzic, I. On the $B \to D^*\tau\bar{\nu}_\tau$ Sensitivity to New Physics. *Phys. Rev. D* **2012**, *85*, 094025, [arXiv:hep-ph/1203.2654]. doi:10.1103/PhysRevD.85.094025.

219. Hiller, G.; Schmaltz, M. R_K and future $b \to s\ell\ell$ physics beyond the standard model opportunities. *Phys. Rev. D* **2014**, *90*, 054014, [arXiv:hep-ph/1408.1627]. doi:10.1103/PhysRevD.90.054014.

220. Fajfer, S.; Košnik, N. Vector leptoquark resolution of R_K and $R_{D^{(*)}}$ puzzles. *Phys. Lett. B* **2016**, *755*, 270–274, [arXiv:hep-ph/1511.06024]. doi:10.1016/j.physletb.2016.02.018.

221. Crivellin, A.; Müller, D.; Ota, T. Simultaneous explanation of $R(D^{(*)})$ and $b \to s\mu^+\mu^-$: the last scalar leptoquarks standing. *JHEP* **2017**, *09*, 040, [arXiv:hep-ph/1703.09226]. doi:10.1007/JHEP09(2017)040.

222. Angelescu, A.; Bečirević, D.; Faroughy, D.A.; Jaffredo, F.; Sumensari, O. Single leptoquark solutions to the B-physics anomalies. *Phys. Rev. D* **2021**, *104*, 055017, [arXiv:hep-ph/2103.12504]. doi:10.1103/PhysRevD.104.055017.

223. Abada, A.; Krauss, M.E.; Porod, W.; Staub, F.; Vicente, A.; Weiland, C. Lepton flavor violation in low-scale seesaw models: SUSY and non-SUSY contributions. *JHEP* **2014**, *11*, 048, [arXiv:hep-ph/1408.0138]. doi:10.1007/JHEP11(2014)048.

224. Gripaios, B.; Nardecchia, M.; Renner, S.A. Composite leptoquarks and anomalies in *B*-meson decays. *JHEP* **2015**, *05*, 006, [arXiv:hep-ph/1412.1791]. doi:10.1007/JHEP05(2015)006.

225. Crivellin, A.; D'Ambrosio, G.; Heeck, J. Explaining $h \to \mu^\pm\tau^\mp$, $B \to K^*\mu^+\mu^-$ and $B \to K\mu^+\mu^-/B \to Ke^+e^-$ in a two-Higgs-doublet model with gauged $L_\mu - L_\tau$. *Phys. Rev. Lett.* **2015**, *114*, 151801, [arXiv:hep-ph/1501.00993]. doi:10.1103/PhysRevLett.114.151801.

226. Descotes-Genon, S.; Hofer, L.; Matias, J.; Virto, J. Global analysis of $b \to s\ell\ell$ anomalies. *JHEP* **2016**, *06*, 092, [arXiv:hep-ph/1510.04239]. doi:10.1007/JHEP06(2016)092.

227. Altmannshofer, W.; Stangl, P.; Straub, D.M. Interpreting Hints for Lepton Flavor Universality Violation. *Phys. Rev. D* **2017**, *96*, 055008, [arXiv:hep-ph/1704.05435]. doi:10.1103/PhysRevD.96.055008.

228. Algueró, M.; Capdevila, B.; Crivellin, A.; Descotes-Genon, S.; Masjuan, P.; Matias, J.; Novoa Brunet, M.; Virto, J. Emerging patterns of New Physics with and without Lepton Flavour Universal contributions. *Eur. Phys. J. C* **2019**, *79*, 714, [arXiv:hep-ph/1903.09578]. [Addendum: Eur.Phys.J.C 80, 511 (2020)], doi:10.1140/epjc/s10052-019-7216-3.

229. Hurth, T.; Mahmoudi, F.; Santos, D.M.; Neshatpour, S. More Indications for Lepton Nonuniversality in $b \to s\ell^+\ell^-$. *Phys. Lett. B* **2022**, *824*, 136838, [arXiv:hep-ph/2104.10058]. doi:10.1016/j.physletb.2021.136838.

230. Dubnička, S.; Dubničková, A.Z.; Issadykov, A.; Ivanov, M.A.; Liptaj, A.; Sakhiyev, S.K. Decay $B_s \to \phi\ell^+\ell^-$ in covariant quark model. *Phys. Rev. D* **2016**, *93*, 094022, [arXiv:hep-ph/1602.07864]. doi:10.1103/PhysRevD.93.094022.

231. Aaij, R.; others. Angular analysis of the rare decay $B_s^0 \to \phi\mu^+\mu^-$. *JHEP* **2021**, *11*, 043, [arXiv:hep-ex/2107.13428]. doi:10.1007/JHEP11(2021)043.

232. Asatryan, H.H.; Asatrian, H.M.; Greub, C.; Walker, M. Calculation of two loop virtual corrections to $b \to sl^+l^-$ in the standard model. *Phys. Rev. D* **2002**, *65*, 074004, [hep-ph/0109140]. doi:10.1103/PhysRevD.65.074004.

233. Greub, C.; Pilipp, V.; Schupbach, C. Analytic calculation of two-loop QCD corrections to $b \to sl^+l^-$ in the high q^2 region. *JHEP* **2008**, *12*, 040, [arXiv:hep-ph/0810.4077]. doi:10.1088/1126-6708/2008/12/040.

234.   Aaboud, M.; others. Angular analysis of $B_d^0 \to K^* \mu^+ \mu^-$ decays in pp collisions at $\sqrt{s} = 8$ TeV with the ATLAS detector. *JHEP* **2018**, *10*, 047, [arXiv:hep-ex/1805.04000]. doi:10.1007/JHEP10(2018)047.

235.   Ivanov, M.A.; Khomutenko, O.E. B and D meson decays with taking into account confinement of light quarks. *Sov. J. Nucl. Phys.* **1991**, *53*, 337–342.

236.   Ivanov, M.A.; Khomutenko, O.E.; Mizutani, T. Form-factors of semileptonic decays of heavy mesons in the quark confinement model. *Phys. Rev. D* **1992**, *46*, 3817–3831. doi:10.1103/PhysRevD.46.3817.

237.   Ivanov, M.A.; Santorelli, P. Leptonic and semileptonic decays of pseudoscalar mesons. *Phys. Lett. B* **1999**, *456*, 248–255, [hep-ph/9903446]. doi:10.1016/S0370-2693(99)00474-8.

238.   Ivanov, M.A.; Santorelli, P.; Tancredi, N. The Semileptonic form-factors of B and D mesons in the quark confinement model. *Eur. Phys. J. A* **2000**, *9*, 109–114, [hep-ph/9905209]. doi:10.1007/s100500070060.

239.   Ivanov, M.A.; Korner, J.G.; Santorelli, P. The Semileptonic decays of the B_c meson. *Phys. Rev. D* **2001**, *63*, 074010, [hep-ph/0007169]. doi:10.1103/PhysRevD.63.074010.

240.   Faessler, A.; Gutsche, T.; Ivanov, M.A.; Korner, J.G.; Lyubovitskij, V.E. The Exclusive rare decays $B \to$ K(K*) $\bar{\ell}\ell$ and $B_c \to$ D(D*) $\bar{\ell}\ell$ in a relativistic quark model. *Eur. Phys. J. direct* **2002**, *4*, 18, [hep-ph/0205287]. doi:10.1007/s1010502c0018.

241.   Ivanov, M.A.; Lyubovitskij, V.E. Exclusive rare decays of B and B_c mesons in a relativistic quark model. *Lect. Notes Phys.* **2004**, *647*, 245–263, [hep-ph/0211077]. doi:10.1007/978-3-540-40975-5_9.

242.   Ivanov, M.A.; Korner, J.G.; Santorelli, P. Semileptonic decays of B_c mesons into charmonium states in a relativistic quark model. *Phys. Rev. D* **2005**, *71*, 094006, [hep-ph/0501051]. [Erratum: Phys.Rev.D 75, 019901 (2007)], doi:10.1103/PhysRevD.75.019901.

243.   Ivanov, M.A.; Korner, J.G.; Santorelli, P. Exclusive semileptonic and nonleptonic decays of the B_c meson. *Phys. Rev. D* **2006**, *73*, 054024, [hep-ph/0602050]. doi:10.1103/PhysRevD.73.054024.

244.   Ivanov, M.A.; Korner, J.G.; Kovalenko, S.G.; Santorelli, P.; Saidullaeva, G.G. Form factors for semileptonic, nonleptonic and rare B (B_s) meson decays. *Phys. Rev. D* **2012**, *85*, 034004, [arXiv:hep-ph/1112.3536]. doi:10.1103/PhysRevD.85.034004.

245.   Dineykhan, M.; Ivanov, M.A.; Saidullaeva, G.G. Exotic states and rare B/s-decays in the covariant quark model. *Phys. Part. Nucl.* **2012**, *43*, 749–782. doi:10.1134/S1063779612060032.

246.   Issadykov, A.; Ivanov, M.A.; Sakhiyev, S.K. Form factors of the B-S-transitions in the covariant quark model. *Phys. Rev. D* **2015**, *91*, 074007, [arXiv:hep-ph/1502.05280]. doi:10.1103/PhysRevD.91.074007.

247.   Ivanov, M.A.; Körner, J.G.; Tran, C.T. Analyzing new physics in the decays $\bar{B}^0 \to D^{(*)}\tau^-\bar{\nu}_\tau$ with form factors obtained from the covariant quark model. *Phys. Rev. D* **2016**, *94*, 094028, [arXiv:hep-ph/1607.02932]. doi:10.1103/PhysRevD.94.094028.

248.   Ivanov, M.A.; Körner, J.G.; Tran, C.T. Probing new physics in $\bar{B}^0 \to D^{(*)}\tau^-\bar{\nu}_\tau$ using the longitudinal, transverse, and normal polarization components of the tau lepton. *Phys. Rev. D* **2017**, *95*, 036021, [arXiv:hep-ph/1701.02937]. doi:10.1103/PhysRevD.95.036021.

249.   Tran, C.T.; Ivanov, M.A.; Körner, J.G.; Santorelli, P. Implications of new physics in the decays $B_c \to (J/\psi, \eta_c)\tau\nu$. *Phys. Rev. D* **2018**, *97*, 054014, [arXiv:hep-ph/1801.06927]. doi:10.1103/PhysRevD.97.054014.

250.   Issadykov, A.; Ivanov, M.A. The decays $B_c \to J/\psi + \bar{\ell}\nu_\ell$ and $B_c \to J/\psi + \pi(K)$ in covariant confined quark model. *Phys. Lett. B* **2018**, *783*, 178–182, [arXiv:hep-ph/1804.00472]. doi:10.1016/j.physletb.2018.06.056.

251.   Issadykov, A.; Ivanov, M.A. b-s Anomaly Decays in Covariant Quark Model. *Phys. Part. Nucl. Lett.* **2018**, *15*, 393–396, [arXiv:hep-ph/1807.04996]. doi:10.1134/S1547477118040118.

252.   Issadykov, A.; Ivanov, M.A. $B \to K^{(*)}\nu\bar{\nu}$ in covariant confined quark model. *Mod. Phys. Lett. A* **2023**, *38*, 2350006, [arXiv:hep-ph/2211.10683]. doi:10.1142/S0217732323500062.

253.   Aaij, R.; others. First observation of $B_s^0 \to J/\psi f_0(980)$ decays. *Phys. Lett. B* **2011**, *698*, 115–122, [arXiv:hep-ex/1102.0206]. doi:10.1016/j.physletb.2011.03.006.

254.   Aaij, R.; others. Observation of $B_c^+ \to J/\psi D_s^+$ and $B_c^+ \to J/\psi D_s^{*+}$ decays. *Phys. Rev. D* **2013**, *87*, 112012, [arXiv:hep-ex/1304.4530]. [Addendum: Phys.Rev.D 89, 019901 (2014)], doi:10.1103/PhysRevD.87.112012.

255.   Aaij, R.; others. Observation of the Decay $B_c^+ \to B_s^0\pi^+$. *Phys. Rev. Lett.* **2013**, *111*, 181801, [arXiv:hep-ex/1308.4544]. doi:10.1103/PhysRevLett.111.181801.

256.   First observation of the $B^+ \to D_s^+ D_s^- K^+$ decay **2022**. [arXiv:hep-ex/2211.05034].

257.   Observation of the $B_s^0 \to D^{*+}D^{*-}$ decay **2022**. [arXiv:hep-ex/2210.14945].

258.   Observation of the $B^+ \to J/\psi\eta' K^+$ decay **2023**. [arXiv:hep-ex/2303.09443].

259.   Observation of the $B_s^0 \to \chi_{c1}(3872)\pi^+\pi^-$ decay **2023**. [arXiv:hep-ex/2302.10629].

260. Aaij, R.; others. Determination of the X(3872) meson quantum numbers. *Phys. Rev. Lett.* **2013**, *110*, 222001, [arXiv:hep-ex/1302.6269]. doi:10.1103/PhysRevLett.110.222001.

261. Aaij, R.; others. Analysis of the resonant components in $B_s \to J/\psi \pi^+ \pi^-$. *Phys. Rev. D* **2012**, *86*, 052006, [arXiv:hep-ex/1204.5643]. doi:10.1103/PhysRevD.86.052006.

262. Aaij, R.; others. Measurement of resonant and CP components in $\bar{B}_s^0 \to J/\psi \pi^+ \pi^-$ decays. *Phys. Rev. D* **2014**, *89*, 092006, [arXiv:hep-ex/1402.6248]. doi:10.1103/PhysRevD.89.092006.

263. Aaij, R.; others. Measurement of the resonant and CP components in $\overline{B}^0 \to J/\psi \pi^+ \pi^-$ decays. *Phys. Rev. D* **2014**, *90*, 012003, [arXiv:hep-ex/1404.5673]. doi:10.1103/PhysRevD.90.012003.

264. Aaij, R.; others. Observation of $J/\psi \phi$ structures consistent with exotic states from amplitude analysis of $B^+ \to J/\psi \phi K^+$ decays. *Phys. Rev. Lett.* **2017**, *118*, 022003, [arXiv:hep-ex/1606.07895]. doi:10.1103/PhysRevLett.118.022003.

265. Aaij, R.; others. Observation of New Resonances Decaying to $J/\psi K^+ +$ and $J/\psi \phi$. *Phys. Rev. Lett.* **2021**, *127*, 082001, [arXiv:hep-ex/2103.01803]. doi:10.1103/PhysRevLett.127.082001.

266. Observation of a $J/\psi \Lambda$ resonance consistent with a strange pentaquark candidate in $B^- \to J/\psi \Lambda \bar{p}$ decays **2022**. [arXiv:hep-ex/2210.10346].

267. Observation of a resonant structure near the $D_s^+ D_s^-$ threshold in the $B^+ \to D_s^+ D_s^- K^+$ decay **2022**. [arXiv:hep-ex/2210.15153].

268. Aaij, R.; others. A model-independent study of resonant structure in $B^+ \to D^+ D^- K^+$ decays. *Phys. Rev. Lett.* **2020**, *125*, 242001, [arXiv:hep-ex/2009.00025]. doi:10.1103/PhysRevLett.125.242001.

269. Aaij, R.; others. Evidence for a new structure in the $J/\psi p$ and $J/\psi \bar{p}$ systems in $B_s^0 \to J/\psi p \bar{p}$ decays. *Phys. Rev. Lett.* **2022**, *128*, 062001, [arXiv:hep-ex/2108.04720]. doi:10.1103/PhysRevLett.128.062001.

270. Evidence of a $J/\psi K_S^0$ structure in $B^0 \to J/\psi \phi K_S^0$ decays **2023**. [arXiv:hep-ex/2301.04899].

271. Aaij, R.; others. Dalitz plot analysis of $B_s^0 \to \bar{D}^0 K^- \pi^+$ decays. *Phys. Rev. D* **2014**, *90*, 072003, [arXiv:hep-ex/1407.7712]. doi:10.1103/PhysRevD.90.072003.

272. Aaij, R.; others. Dalitz plot analysis of $B^0 \to \overline{D}^0 \pi^+ \pi^-$ decays. *Phys. Rev. D* **2015**, *92*, 032002, [arXiv:hep-ex/1505.01710]. doi:10.1103/PhysRevD.92.032002.

273. Aaij, R.; others. Amplitude analysis of $B^- \to D^+ \pi^- \pi^-$ decays. *Phys. Rev. D* **2016**, *94*, 072001, [arXiv:hep-ex/1608.01289]. doi:10.1103/PhysRevD.94.072001.

274. Aaij, R.; others. Amplitude analysis of $B^+ \to J/\psi \phi K^+$ decays. *Phys. Rev. D* **2017**, *95*, 012002, [arXiv:hep-ex/1606.07898]. doi:10.1103/PhysRevD.95.012002.

275. Aaij, R.; others. Amplitude analysis of the $B^+ \to D^+ D^- K^+$ decay. *Phys. Rev. D* **2020**, *102*, 112003, [arXiv:hep-ex/2009.00026]. doi:10.1103/PhysRevD.102.112003.

276. Amplitude analysis of the $D_s^+ \to \pi^- \pi^+ \pi^+$ decay **2022**. [arXiv:hep-ex/2209.09840].

277. Amplitude analysis of $B^0 \to \overline{D}^0 D_s^+ \pi^-$ and $B^+ \to D^- D_s^+ \pi^+$ decays **2022**. [arXiv:hep-ex/2212.02717].

278. Aaij, R.; others. Measurement of the CP-violating phase ϕ_s in the decay $B_s^0 \to J/\psi \phi$. *Phys. Rev. Lett.* **2012**, *108*, 101803, [arXiv:hep-ex/1112.3183]. doi:10.1103/PhysRevLett.108.101803.

279. Aaij, R.; others. First evidence of direct *CP* violation in charmless two-body decays of B_s^0 mesons. *Phys. Rev. Lett.* **2012**, *108*, 201601, [arXiv:hep-ex/1202.6251]. doi:10.1103/PhysRevLett.108.201601.

280. Aaij, R.; others. Measurement of the $B_s^0 - \bar{B}_s^0$ oscillation frequency Δm_s in $B_s^0 \to D_s^-(3)\pi$ decays. *Phys. Lett. B* **2012**, *709*, 177–184, [arXiv:hep-ex/1112.4311]. doi:10.1016/j.physletb.2012.02.031.

281. Aaij, R.; others. Measurement of CP violation in the phase space of $B^\pm \to K^\pm \pi^+ \pi^-$ and $B^\pm \to K^\pm K^+ K^-$ decays. *Phys. Rev. Lett.* **2013**, *111*, 101801, [arXiv:hep-ex/1306.1246]. doi:10.1103/PhysRevLett.111.101801.

282. Aaij, R.; others. Measurement of CP violation in the phase space of $B^\pm \to K^+ K^- \pi^\pm$ and $B^\pm \to \pi^+ \pi^- \pi^\pm$ decays. *Phys. Rev. Lett.* **2014**, *112*, 011801, [arXiv:hep-ex/1310.4740]. doi:10.1103/PhysRevLett.112.011801.

283. Aaij, R.; others. Precision measurement of the B_s^0-$\bar{B}_s^0$ oscillation frequency with the decay $B_s^0 \to D_s^- \pi^+$. *New J. Phys.* **2013**, *15*, 053021, [arXiv:hep-ex/1304.4741]. doi:10.1088/1367-2630/15/5/053021.

284. Aaij, R.; others. Observation of CP violation in $B^\pm \to DK^\pm$ decays. *Phys. Lett. B* **2012**, *712*, 203–212, [arXiv:hep-ex/1203.3662]. [Erratum: Phys.Lett.B 713, 351 (2012)], doi:10.1016/j.physletb.2012.04.060.

285. Aaij, R.; others. First observation of *CP* violation in the decays of B_s^0 mesons. *Phys. Rev. Lett.* **2013**, *110*, 221601, [arXiv:hep-ex/1304.6173]. doi:10.1103/PhysRevLett.110.221601.

286. Aaij, R.; others. Measurement of CP violation and the B_s^0 meson decay width difference with $B_s^0 \to J/\psi K^+ K^-$ and $B_s^0 \to J/\psi \pi^+ \pi^-$ decays. *Phys. Rev. D* **2013**, *87*, 112010, [arXiv:hep-ex/1304.2600]. doi:10.1103/PhysRevD.87.112010.

287. Aaij, R.; others. Measurement of the CP-violating phase ϕ_s in $\overline{B}_s^0 \to J/\psi \pi^+ \pi^-$ decays. *Phys. Lett. B* **2014**, *736*, 186–195, [arXiv:hep-ex/1405.4140]. doi:10.1016/j.physletb.2014.06.079.

288. Aaij, R.; others. Measurement of *CP* violation in $B^0 \to J/\psi K_S^0$ decays. *Phys. Rev. Lett.* **2015**, *115*, 031601, [arXiv:hep-ex/1503.07089]. doi:10.1103/PhysRevLett.115.031601.

289. Aaij, R.; others. Precision measurement of *CP* violation in $B_s^0 \to J/\psi K^+ K^-$ decays. *Phys. Rev. Lett.* **2015**, *114*, 041801, [arXiv:hep-ex/1411.3104]. doi:10.1103/PhysRevLett.114.041801.

290. Measurement of the CKM angle γ with $B^\pm \to D[K^\mp \pi^\pm \pi^\pm \pi^\mp] h^\pm$ decays using a binned phase-space approach **2022**. [arXiv:hep-ex/2209.03692].

291. A study of *CP* violation in the decays $B^\pm \to [K^+ K^- \pi^+ \pi^-]_D h^\pm$ ($h = K, \pi$) and $B^\pm \to [\pi^+ \pi^- \pi^+ \pi^-]_D h^\pm$ **2023**. [arXiv:hep-ex/2301.10328].

292. Aaij, R.; others. Measurements of B_c^+ production and mass with the $B_c^+ \to J/\psi \pi^+$ decay. *Phys. Rev. Lett.* **2012**, *109*, 232001, [arXiv:hep-ex/1209.5634]. doi:10.1103/PhysRevLett.109.232001.

293. Aaij, R.; others. Measurement of *b*-hadron branching fractions for two-body decays into charmless charged hadrons. *JHEP* **2012**, *10*, 037, [arXiv:hep-ex/1206.2794]. doi:10.1007/JHEP10(2012)037.

294. Aaij, R.; others. Measurement of the ratio of branching fractions $BR(B_0 \to K^{*0}\gamma)/BR(B_{s0} \to \phi\gamma)$ and the direct CP asymmetry in $B_0 \to K^{*0}\gamma$. *Nucl. Phys. B* **2013**, *867*, 1–18, [arXiv:hep-ex/1209.0313]. doi:10.1016/j.nuclphysb.2012.09.013.

295. Aaij, R.; others. Measurement of the fragmentation fraction ratio f_s/f_d and its dependence on *B* meson kinematics. *JHEP* **2013**, *04*, 001, [arXiv:hep-ex/1301.5286]. doi:10.1007/JHEP04(2013)001.

296. Aaij, R.; others. Measurement of *b* hadron fractions in 13 TeV *pp* collisions. *Phys. Rev. D* **2019**, *100*, 031102, [arXiv:hep-ex/1902.06794]. doi:10.1103/PhysRevD.100.031102.

297. Aaij, R.; others. Precise measurement of the f_s/f_d ratio of fragmentation fractions and of B_s^0 decay branching fractions. *Phys. Rev. D* **2021**, *104*, 032005, [arXiv:hep-ex/2103.06810]. doi:10.1103/PhysRevD.104.032005.

298. Study of B_c^+ meson decays to charmonia plus multihadron final states **2022**. [arXiv:hep-ex/2208.08660].

299. Measurement of the ratio of branching fractions $\mathcal{B}(B_c^+ \to B_s^0 \pi^+)/\mathcal{B}(B_c^+ \to J/\psi \pi^+)$ **2022**. [arXiv:hep-ex/2210.12000].

300. Study of the $B^- \to \Lambda_c^+ \bar{\Lambda}_c^- K^-$ decay **2022**. [arXiv:hep-ex/2211.00812].

301. Aaij, R.; others. Study of charmonium decays to $K_S^0 K \pi$ in the $B \to (K_S^0 K \pi) K$ channels **2023**. [arXiv:hep-ex/2304.14891].

302. Aubert, B.; others. Observation of CP violation in the B^0 meson system. *Phys. Rev. Lett.* **2001**, *87*, 091801, [hep-ex/0107013]. doi:10.1103/PhysRevLett.87.091801.

303. Aubert, B.; others. Measurement of CP violating asymmetries in B^0 decays to CP eigenstates. *Phys. Rev. Lett.* **2001**, *86*, 2515–2522, [hep-ex/0102030]. doi:10.1103/PhysRevLett.86.2515.

304. Aubert, B.; others. Measurement of sin 2 beta in $B^0 \to \phi K_S^0$. 31st International Conference on High Energy Physics, 2002, [hep-ex/0207070].

305. Aubert, B.; others. A study of time dependent CP-violating asymmetries and flavor oscillations in neutral *B* decays at the $\Upsilon(4S)$. *Phys. Rev. D* **2002**, *66*, 032003, [hep-ex/0201020]. doi:10.1103/PhysRevD.66.032003.

306. Aubert, B.; others. Observation of direct CP violation in $B^0 \to K^+ \pi^-$ decays. *Phys. Rev. Lett.* **2004**, *93*, 131801, [hep-ex/0407057]. doi:10.1103/PhysRevLett.93.131801.

307. Aubert, B.; others. Improved measurement of CP asymmetries in $B^0 \to (c\bar{c}) K^{(*)0}$ decays. *Phys. Rev. Lett.* **2005**, *94*, 161803, [hep-ex/0408127]. doi:10.1103/PhysRevLett.94.161803.

308. Aubert, B.; others. Ambiguity-free measurement of $\cos(2\beta)$: Time-integrated and time-dependent angular analyses of $B \to J/\psi K\pi$. *Phys. Rev. D* **2005**, *71*, 032005, [hep-ex/0411016]. doi:10.1103/PhysRevD.71.032005.

309. Aubert, B.; others. Observation of CP violation in $B^0 \to K^+ \pi^-$ and $B^0 \to \pi^+ \pi^-$. *Phys. Rev. Lett.* **2007**, *99*, 021603, [hep-ex/0703016]. doi:10.1103/PhysRevLett.99.021603.

310. Aubert, B.; others. Measurement of Time-Dependent CP Asymmetry in B0 —> c anti-c K(*)0 Decays. *Phys. Rev. D* **2009**, *79*, 072009, [arXiv:hep-ex/0902.1708]. doi:10.1103/PhysRevD.79.072009.

311. Adachi, I.; others. Measurement of $\cos 2\beta$ in $B^0 \to D^{(*)} h^0$ with $D \to K_S^0 \pi^+ \pi^-$ decays by a combined time-dependent Dalitz plot analysis of BaBar and Belle data. *Phys. Rev. D* **2018**, *98*, 112012, [arXiv:hep-ex/1804.06153]. doi:10.1103/PhysRevD.98.112012.

312.   Aubert, B.; others. Evidence for Direct CP Violation from Dalitz-plot analysis of $B^\pm \to K^\pm \pi^\mp \pi^\pm$. *Phys. Rev. D* **2008**, *78*, 012004, [arXiv:hep-ex/0803.4451]. doi:10.1103/PhysRevD.78.012004.

313.   del Amo Sanchez, P.; others.   Evidence for direct CP violation in the measurement of the Cabibbo-Kobayashi-Maskawa angle gamma with B-+ —> D(*) K(*)-+ decays. *Phys. Rev. Lett.* **2010**, *105*, 121801, [arXiv:hep-ex/1005.1096]. doi:10.1103/PhysRevLett.105.121801.

314.   Lees, J.P.; others.   Study of CP violation in Dalitz-plot analyses of B0 —> K+K-K0(S), B+ —> K+K-K+, and B+ —> K0(S)K0(S)K+. *Phys. Rev. D* **2012**, *85*, 112010, [arXiv:hep-ex/1201.5897]. doi:10.1103/PhysRevD.85.112010.

315.   Lees, J.P.; others.   Measurement of B($B \to X_s\gamma$), the $B \to X_s\gamma$ photon energy spectrum, and the direct CP asymmetry in $B \to X_{s+d}\gamma$ decays. *Phys. Rev. D* **2012**, *86*, 112008, [arXiv:hep-ex/1207.5772]. doi:10.1103/PhysRevD.86.112008.

316.   Aubert, B.; others. Measurement of branching fractions and search for CP-violating charge asymmetries in charmless two-body *B* decays into pions and kaons. *Phys. Rev. Lett.* **2001**, *87*, 151802, [hep-ex/0105061]. doi:10.1103/PhysRevLett.87.151802.

317.   Aubert, B.; others.   Measurements of branching fractions and CP-violating asymmetries in $B^0 \to \pi^+\pi^-$, $K^+\pi^-$, K^+K^- decays. *Phys. Rev. Lett.* **2002**, *89*, 281802, [hep-ex/0207055]. doi:10.1103/PhysRevLett.89.281802.

318.   Aubert, B.; others. Measurements of branching fractions and CP-violating asymmetries in $B^0 \to \rho^\pm h^\mp$ decays. *Phys. Rev. Lett.* **2003**, *91*, 201802, [hep-ex/0306030]. doi:10.1103/PhysRevLett.91.201802.

319.   Aubert, B.; others. Measurement of branching fractions, and CP and isospin asymmetries, for $B \to K^*\gamma$. *Phys. Rev. D* **2004**, *70*, 112006, [hep-ex/0407003]. doi:10.1103/PhysRevD.70.112006.

320.   Aubert, B.; others.   Measurement of the branching fraction and photon energy moments of $B \to X_s\gamma$ and $A_{CP}(B \to X_{s+d}\gamma)$. *Phys. Rev. Lett.* **2006**, *97*, 171803, [hep-ex/0607071]. doi:10.1103/PhysRevLett.97.171803.

321.   Lees, J.P.; others. Precision Measurement of the $B \to X_s\gamma$ Photon Energy Spectrum, Branching Fraction, and Direct CP Asymmetry $A_{CP}(B \to X_{s+d}\gamma)$. *Phys. Rev. Lett.* **2012**, *109*, 191801, [arXiv:hep-ex/1207.2690]. doi:10.1103/PhysRevLett.109.191801.

322.   Aubert, B.; others. Study of the decay $B^0(\overline{B}^0) \to \rho^+\rho^-$, and constraints on the CKM angle α. *Phys. Rev. Lett.* **2004**, *93*, 231801, [hep-ex/0404029]. doi:10.1103/PhysRevLett.93.231801.

323.   Aubert, B.; others. Measurement of γ in $B^\mp \to D^{(*)}K^\mp$ decays with a Dalitz analysis of $D \to K_S^0\pi^-\pi^+$. *Phys. Rev. Lett.* **2005**, *95*, 121802, [hep-ex/0504039]. doi:10.1103/PhysRevLett.95.121802.

324.   Aubert, B.; others. A Study of B0 —> rho+ rho- Decays and Constraints on the CKM Angle alpha. *Phys. Rev. D* **2007**, *76*, 052007, [arXiv:hep-ex/0705.2157]. doi:10.1103/PhysRevD.76.052007.

325.   Aubert, B.; others.   Improved measurement of the CKM angle γ in $B^\mp \to D^{(*)}K^{(*\mp)}$ decays with a Dalitz plot analysis of D decays to $K_S^0\pi^+\pi^-$ and $K_S^0K^+K^-$. *Phys. Rev. D* **2008**, *78*, 034023, [arXiv:hep-ex/0804.2089]. doi:10.1103/PhysRevD.78.034023.

326.   Aubert, B.; others.   Measurement of the $B \to J/\psi K^*(892)$ decay amplitudes. *Phys. Rev. Lett.* **2001**, *87*, 241801, [hep-ex/0107049]. doi:10.1103/PhysRevLett.87.241801.

327.   Aubert, B.; others. Measurement of branching fractions for exclusive *B* decays to charmonium final states. *Phys. Rev. D* **2002**, *65*, 032001, [hep-ex/0107025]. doi:10.1103/PhysRevD.65.032001.

328.   Aubert, B.; others. Rates, polarizations, and asymmetries in charmless vector-vector *B* meson decays. *Phys. Rev. Lett.* **2003**, *91*, 171802, [hep-ex/0307026]. doi:10.1103/PhysRevLett.91.171802.

329.   Aubert, B.; others. Measurement of the $B^0 \to \phi K^0$ decay amplitudes. *Phys. Rev. Lett.* **2004**, *93*, 231804, [hep-ex/0408017]. doi:10.1103/PhysRevLett.93.231804.

330.   Aubert, B.; others. Measurements of the $B \to X_s\gamma$ branching fraction and photon spectrum from a sum of exclusive final states. *Phys. Rev. D* **2005**, *72*, 052004, [hep-ex/0508004]. doi:10.1103/PhysRevD.72.052004.

331.   Aubert, B.; others. Measurement of the $B^+ \to p\bar{p}K^+$ branching fraction and study of the decay dynamics. *Phys. Rev. D* **2005**, *72*, 051101, [hep-ex/0507012]. doi:10.1103/PhysRevD.72.051101.

332.   Aubert, B.; others. Measurements of the absolute branching fractions of $B^\pm \to K^\pm X(c\bar{c})$. *Phys. Rev. Lett.* **2006**, *96*, 052002, [hep-ex/0510070]. doi:10.1103/PhysRevLett.96.052002.

333.   Aubert, B.; others. Dalitz plot analysis of the decay $B^\pm \to K^\pm K^\pm K^\mp$. *Phys. Rev. D* **2006**, *74*, 032003, [hep-ex/0605003]. doi:10.1103/PhysRevD.74.032003.

334. Aubert, B.; others. Study of $B^0 \rightarrow \pi^0 \pi^0$, $B^{\pm} \rightarrow \pi^{\pm} \pi^0$, and $B^{\pm} \rightarrow K^{\pm} \pi^0$ Decays, and Isospin Analysis of $B \rightarrow \pi\pi$ Decays. *Phys. Rev. D* **2007**, *76*, 091102, [arXiv:hep-ex/0707.2798]. doi:10.1103/PhysRevD.76.091102.

335. Aubert, B.; others. Measurement of decay amplitudes of $B \rightarrow J/\psi K^*$, $\psi(2S)K^*$, and $\chi_{c1}K^*$ with an angular analysis. *Phys. Rev. D* **2007**, *76*, 031102, [arXiv:hep-ex/0704.0522]. doi:10.1103/PhysRevD.76.031102.

336. Aubert, B.; others. Measurement of the $B \rightarrow X_s \gamma$ branching fraction and photon energy spectrum using the recoil method. *Phys. Rev. D* **2008**, *77*, 051103, [arXiv:hep-ex/0711.4889]. doi:10.1103/PhysRevD.77.051103.

337. Lees, J.P.; others. Exclusive Measurements of $b \rightarrow s\gamma$ Transition Rate and Photon Energy Spectrum. *Phys. Rev. D* **2012**, *86*, 052012, [arXiv:hep-ex/1207.2520]. doi:10.1103/PhysRevD.86.052012.

338. Aubert, B.; others. Dalitz-plot analysis of the decays $B^{\pm} \rightarrow K^{\pm} \pi^{\mp} \pi^{\pm}$. *Phys. Rev. D* **2005**, *72*, 072003, [hep-ex/0507004]. [Erratum: Phys.Rev.D 74, 099903 (2006)], doi:10.1103/PhysRevD.72.072003.

339. Aubert, B.; others. Study of Resonances in Exclusive B Decays to anti-D(*) D(*) K. *Phys. Rev. D* **2008**, *77*, 011102, [arXiv:hep-ex/0708.1565]. doi:10.1103/PhysRevD.77.011102.

340. Aubert, B.; others. Dalitz Plot Analysis of B+- —> pi+-pi+-pi-+ Decays. *Phys. Rev. D* **2009**, *79*, 072006, [arXiv:hep-ex/0902.2051]. doi:10.1103/PhysRevD.79.072006.

341. Aubert, B.; others. Observation of the decay $B \rightarrow J/\psi \eta K$ and search for $X(3872) \rightarrow J/\psi \eta$. *Phys. Rev. Lett.* **2004**, *93*, 041801, [hep-ex/0402025]. doi:10.1103/PhysRevLett.93.041801.

342. Aubert, B.; others. Study of the $B \rightarrow J/\psi K^- \pi^+ \pi^-$ decay and measurement of the $B \rightarrow X(3872)K^-$ branching fraction. *Phys. Rev. D* **2005**, *71*, 071103, [hep-ex/0406022]. doi:10.1103/PhysRevD.71.071103.

343. Aubert, B.; others. Search for a charged partner of the X(3872) in the B meson decay $B \rightarrow X^- K$, $X^- \rightarrow J/\psi \pi^- \pi^0$. *Phys. Rev. D* **2005**, *71*, 031501, [hep-ex/0412051]. doi:10.1103/PhysRevD.71.031501.

344. Aubert, B.; others. Search for $B^+ \rightarrow X(3872)K^+$, $X_{3872} \rightarrow J/\psi \gamma$. *Phys. Rev. D* **2006**, *74*, 071101, [hep-ex/0607050]. doi:10.1103/PhysRevD.74.071101.

345. Aubert, B.; others. Study of $J/\psi \pi^+ \pi^-$ states produced in $B^0 \rightarrow J/\psi \pi^+ \pi^- K^0$ and $B^- \rightarrow J/\psi \pi^+ \pi^- K^-$. *Phys. Rev. D* **2006**, *73*, 011101, [hep-ex/0507090]. doi:10.1103/PhysRevD.73.011101.

346. Aubert, B.; others. A Study of $B \rightarrow X(3872)K$, with $X_{3872} \rightarrow J/\Psi \pi^+ \pi^-$. *Phys. Rev. D* **2008**, *77*, 111101, [arXiv:hep-ex/0803.2838]. doi:10.1103/PhysRevD.77.111101.

347. Aubert, B.; others. Evidence for $X(3872) \rightarrow \psi_{2S} \gamma$ in $B^{\pm} \rightarrow X_{3872} K^{\pm}$ decays, and a study of $B \rightarrow c\bar{c}\gamma K$. *Phys. Rev. Lett.* **2009**, *102*, 132001, [arXiv:hep-ex/0809.0042]. doi:10.1103/PhysRevLett.102.132001.

348. del Amo Sanchez, P.; others. Evidence for the decay X(3872) —> J/ psi omega. *Phys. Rev. D* **2010**, *82*, 011101, [arXiv:hep-ex/1005.5190]. doi:10.1103/PhysRevD.82.011101.

349. Lees, J.P.; others. Measurements of the Absolute Branching Fractions of $B^{\pm} \rightarrow K^{\pm} X_{c\bar{c}}$. *Phys. Rev. Lett.* **2020**, *124*, 152001, [arXiv:hep-ex/1911.11740]. doi:10.1103/PhysRevLett.124.152001.

350. Choi, S.K.; others. Observation of a narrow charmonium-like state in exclusive $B^{\pm} \rightarrow K^{\pm} \pi^+ \pi^- J/\psi$ decays. *Phys. Rev. Lett.* **2003**, *91*, 262001, [hep-ex/0309032]. doi:10.1103/PhysRevLett.91.262001.

351. Choi, S.K.; others. Observation of a resonance-like structure in the $pi^{\pm} \psi'$ mass distribution in exclusive $B \rightarrow K\pi^{\pm}\psi'$ decays. *Phys. Rev. Lett.* **2008**, *100*, 142001, [arXiv:hep-ex/0708.1790]. doi:10.1103/PhysRevLett.100.142001.

352. Abe, K.; others. Observation of a near-threshold omega J/ψ mass enhancement in exclusive $B \rightarrow K\omega J/\psi$ decays. *Phys. Rev. Lett.* **2005**, *94*, 182002, [hep-ex/0408126]. doi:10.1103/PhysRevLett.94.182002.

353. Abe, K.; others. Experimental constraints on the possible J^{PC} quantum numbers of the $X(3872)$. 22nd International Symposium on Lepton-Photon Interactions at High Energy (LP 2005), 2005, [hep-ex/0505038].

354. Gokhroo, G.; others. Observation of a Near-threshold D0 anti-D0 pi0 Enhancement in B —> D0 anti-D0 pi0 K Decay. *Phys. Rev. Lett.* **2006**, *97*, 162002, [hep-ex/0606055]. doi:10.1103/PhysRevLett.97.162002.

355. Mizuk, R.; others. Observation of two resonance-like structures in the pi+ chi(c1) mass distribution in exclusive anti-B0 —> K- pi+ chi(c1) decays. *Phys. Rev. D* **2008**, *78*, 072004, [arXiv:hep-ex/0806.4098]. doi:10.1103/PhysRevD.78.072004.

356. Aushev, T.; others. Study of the B —> X(3872)(D*0 anti-D0) K decay. *Phys. Rev. D* **2010**, *81*, 031103, [arXiv:hep-ex/0810.0358]. doi:10.1103/PhysRevD.81.031103.

357. Mizuk, R.; others. Dalitz analysis of B —> K pi+ psi-prime decays and the Z(4430)+. *Phys. Rev. D* **2009**, *80*, 031104, [arXiv:hep-ex/0905.2869]. doi:10.1103/PhysRevD.80.031104.

358. Choi, S.K.; others. Bounds on the width, mass difference and other properties of $X(3872) \rightarrow \pi^+ \pi^- J/\psi$ decays. *Phys. Rev. D* **2011**, *84*, 052004, [arXiv:hep-ex/1107.0163]. doi:10.1103/PhysRevD.84.052004.

359. Bhardwaj, V.; others. Observation of $X(3872) \to J/\psi\gamma$ and search for $X(3872) \to \psi'\gamma$ in B decays. *Phys. Rev. Lett.* **2011**, *107*, 091803, [arXiv:hep-ex/1105.0177]. doi:10.1103/PhysRevLett.107.091803.

360. Bhardwaj, V.; others. Evidence of a new narrow resonance decaying to $\chi_{c1}\gamma$ in $B \to \chi_{c1}\gamma K$. *Phys. Rev. Lett.* **2013**, *111*, 032001, [arXiv:hep-ex/1304.3975]. doi:10.1103/PhysRevLett.111.032001.

361. Chilikin, K.; others. Observation of a new charged charmoniumlike state in $\bar{B}^0 \to J/\psi K^- \pi^+$ decays. *Phys. Rev. D* **2014**, *90*, 112009, [arXiv:hep-ex/1408.6457]. doi:10.1103/PhysRevD.90.112009.

362. Hirata, H.; others. Study of the lineshape of $X(3872)$ using B decays to $D^0\overline{D}^{*0}K$ **2023**. [arXiv:hep-ex/2302.02127].

363. Abe, K.; others. Observation of large CP violation in the neutral *B* meson system. *Phys. Rev. Lett.* **2001**, *87*, 091802, [hep-ex/0107061]. doi:10.1103/PhysRevLett.87.091802.

364. Abe, K.; others. An Improved measurement of mixing induced CP violation in the neutral B meson system. *Phys. Rev. D* **2002**, *66*, 071102, [hep-ex/0208025]. doi:10.1103/PhysRevD.66.071102.

365. Abe, K.; others. Observation of large *CP* violation and evidence for direct *CP* violation in $B^0 \to \pi^+\pi^-$ decays. *Phys. Rev. Lett.* **2004**, *93*, 021601, [hep-ex/0401029]. doi:10.1103/PhysRevLett.93.021601.

366. Chao, Y.; others. Evidence for direct CP violation in B0 —> K+ pi- decays. *Phys. Rev. Lett.* **2004**, *93*, 191802, [hep-ex/0408100]. doi:10.1103/PhysRevLett.93.191802.

367. Abashian, A.; others. Measurement of the CP violation parameter $\sin 2\phi_1$ in B_d^0 meson decays. *Phys. Rev. Lett.* **2001**, *86*, 2509–2514, [hep-ex/0102018]. doi:10.1103/PhysRevLett.86.2509.

368. Abe, K.; others. Evidence for CP violating asymmetries B0 —> pi+ pi- decays and constraints on the CKM angle phi(2). *Phys. Rev. D* **2003**, *68*, 012001, [hep-ex/0301032]. doi:10.1103/PhysRevD.68.012001.

369. Abe, K.; others. Measurement of time dependent CP violating asymmetries in B0 —> phi K0(s), K+ K- K0(s), and eta-prime K0(s) decays. *Phys. Rev. Lett.* **2003**, *91*, 261602, [hep-ex/0308035]. doi:10.1103/PhysRevLett.91.261602.

370. Poluektov, A.; others. Measurement of phi(3) with Dalitz plot analysis of B+- —> D**(*) K+- decay. *Phys. Rev. D* **2004**, *70*, 072003, [hep-ex/0406067]. doi:10.1103/PhysRevD.70.072003.

371. Chen, K.F.; others. Time-dependent CP-violating asymmetries in b —> s anti-q q transitions. *Phys. Rev. D* **2005**, *72*, 012004, [hep-ex/0504023]. doi:10.1103/PhysRevD.72.012004.

372. Itoh, R.; others. Studies of CP violation in B —> J/psi K* decays. *Phys. Rev. Lett.* **2005**, *95*, 091601, [hep-ex/0504030]. doi:10.1103/PhysRevLett.95.091601.

373. Garmash, A.; others. Evidence for large direct CP violation in B+- —> rho(770)0K+- from analysis of the three-body charmless B+- —>K+- pi+- pi-+ decay. *Phys. Rev. Lett.* **2006**, *96*, 251803, [hep-ex/0512066]. doi:10.1103/PhysRevLett.96.251803.

374. Poluektov, A.; others. Measurement of phi(3) with Dalitz plot analysis of B+ —> D(*)K(*)+ decay. *Phys. Rev. D* **2006**, *73*, 112009, [hep-ex/0604054]. doi:10.1103/PhysRevD.73.112009.

375. Abe, K.; others. Observation of b —> d gamma and determination of |V(td)/V(ts)|. *Phys. Rev. Lett.* **2006**, *96*, 221601, [hep-ex/0506079]. doi:10.1103/PhysRevLett.96.221601.

376. Ushiroda, Y.; others. Time-Dependent CP Asymmetries in $B^0 \to K_S^0\pi^0\gamma$ transitions. *Phys. Rev. D* **2006**, *74*, 111104, [hep-ex/0608017]. doi:10.1103/PhysRevD.74.111104.

377. Somov, A.; others. Measurement of the branching fraction, polarization, and CP asymmetry for B0 —> rho+ rho- decays, and determination of the CKM phase phi(2). *Phys. Rev. Lett.* **2006**, *96*, 171801, [hep-ex/0601024]. doi:10.1103/PhysRevLett.96.171801.

378. Chen, K.F.; others. Observation of time-dependent CP violation in B0 —> eta-prime K0 decays and improved measurements of CP asymmetries in B0 —> phi K0, K0(s) K0(s) K0(s) and B0 —> J/psi K0 decays. *Conf. Proc. C* **2006**, *060726*, 823–826, [hep-ex/0608039]. doi:10.1103/PhysRevLett.98.031802.

379. Ishino, H.; others. Observation of Direct CP-Violation in B0 —> pi+ pi- Decays and Model-Independent Constraints on phi(2). *Phys. Rev. Lett.* **2007**, *98*, 211801, [hep-ex/0608035]. doi:10.1103/PhysRevLett.98.211801.

380. Lin, S.W.; others. Difference in direct charge-parity violation between charged and neutral *B* meson decays. *Nature* **2008**, *452*, 332–335. doi:10.1038/nature06827.

381. Poluektov, A.; others. Evidence for direct CP violation in the decay B->D(*)K, D->KsPi+Pi- and measurement of the CKM phase phi3. *Phys. Rev. D* **2010**, *81*, 112002, [arXiv:hep-ex/1003.3360]. doi:10.1103/PhysRevD.81.112002.

382.   Adachi, I.; others. Precise measurement of the CP violation parameter $\sin 2\phi_1$ in $B^0 \to (c\bar{c})K^0$ decays. *Phys. Rev. Lett.* **2012**, *108*, 171802, [arXiv:hep-ex/1201.4643]. doi:10.1103/PhysRevLett.108.171802.

383.   Duh, Y.T.; others. Measurements of branching fractions and direct CP asymmetries for $B \to K\pi, B \to \pi\pi$ and $B \to KK$ decays. *Phys. Rev. D* **2013**, *87*, 031103, [arXiv:hep-ex/1210.1348]. doi:10.1103/PhysRevD.87.031103.

384.   Kang, K.H.; others. Measurement of time-dependent *CP* violation parameters in $B^0 \to K_0^S K_0^S K_0^S$ decays at Belle. *Phys. Rev. D* **2021**, *103*, 032003, [arXiv:hep-ex/2011.00793]. doi:10.1103/PhysRevD.103.032003.

385.   Adachi, I.; others. Measurement of *CP* violation in $B^0 \to K_S^0 \pi^0$ decays at Belle II **2023**. [arXiv:hep-ex/2305.07555].

386.   Abudinén, F.; others. Measurement of the B0 lifetime and flavor-oscillation frequency using hadronic decays reconstructed in 2019–2021 Belle II data. *Phys. Rev. D* **2023**, *107*, L091102, [arXiv:hep-ex/2302.12791]. doi:10.1103/PhysRevD.107.L091102.

387.   Adachi, I.; others. Measurement of decay-time-dependent *CP* violation in $B^0 \to J/\psi K_S^0$ decays using 2019-2021 Belle II data **2023**. [arXiv:hep-ex/2302.12898].

388.   Abe, K.; others. A Measurement of the branching fraction for the inclusive B —> X(s) gamma decays with BELLE. *Phys. Lett. B* **2001**, *511*, 151–158, [hep-ex/0103042]. doi:10.1016/S0370-2693(01)00626-8.

389.   Abe, K.; others. Measurement of branching fractions for B —> pi pi, K pi and K K decays. *Phys. Rev. Lett.* **2001**, *87*, 101801, [hep-ex/0104030]. doi:10.1103/PhysRevLett.87.101801.

390.   Abe, K.; others. Study of three-body charmless B decays. *Phys. Rev. D* **2002**, *65*, 092005, [hep-ex/0201007]. doi:10.1103/PhysRevD.65.092005.

391.   Garmash, A.; others. Study of B meson decays to three body charmless hadronic final states. *Phys. Rev. D* **2004**, *69*, 012001, [hep-ex/0307082]. doi:10.1103/PhysRevD.69.012001.

392.   Nakao, M.; others. Measurement of the $B \to K^*\gamma$ branching fractions and asymmetries. *Phys. Rev. D* **2004**, *69*, 112001, [hep-ex/0402042]. doi:10.1103/PhysRevD.69.112001.

393.   Abe, K.; others. Study of B- —> D**0 pi- (D**0 —> D(*)+ pi-) decays. *Phys. Rev. D* **2004**, *69*, 112002, [hep-ex/0307021]. doi:10.1103/PhysRevD.69.112002.

394.   Garmash, A.; others. Dalitz analysis of the three-body charmless decays B+ —> K+ pi+ pi- and B+ —> K+ K+ K-. *Phys. Rev. D* **2005**, *71*, 092003, [hep-ex/0412066]. doi:10.1103/PhysRevD.71.092003.

395.   Limosani, A.; others. Measurement of Inclusive Radiative B-meson Decays with a Photon Energy Threshold of 1.7-GeV. *Phys. Rev. Lett.* **2009**, *103*, 241801, [arXiv:hep-ex/0907.1384]. doi:10.1103/PhysRevLett.103.241801.

396.   Chen, Y.Q.; others. Dalitz analysis of $D^0 \to K^-\pi^+\eta$ decays at Belle. *Phys. Rev. D* **2020**, *102*, 012002, [arXiv:hep-ex/2003.07759]. doi:10.1103/PhysRevD.102.012002.

397.   Abudinén, F.; others. Measurement of the branching fraction and *CP* asymmetry of $B^0 \to \pi^0\pi^0$ decays using $198 \times 10^6 B\bar{B}$ pairs in Belle II data **2023**. [arXiv:hep-ex/2303.08354].

398.   Abe, K.; others. Observation of B+- —> p anti-p K+-. *Phys. Rev. Lett.* **2002**, *88*, 181803, [hep-ex/0202017]. doi:10.1103/PhysRevLett.88.181803.

399.   Choi, S.K.; others. Observation of the eta(c)(2S) in exclusive B —> K K(S) K- pi+ decays. *Phys. Rev. Lett.* **2002**, *89*, 102001, [hep-ex/0206002]. [Erratum: Phys.Rev.Lett. 89, 129901 (2002)], doi:10.1103/PhysRevLett.89.102001.

400.   Abe, K.; others. Observation of anti-B0 —> D0(*) p anti-p. *Phys. Rev. Lett.* **2002**, *89*, 151802, [hep-ex/0205083]. doi:10.1103/PhysRevLett.89.151802.

401.   Lee, S.H.; others. Evidence for $B^0 \to \pi^0\pi^0$. *Phys. Rev. Lett.* **2003**, *91*, 261801, [hep-ex/0308040]. doi:10.1103/PhysRevLett.91.261801.

402.   Krokovny, P.; others. Observation of the D(sJ)(2317) and D(sJ)(2457) in B decays. *Phys. Rev. Lett.* **2003**, *91*, 262002, [hep-ex/0308019]. doi:10.1103/PhysRevLett.91.262002.

403.   Zhang, J.; others. Observation of B+ —> rho+ rho0. *Phys. Rev. Lett.* **2003**, *91*, 221801, [hep-ex/0306007]. doi:10.1103/PhysRevLett.91.221801.

404.   Wang, M.Z.; others. Observation of B+ —> p anti-p pi+, B0 —> p anti-p K0, and B+ —> p anti-p K*+. *Phys. Rev. Lett.* **2004**, *92*, 131801, [hep-ex/0310018]. doi:10.1103/PhysRevLett.92.131801.

405.   Brodzicka, J.; others. Observation of a new D(sJ) meson in B+ —> anti-D0 D0 K+ decays. *Phys. Rev. Lett.* **2008**, *100*, 092001, [arXiv:hep-ex/0707.3491]. doi:10.1103/PhysRevLett.100.092001.

406. Li, Y.B.; others. Observation of $\Xi_c(2930)^0$ and updated measurement of $B^- \to K^- \Lambda_c^+ \bar{\Lambda}_c^-$ at Belle. *Eur. Phys. J. C* **2018**, *78*, 252, [arXiv:hep-ex/1712.03612]. doi:10.1140/epjc/s10052-018-5720-5.

407. Chen, K.F.; others. Measurement of branching fractions and polarization in B —> phi K(*) decays. *Phys. Rev. Lett.* **2003**, *91*, 201801, [hep-ex/0307014]. doi:10.1103/PhysRevLett.91.201801.

408. Chen, K.F.; others. Measurement of polarization and triple-product correlations in B —> phi K* decays. *Phys. Rev. Lett.* **2005**, *94*, 221804, [hep-ex/0503013]. doi:10.1103/PhysRevLett.94.221804.

409. Koppenburg, P.; others. An Inclusive measurement of the photon energy spectrum in b —> s gamma decays. *Phys. Rev. Lett.* **2004**, *93*, 061803, [hep-ex/0403004]. doi:10.1103/PhysRevLett.93.061803.

410. Abudinén, F.; others. Measurement of the photon-energy spectrum in inclusive $B \to X_s\gamma$ decays identified using hadronic decays of the recoil B meson in 2019-2021 Belle II data **2022**. [arXiv:hep-ex/2210.10220].

411. Cabibbo, N. Unitary Symmetry and Leptonic Decays. *Phys. Rev. Lett.* **1963**, *10*, 531–533. doi:10.1103/PhysRevLett.10.531.

412. Kobayashi, M.; Maskawa, T. CP Violation in the Renormalizable Theory of Weak Interaction. *Prog. Theor. Phys.* **1973**, *49*, 652–657. doi:10.1143/PTP.49.652.

413. Bander, M.; Silverman, D.; Soni, A. CP Noninvariance in the Decays of Heavy Charged Quark Systems. *Phys. Rev. Lett.* **1979**, *43*, 242. doi:10.1103/PhysRevLett.43.242.

414. Carter, A.B.; Sanda, A.I. CP Violation in B Meson Decays. *Phys. Rev. D* **1981**, *23*, 1567. doi:10.1103/PhysRevD.23.1567.

415. Bigi, I.I.Y.; Sanda, A.I. Notes on the Observability of CP Violations in B Decays. *Nucl. Phys. B* **1981**, *193*, 85–108. doi:10.1016/0550-3213(81)90519-8.

416. Chernyak, V.L.; Zhitnitsky, A.R. Asymptotic Behavior of Exclusive Processes in QCD. *Phys. Rept.* **1984**, *112*, 173. doi:10.1016/0370-1573(84)90126-1.

417. Godfrey, S.; Isgur, N. Mesons in a Relativized Quark Model with Chromodynamics. *Phys. Rev. D* **1985**, *32*, 189–231. doi:10.1103/PhysRevD.32.189.

418. Bauer, M.; Stech, B.; Wirbel, M. Exclusive Nonleptonic Decays of D, D(s), and B Mesons. *Z. Phys. C* **1987**, *34*, 103. doi:10.1007/BF01561122.

419. Buras, A.J.; Jamin, M.; Lautenbacher, M.E.; Weisz, P.H. Effective Hamiltonians for $\Delta S = 1$ and $\Delta B = 1$ nonleptonic decays beyond the leading logarithmic approximation. *Nucl. Phys. B* **1992**, *370*, 69–104. [Addendum: Nucl.Phys.B 375, 501 (1992)], doi:10.1016/0550-3213(92)90345-C.

420. Isgur, N.; Wise, M.B. Spectroscopy with heavy quark symmetry. *Phys. Rev. Lett.* **1991**, *66*, 1130–1133. doi:10.1103/PhysRevLett.66.1130.

421. Neubert, M.; Stech, B. Nonleptonic weak decays of B mesons. *Adv. Ser. Direct. High Energy Phys.* **1998**, *15*, 294–344, [hep-ph/9705292]. doi:10.1142/9789812812667_0004.

422. Chetyrkin, K.G.; Misiak, M.; Munz, M. Weak radiative B meson decay beyond leading logarithms. *Phys. Lett. B* **1997**, *400*, 206–219, [hep-ph/9612313]. [Erratum: Phys.Lett.B 425, 414 (1998)], doi:10.1016/S0370-2693(97)00324-9.

423. Ciuchini, M.; Franco, E.; Martinelli, G.; Silvestrini, L. Charming penguins in B decays. *Nucl. Phys. B* **1997**, *501*, 271–296, [hep-ph/9703353]. doi:10.1016/S0550-3213(97)00388-X.

424. Kagan, A.L.; Neubert, M. QCD anatomy of B —> X(s gamma) decays. *Eur. Phys. J. C* **1999**, *7*, 5–27, [hep-ph/9805303]. doi:10.1007/s100529800959.

425. Dunietz, I.; Rosner, J.L. Time Dependent CP Violation Effects in B0 anti-B0 Systems. *Phys. Rev. D* **1986**, *34*, 1404. doi:10.1103/PhysRevD.34.1404.

426. Gronau, M.; London, D. Isospin analysis of CP asymmetries in B decays. *Phys. Rev. Lett.* **1990**, *65*, 3381–3384. doi:10.1103/PhysRevLett.65.3381.

427. Ali, A.; Kramer, G.; Lu, C.D. Experimental tests of factorization in charmless nonleptonic two-body B decays. *Phys. Rev. D* **1998**, *58*, 094009, [hep-ph/9804363]. doi:10.1103/PhysRevD.58.094009.

428. Beneke, M.; Buchalla, G.; Neubert, M.; Sachrajda, C.T. QCD factorization for exclusive, nonleptonic B meson decays: General arguments and the case of heavy light final states. *Nucl. Phys. B* **2000**, *591*, 313–418, [hep-ph/0006124]. doi:10.1016/S0550-3213(00)00559-9.

429. Beneke, M.; Buchalla, G.; Neubert, M.; Sachrajda, C.T. QCD factorization in $B \to \pi K, \pi\pi$ decays and extraction of Wolfenstein parameters. *Nucl. Phys. B* **2001**, *606*, 245–321, [hep-ph/0104110]. doi:10.1016/S0550-3213(01)00251-6.

430. Bauer, C.W.; Pirjol, D.; Stewart, I.W. A Proof of factorization for $B \to D\pi$. *Phys. Rev. Lett.* **2001**, *87*, 201806, [hep-ph/0107002]. doi:10.1103/PhysRevLett.87.201806.

431. Beneke, M.; Neubert, M. QCD factorization for $B \to PP$ and $B \to PV$ decays. *Nucl. Phys. B* **2003**, *675*, 333–415, [hep-ph/0308039]. doi:10.1016/j.nuclphysb.2003.09.026.

432. Bauer, C.W.; Pirjol, D.; Rothstein, I.Z.; Stewart, I.W. $B \to M(1)M(2)$: Factorization, charming penguins, strong phases, and polarization. *Phys. Rev. D* **2004**, *70*, 054015, [hep-ph/0401188]. doi:10.1103/PhysRevD.70.054015.

433. Buras, A.J.; Fleischer, R.; Recksiegel, S.; Schwab, F. $B \to \pi\pi$, new physics in $B \to \pi K$ and implications for rare K and B decays. *Phys. Rev. Lett.* **2004**, *92*, 101804, [hep-ph/0312259]. doi:10.1103/PhysRevLett.92.101804.

434. Buras, A.J.; Fleischer, R.; Recksiegel, S.; Schwab, F. Anatomy of prominent B and K decays and signatures of CP violating new physics in the electroweak penguin sector. *Nucl. Phys. B* **2004**, *697*, 133–206, [hep-ph/0402112]. doi:10.1016/j.nuclphysb.2004.07.009.

435. Cheng, H.Y.; Chua, C.K.; Soni, A. Final state interactions in hadronic B decays. *Phys. Rev. D* **2005**, *71*, 014030, [hep-ph/0409317]. doi:10.1103/PhysRevD.71.014030.

436. Ball, P.; Zwicky, R. New results on $B \to \pi, K, \eta$ decay formfactors from light-cone sum rules. *Phys. Rev. D* **2005**, *71*, 014015, [hep-ph/0406232]. doi:10.1103/PhysRevD.71.014015.

437. Gorbahn, M.; Haisch, U. Effective Hamiltonian for non-leptonic $|\Delta F| = 1$ decays at NNLO in QCD. *Nucl. Phys. B* **2005**, *713*, 291–332, [hep-ph/0411071]. doi:10.1016/j.nuclphysb.2005.01.047.

438. Beneke, M.; Rohrer, J.; Yang, D. Branching fractions, polarisation and asymmetries of B —> VV decays. *Nucl. Phys. B* **2007**, *774*, 64–101, [hep-ph/0612290]. doi:10.1016/j.nuclphysb.2007.03.020.

439. Charles, J.; others. Current status of the Standard Model CKM fit and constraints on $\Delta F = 2$ New Physics. *Phys. Rev. D* **2015**, *91*, 073007, [arXiv:hep-ph/1501.05013]. doi:10.1103/PhysRevD.91.073007.

440. Dubnicka, S.; Dubnickova, A.Z.; Ivanov, M.A.; Liptaj, A. Decays $B_s \to J/\psi + \eta$ and $B_s \to J/\psi + \eta'$ in the framework of covariant quark model. *Phys. Rev. D* **2013**, *87*, 074201, [arXiv:hep-ph/1301.0738]. doi:10.1103/PhysRevD.87.074021.

441. Ambrosino, F.; others. Measurement of the pseudoscalar mixing angle and eta-prime gluonium content with KLOE detector. *Phys. Lett. B* **2007**, *648*, 267–273, [hep-ex/0612029]. doi:10.1016/j.physletb.2007.03.032.

442. Li, J.; others. First observation of $B_s^0 \to J/\psi\eta$ and $B_s^0 \to J/\psi\eta'$. *Phys. Rev. Lett.* **2012**, *108*, 181808, [arXiv:hep-ex/1202.0103]. doi:10.1103/PhysRevLett.108.181808.

443. Aaij, R.; others. Evidence for the decay $B^0 \to J/\psi\omega$ and measurement of the relative branching fractions of B_s^0 meson decays to $J/\psi\eta$ and $J/\psi\eta'$. *Nucl. Phys. B* **2013**, *867*, 547–566, [arXiv:hep-ex/1210.2631]. doi:10.1016/j.nuclphysb.2012.10.021.

444. Dubnička, S.; Dubničková, A.Z.; Ivanov, M.A.; Liptaj, A. Decays $B \to D(s)(*)h$ ($h = \pi, \rho$) in a confined covariant quark model. *Phys. Rev. D* **2022**, *106*, 033006, [arXiv:hep-ph/2204.11599]. doi:10.1103/PhysRevD.106.033006.

445. Huber, T.; Kränkl, S.; Li, X.Q. Two-body non-leptonic heavy-to-heavy decays at NNLO in QCD factorization. *JHEP* **2016**, *09*, 112, [arXiv:hep-ph/1606.02888]. doi:10.1007/JHEP09(2016)112.

446. Bordone, M.; Gubernari, N.; Huber, T.; Jung, M.; van Dyk, D. A puzzle in $\bar{B}_{(s)}^0 \to D_{(s)}^{(*)+}\{\pi^-, K^-\}$ decays and extraction of the f_s/f_d fragmentation fraction. *Eur. Phys. J. C* **2020**, *80*, 951, [arXiv:hep-ph/2007.10338]. doi:10.1140/epjc/s10052-020-08512-8.

447. Iguro, S.; Kitahara, T. Implications for new physics from a novel puzzle in $\bar{B}_{(s)}^0 \to D_{(s)}^{(*)+}\{\pi^-, K^-\}$ decays. *Phys. Rev. D* **2020**, *102*, 071701, [arXiv:hep-ph/2008.01086]. doi:10.1103/PhysRevD.102.071701.

448. Ivanov, M.A.; Korner, J.G.; Pakhomova, O.N. The Nonleptonic decays $B_c^+ \to D_s^+\bar{D}^0$ and $B_c^+ \to D_s^+D^0$ in a relativistic quark model. *Phys. Lett. B* **2003**, *555*, 189–196, [hep-ph/0212291]. doi:10.1016/S0370-2693(03)00052-2.

449. Dubnicka, S.; Dubnickova, A.Z.; Issadykov, A.; Ivanov, M.A.; Liptaj, A. Study of B_c decays into charmonia and D mesons. *Phys. Rev. D* **2017**, *96*, 076017, [arXiv:hep-ph/1708.09607]. doi:10.1103/PhysRevD.96.076017.

450. Aad, G.; others. Study of the $B_c^+ \to J/\psi D_s^+$ and $B_c^+ \to J/\psi D_s^{*+}$ decays with the ATLAS detector. *Eur. Phys. J. C* **2016**, *76*, 4, [arXiv:hep-ex/1507.07099]. doi:10.1140/epjc/s10052-015-3743-8.

451. Ivanov, M.A.; Tyulemissov, Z.; Tyulemissova, A. Weak nonleptonic decays of vector B-mesons. *Phys. Rev. D* **2023**, *107*, 013009, [arXiv:hep-ph/2212.10161]. doi:10.1103/PhysRevD.107.013009.

452. Aaij, R.; others. Measurement of the $B_s^0 \to \mu^+\mu^-$ decay properties and search for the $B^0 \to \mu^+\mu^-$ and $B_s^0 \to \mu^+\mu^-\gamma$ decays. *Phys. Rev. D* **2022**, *105*, 012010, [arXiv:hep-ex/2108.09283]. doi:10.1103/PhysRevD.105.012010.

453. Aad, G.; others. Study of $B_c^+ \to J/\psi D_s^+$ and $B_c^+ \to J/\psi D_s^{*+}$ decays in pp collisions at $\sqrt{s}$ = 13 TeV with the ATLAS detector. *JHEP* **2022**, *08*, 087, [arXiv:hep-ex/2203.01808]. doi:10.1007/JHEP08(2022)087.